

N O T I C E

THIS DOCUMENT HAS BEEN REPRODUCED FROM
MICROFICHE. ALTHOUGH IT IS RECOGNIZED THAT
CERTAIN PORTIONS ARE ILLEGIBLE, IT IS BEING RELEASED
IN THE INTEREST OF MAKING AVAILABLE AS MUCH
INFORMATION AS POSSIBLE

(NASA-CR-163296) STRAIN MEASUREMENTS IN
COMPOSITE BOLTED-JOINT SPECIMENS (Virginia
Polytechnic Inst. and State Univ.) 87 p
HC A05/MF A01 CSCL 20K

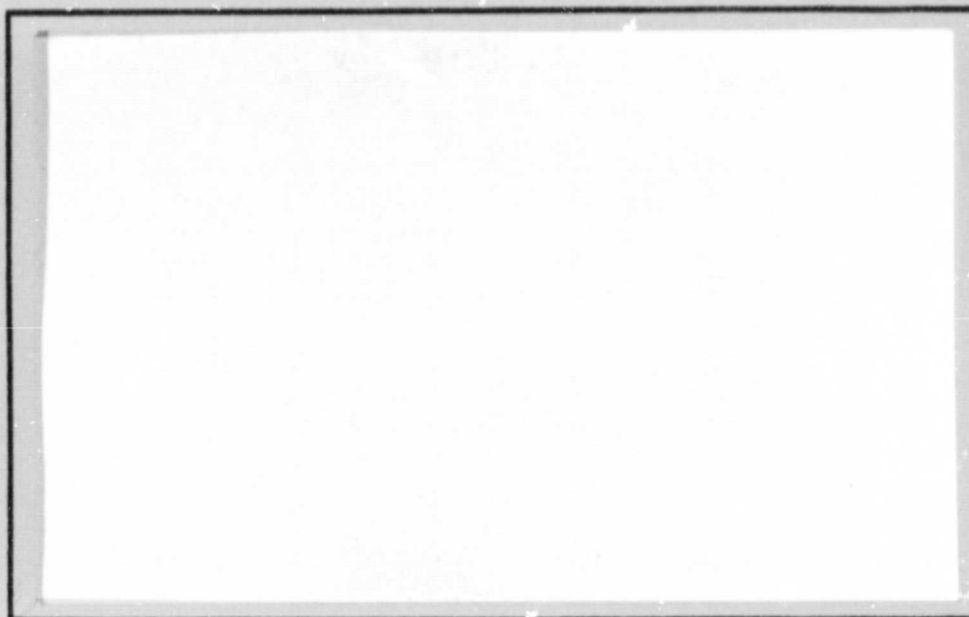
a80-26698

Unclass

G3/39 24246



**COLLEGE
OF
ENGINEERING**



**VIRGINIA
POLYTECHNIC
INSTITUTE
AND
STATE
UNIVERSITY**

**BLACKSBURG,
VIRGINIA**

VPI-E-79-17

May 1979

STRAIN MEASUREMENTS IN COMPOSITE
BOLTED-JOINT SPECIMENTS

By

Michael W. Hyer

Michael C. Lightfoot

and

James C. Perry

BIBLIOGRAPHIC DATA SHEET	1. Report No. VPI-E-79-17	2.	3. Recipient's Accession No.
4. Title and Subtitle Strain Measurements in Composite Bolted-Joint Specimens		5. Report Date May 1979	
		6.	
7. Author(s) Michael W. Hyer (VPI&SU) Michael C. Lightfoot and James C. Perry (ODU)		8. Performing Organization Rept. No.	
9. Performing Organization Name and Address Virginia Polytechnic Institute and State University Department of Engineering Science and Mechanics Blacksburg, VA 24061		10. Project/Task/Work Unit No. 802-068-1 (VPI&SU)	
		11. Contract/Grant No. NSG 1167 (NASA/LARC)	
12. Sponsoring Organization Name and Address Old Dominion University Research Foundation P.O. Box 6369 Norfolk, VA 23508		13. Type of Report & Period Covered Interim Report 9/1/78 to 12/15/78	
		14.	
15. Supplementary Notes The grantee for this project is the Old Dominion University Research Foundation (grant NSG 1167 with NASA/Langley Research Center); Dr. Hyer is now affiliated with Virginia Polytechnic Institute and State University.			
16. Abstracts Strain data from a series of bolted-joint tests is presented. Double-lap, double-hole, double-lap, single-hole, and open-hole tensile specimens were tested and the strain gage locations, load-strain responses, and load-axial displacement responses are presented. The open-hole specimens were gaged to determine strain concentration factors. The double-lap, double-hole specimens were gaged to determine the uniformity of the strain in the joint and the amount of load transferred past the first bolt. The measurements indicated roughly half the load passed the first bolt to be reacted by the second bolt.			
17. Key Words and Document Analysis. 17a. Descriptors Bolted-joints Strain concentration factors Stress concentration factors Load transfer Holes in tensile specimens Composites Strain gages 17b. Identifiers/Open-Ended Terms 17c. COSATI Field Group			
18. Availability Statement		19. Security Class (This Report) UNCLASSIFIED	21. No. of Pages 88
		20. Security Class (This Page) UNCLASSIFIED	22. Price

TABLE OF CONTENTS

	<u>Page</u>
ABSTRACT	1
INTRODUCTION	2
DESCRIPTION OF SPECIMENS	2
STRAIN GAGE LOCATIONS	4
Open-Hole Specimens	4
Double-Lap, Single-Hole Specimen	5
Double-Lap, Double-Hole Specimens	6
EXPERIMENTAL RESULTS	6
Double-Lap, Single-Hole Specimen	6
Open-Hole Specimens	7
Double-Lap, Double-Hole Specimens	7
DISCUSSION OF RESULTS	8
Open-Hole Specimens	8
Double-Lap, Double-Hole Specimens	11
CONCLUDING REMARKS	12
APPENDIX A: LOCATION OF GAGES ON COMPOSITE OPEN-HOLE SPECIMENS	14
APPENDIX B: STRAIN GAGE SPECIFICATIONS FOR COMPOSITE OPEN-HOLE SPECIMENS	16
APPENDIX C: LOCATION OF STRAIN GAGES ON DOUBLE-LAP, SINGLE-HOLE SPECIMEN 11	17
APPENDIX D: STRAIN GAGE SPECIFICATION FOR DOUBLE-LAP, SINGLE-HOLE SPECIMEN 11	18
APPENDIX E: LOCATION OF STRAIN GAGES ON DOUBLE-LAP, DOUBLE-HOLE SPECIMENS	19
APPENDIX F: STRAIN GAGE SPECIFICATIONS FOR DOUBLE-LAP, DOUBLE-HOLE SPECIMENS	20
REFERENCES	21

LIST OF TABLES

<u>Table</u>	<u>Page</u>
1 Strain concentration data for aluminum open-hole specimen 1	22
2 Strain concentration data for aluminum open-hole specimen 11	23
3 Strain concentration data for composite open-hole specimen 1	24
4 Strain concentration data for composite open-hole specimen 11	25

LIST OF FIGURES

<u>Figure</u>	<u>Page</u>
1 Specimens for open-hole tests	26
2 Specimens for double-lap, single-hole tests	27
3 Specimens for double-lap, double-hole tests	28
4 Double-lap, single-hole test setup	29
5 Strain gage locations for open-hole specimens 4 and 7	30
6 Strain gage locations for open-hole specimens 5 and 9	31
7 Strain gage locations for open-hole specimen 1	32
8 Strain gage locations for open-hole specimen 11	33
9 Strain gage locations for double-lap, single-hole specimen 11	34
10 Strain gage locations for double-lap, double-hole specimens	35
11 Load-strain responses for double-lap, single-hole specimen 11, axial gages	36
12 Load-strain responses for double-lap, single-hole specimen 11, lateral gages	37
13 Load-strain responses for double-lap, single-hole specimen 11, 45° gages	38

LIST OF FIGURES (CONT'D)

<u>Figure</u>		<u>Page</u>
14	Load-head displacement for double-lap, single-hole specimen 11	39
15	Load-strain responses for open-hole specimen 4	40
16	Load-strain responses for open-hole specimen 5	41
17	Load-strain responses for open-hole specimen 7	42
18	Load-strain responses for open-hole specimen 9	43
19	Load-strain responses for open-hole specimen 1	44
20	Load-strain responses for open-hole specimen 11	45
21	Load-head displacement for open-hole specimen 4	46
22	Load-head displacement for open-hole specimen 5	47
23	Load-head displacement for open-hole specimen 7	48
24	Load-head displacement for open-hole specimen 9	49
25	Load-head displacement for open-hole specimen 1	50
26	Load-head displacement for open-hole specimen 11	51
27	Load-strain responses for double-lap, double-hole specimen 1	52
28	Load-strain responses for double-lap, double-hole specimen 3	53
29	Load-strain responses for double-lap, double-hole specimen 7	54
30	Load-strain responses for double-lap, double-hole specimen 17	55
31	Load-strain responses for double-lap, double-hole specimen 18	56
32	Load-strain responses for double-lap, double-hole specimen 20	57
33	Load-strain responses for double-lap, double-hole specimen 22	58

LIST OF FIGURES (CONT'D)

<u>Figure</u>		<u>Page</u>
34	Load-head displacement for double-lap, double-hole specimen 1	59
35	Load-head displacement for double-lap, double-hole specimen 3	60
36	Load-head displacement for double-lap, double-hole specimen 7	61
37	Load-head displacement for double-lap, double-hole specimen 17	62
38	Load-head displacement for double-lap, double-hole specimen 18	63
39	Load-head displacement for double-lap, double-hole specimen 20	64
40	Load-head displacement for double-lap, double-hole specimen 22	65
41	Strain gage locations for aluminum open-hole specimen 1	66
42	Strain gage locations for aluminum open-hole specimen 11	67
43	Aluminum open-hole specimens 1 (left) and 11 (right)	68
44	Load-strain responses for aluminum open-hole specimen 1	71
45	Load-strain responses for aluminum open-hole specimen 11	72
46	Load-head displacement for aluminum open-hole specimen 1	73
47	Load-head displacement for aluminum open-hole specimen 11	74
48	Stress concentration factors for aluminum and composite specimens 1 and 11	75
49	Uniformity of strain across double-lap, double-hole specimens between doubler and first bolt	76
50	Uniformity of strain across double-lap, double-hole specimens between bolts	77

LIST OF FIGURES (CONCL'D)

<u>Figure</u>		<u>Page</u>
51	Ratio of strains before and after first bolt in double-lap, double-hole specimens, outer gages	78
52	Ratio of strains before and after first bolt in double-lap, double-hole specimens, centerline gages	79

STRAIN MEASUREMENTS IN COMPOSITE BOLTED-JOINT SPECIMENS

By

Michael W. Hyer¹, Michael C. Lightfoot², and James C. Perry²

ABSTRACT

This report presents strain data resulting from the testing of a series of specimens designed to determine the load-carrying capacity of quasi-isotropic composite bolted joints. Three types of specimens: double-lap, double-hole bolted joints, double-lap, single-hole bolted joints, and open-hole tensile specimens were tested, and the strain gage locations, load-strain responses, and load-axial displacement responses are presented. The open-hole specimens were gaged in such a way as to measure strains inside the hole, and strain concentration values were computed. To check the accuracy of the strain measurements, identical aluminum specimens were fabricated, tested, and the results of strain concentration calculations compared with handbook values. Agreement was good, and so the results from the composite specimens, which showed higher strain concentration values than the identical isotropic specimens, were felt to be reliable. However, results from the aluminum specimens, which had more gages than their composite counterparts, showed the composite test specimens may have been made too short, in an effort to conserve material, and the load-introduction doublers could have interfered with the test holes. The double-lap, double-hole specimens were gaged to measure the amount of load transferred past the first bolt and the uniformity of strain across the specimen. Overall, the measurements indicated roughly half the load passed the first bolt to be reacted by the second bolt. Only one double-lap, single-hole specimen was strain gaged, and the data was used to determine elastic properties of the material used in the specimens.

¹ Assistant Professor, Department of Engineering Science and Mechanics, Virginia Polytechnic Institute and State University, Blacksburg, Virginia 24061.

² Research Assistant, Old Dominion University Research Foundation, P.O. Box 6369, Norfolk, Virginia 23508.

INTRODUCTION

In an effort to better understand the behavior of composite bolted joints, a series of specimens was fabricated and tested to failure. The joint specimens were designed to determine the effects of specimen width, specimen thickness, bolt size and the number of bolts on the load-carrying capacity of the joints. The specimens were measured carefully, tested to failure, and the load capacity determined as a function of the various parameters. Reference 1 summarizes that work in detail, and reference 2 further discusses the results. To obtain additional information on the behavior of the joints, some of the specimens were strain gaged and those responses measured as a function of applied load. The results of the strain gage measurements are presented here. This document is intended as a companion document to reference 1, and the reader is urged to consult it for more details since much of the information is not repeated here.

DESCRIPTION OF SPECIMENS

Three specimen configurations were tested: open-hole (OH), double-lap, single-hole (DLSH) and double-lap, double-hole (DLDH). The configurations of the three specimens are shown in figures 1, 2, and 3.

The open-hole specimen is not a joint, rather it is a tensile specimen and serves to determine the effect of simply putting a hole in a laminate. Work on this configuration has been done by other investigators (ref. 3). By the geometry of the open-hole specimens, two tests could be conducted on each specimen: one on the hole on the left (L) end of the specimen and one on the hole on the right (R) end of the specimen. The specimens were loaded through holes reinforced with aluminum doublers. To test the hole on the right end, the tensile loads were applied through the central reinforced hole and the right reinforced hole. The left test hole was tested by loading the specimen through the central reinforced hole and the left reinforced hole. The specimen widths, W , ranged from 44.4 to 127 mm (1.75 to 5.00 in.), and the hole diameters, D , ranged from 11.1 to 15.9 mm (0.438 to 0.625 in.). All open-hole specimens were 32 plies in thickness and were nominally 4.30-mm (0.169-in.) thick. The ratios of W/D were chosen

to be 4, 6, and 8. The material system for all three specimen types was Narmco T-300/Narmco 5208 in a quasi-isotropic layup. The volume fraction was 59.2 percent fibers. The specific layup for the open-hole specimens was $[(0^\circ/90^\circ/45^\circ/-45^\circ)_4]_S$. There were 12 open-hole specimens, 8 of which were gaged.

The double-lap, single-hole configuration represents the inner lap of a lapped joint. This idea is shown in figure 4. To reduce the cost of specimens, the outer laps were steel, rather than graphite-epoxy, and were reusable. The primary effect being tested was the load capacity of a composite loaded through a single hole by a bolt. This loading results in a net-section tensile failure, bearing failure, shear-out failure or some combination of these. With this specimen configuration four tests could be conducted per specimen. To force failure at the holes designated as test holes, aluminum doublers were used at the central hole transmitting the load to the specimen. The specimen widths, W , ranged from 44.4 to 127.0 mm (1.75 to 5.00 in.), and the hole diameters, D , varied from 11.1 to 15.9 mm (0.438 to 0.625 in.). The values of W/D were chosen to be 4, 6, and 8. There were 2 specimen thicknesses, 32-ply and 96-ply. The layup for the 32-ply specimens was $[(0^\circ/90^\circ/45^\circ/-45^\circ)_4]_S$, and the layup for the 96-ply specimens was $[(0^\circ/90^\circ/45^\circ/-45^\circ)_{12}]_S$. The average thickness for the 32-ply specimens was 4.30 mm (0.169 in.), while for the 96-ply specimens the nominal thickness was 12.3 mm (0.485 in.). There were 32 double-lap, single-hole specimens, but, as explained later, only one specimen was gaged. For all specimens, the distance from the center of the test hole to the end of the specimen was approximately three bolt diameters.

The double-lap, double-hole specimens represent the only true joint. For this configuration the interaction of the bolts was being investigated and it was necessary to have the inner and outer laps of equal stiffness to obtain correct bolt-lap interaction. Thus, except for the aluminum doublers, the entire joint was made of graphite-epoxy. Only one test could be conducted per specimen. The specimen widths, W , ranged from 44.0 to 127.0 mm (1.75 to 5.00 in.) and the hole diameter, D , from 11.1 to 19.0 mm (0.438 to 0.750 in.). Actually the largest hole size was intended to be 15.9 mm (0.625 in.), but several specimens were misdrilled and the holes were over-

sized. The values of W/D were originally intended to be 4, 6, and 8, but the oversized hole produced some specimens with $W/D = 2.35$. There were two thicknesses, 32-ply and 96-ply, representing the thicknesses of the inner lap. Each outer lap was one-half the thickness of the inner lap. The inner lap of the 32-ply specimens averaged 4.30 mm (0.169 in.) while the 92-ply specimens averaged 12.3 mm (0.485 in.) in thickness. Except for the specimens with oversized holes, the distance from the center of the bolt to the end of the specimen was three bolt diameters while the distance between bolts was twice that. There was 32 double-lap, double hole specimens, of which 7 were strain gaged.

In addition to having the left and right ends of the specimens identified, all specimens were coded with an abbreviation as to their type and a number: e.g. DLDH-7 denoted specimen number 7 of the double-lap, double-hole variety.

STRAIN GAGE LOCATIONS

Open-Hole Specimens

In order to determine the strain concentration factors at the holes in the open-hole specimens, strain gages were positioned near the hole. Two of the six specimens gaged had strain gages mounted circumferentially inside the hole. The strain gage locations for specimens 4 and 7 are shown in figure 5, the locations for specimens 5 and 9 in figure 6, the locations for specimen 1 in figure 7, and the locations for specimen 11 in figure 8. The gages were placed symmetrically on either side of the hole to determine if the loading mechanism was applying pure tension to the specimens. Referring to these figures, gages 1 and 7 measured the strain at the outer edges on the upper surface of the specimen while gage 8 was a back-to-back mate with gage 7 to check for through-the-thickness bending. Gages 2 and 3 measured strain on the upper surface at the edge of the hole. These gages were trimmed so the gage-sensing material was as close to the hole edge as possible, generally less than 0.254 mm (0.01 in.). These gages were 1.58×1.58 mm (0.062×0.062 in.) in size, 7 to 10 times smaller than the hole radii being considered. On specimens 5, 9, and 11, gages 4, 5, and 6 were stacked rosettes.

Since there are high strain gradients associated with strain concentrations, several other gages were mounted on specimens 1 and 11 to determine the severity of these gradients. Referring to figures 7 and 8, gages 9 and 12 were positioned on the extreme outer edges of the specimens. Comparisons of gages 1, 7, 8, 9, and 12 would indicate the magnitude of the strain gradient near the outer edge, an effect felt to be small. It was felt placement of gages 2 and 3 would give a good indication of the strain at the hole edge. However, the strain gradients were high there, and, as a check, gages 10 and 11 were installed circumferentially inside the hole. Comparison of strain values from gages 2, 3, 10, and 11 would then indicate the severity of the gradient. If the gradient were high, gages 2 and 3 would not agree with gages 10 and 11. It was felt that, by using the strain values and relative distance to the hole edge of each gage, gages 1, 2, 3, 4, 7, 8, 9, and 12 on specimen 11 could be used to obtain an extrapolated value of strain at the hole edge. This extrapolated value would perhaps be closer to the value measured by gages 10 and 11 than the values from just 2 and 3 alone. Unfortunately, even for the larger holes, the strain gradients were so high near the hole edge only gages mounted inside the hole could accurately describe the strain there.

Appendixes A and B summarize the locations and specifications of the gages used on the open-hole specimens.

Double-Lap, Single-Hole Specimen

In the double-lap, single-hole specimens, the regions which experienced the maximum strain were under the steel outer laps. Thus, strain gages could not be used to advantage with this configuration. Only one specimen, number 11, was instrumented, and the gages, stacked rosettes, were positioned as shown in figure 9. The gages were positioned to determine if the two test holes were interacting, an undesirable situation which would lead to erroneous conclusions regarding the behavior of a single loaded hole. If the holes were interacting, the stress would not be uniform across the width of the specimen. If the holes were not interacting, the stress would be uniform across the specimen and the data could be used to determine some of the elastic properties of the material. The specimen gaged was 127-mm (5.00-in.) wide, and the holes were 15.9 mm in diameter (0.625 in.). The specimen was 96 plys thick.

Appendixes C and D summarize the locations and specifications of the gages used on the double-lap, single-hole specimens.

Double-Lap, Double-Hole Specimens

With the double-lap, double-hole configuration, the main issue to be investigated was the effect of the second bolt. In particular, the question was the percentage of load being transmitted to the second bolt. Seven specimens were gaged in the configuration shown in figure 10. With this arrangement the uniformity of the loading across the specimen and the strain levels before and after the first bolt could be studied. One of the specimens, DLDH-20, had a rosette installed in place of a single gage.

Appendixes E and F summarize the gage locations and specifications for the double-lap, double-hole specimens. The centerline of the first row of gages was halfway between the edge of the doubler and the first bolt, and the centerline of the second row of gages was halfway between the hole centers.

During the testing of all specimens, a direct-current displacement transducer (DCDT) was used to measure the change in distance between the loading heads as the load was applied to the specimen. Although this measurement includes elastic deformations of the loading fixture, it provided some measure of the axial stiffness of various joint configurations.

EXPERIMENTAL RESULTS

Double-Lap, Single-Hole Specimen

Figures 11 to 14 show the load-strain and load-head displacement behavior for the double-lap, single-hole specimen. The closeness of the responses of gages 1, 4, and 7 make it apparent the axial strain was quite uniform across the width. In addition, comparing the back gage, B, with gages 1, 4, and 7, it appears there was little bending from side to side or through the thickness. Using the cross-sectional area of the specimen, 1187 mm^2 (1.8396 in.^2), and the slope of the load-axial strain relation, Young's modulus of the material was computed to be 56.26 MPa ($8.16 \times 10^6 \text{ psi}$). The ratio of the response from gages 2, 5, and 8 to the response from gages 1, 4, and 7 led to a value of 0.31 for Poisson's ratio.

Open-Hole Specimens

Figures 15 to 18 show the load-strain behavior for the gages on specimens 4, 5, 7, and 9, respectively. The closeness of gages 1, 7, and 8 make it evident there was little bending, both through the thickness of the specimen or across the width. All gages responded linearly until failure of the specimen, indicating a brittle-type failure. All specimens failed in the net-section tension with the failure surface, on-the-whole, perpendicular to the direction of the loading. The initial failure surface was at the hole edge and did not emanate from the minimum cross section, but rather approximately 15 to 20° around the hole circumference from the minimum cross section.

Figures 19 and 20 show the responses for specimens 1 and 11, respectively. Bending was evident but again not significant. The prominent feature of these figures, however, was the large strain response from gages 10 and 11, the gages inside the holes. There was a large difference between gages 2 and 3, located at the top edges of the hole, and gages 10 and 11. Based on these differences, there appeared to be a large strain gradient at the hole edge, much larger than expected. Using the extrapolation scheme, involving the other gages on the top surface, led to an estimate for strain at the hole edge smaller than the strain as measured by gages 10 and 11. Although this estimate was better than that obtained by using gages 2 and 3 alone, it was still 50 to 60 percent low. There did not appear to be large gradients at the specimen edge, and the differences among gages 1, 7, 8, 9, and 12 were more closely related to bending effects than to strain gradients. The shear strains at the rosettes on specimens 5, 9, and 11 were insignificant, as expected, and are not shown.

Figures 21 to 26 show the load-head displacement behavior for the open-hole specimens. The nonlinearity at the low load level for each was due to slack in the various connections in the loading fixture.

Double-Lap, Double-Hole Specimens

Figures 27 to 33 indicate the load-strain responses for double-lap, double-hole specimens 1, 3, 7, 17, 18, 20, and 22, respectively. For these tests, as seen by the closeness of gages 1 and 3 and 4 and 6, the bending across the width was minimal. From the higher strains at gages 1 and 3, as

opposed to gage 2, and at 4 and 6 as opposed to 5, it is apparent the material on the centerline of the specimen was not stressed as highly in tension as the material on either side of the centerline. The tensile load apparently came into the bolt from either side of the centerline, and whatever tensile load wasn't reacted by the first bolt was transmitted to the second bolt, again on either side of the centerline. It is safe to conclude that, had gages been mounted transverse to the load axis where the axial gages were, the transverse compressive strain would have been higher on the centerline than at the outer gage locations.

The load-head displacement responses for the double-lap, double-hole specimens are illustrated in figures 34 to 40.

DISCUSSION OF RESULTS

Open-Hole Specimens

As mentioned earlier, the strain gradients near the edge of the hole were quite high. The only way to measure them appeared to be with a gage mounted circumferentially inside the hole. However, there was still the basic question of the interpretation of the response of the circumferential gages. The gages were mounted on a concave surface and, with the high strain gradients, the bond thickness of the strain adhesive could affect the results. To quantify the effects, two aluminum specimens with the exact dimensions as open-hole specimens 1 and 11 were fabricated and instrumented. The gage arrangement and specifications were identical to the composite specimens with the addition of three gages between the hole and the aluminum doubler. Figures 41 and 42 indicate the gage arrangements and the 3 additional gages, 13, 14, and 15, which were added to measure the uniformity of the strain between the hole and the aluminum doubler. Figure 43 shows these specimens.

The specimens were loaded to failure, and, based on the strain gage outputs and specimen geometry, the strain (stress) concentration factors for the two specimens were computed. These results were then compared with commonly accepted stress-concentration values for finite-width plates with circular holes. The values were obtained from reference 4. If good agreement could be obtained for the measured and commonly accepted values, then some degree of confidence could be placed in using gages inside holes to measure strain concentration factors.

Figure 44 shows the load-strain response for open-hole aluminum specimen 1. As shown by the closeness of the responses of gages 1, 7, 8, 9, and 12, there was little bending. The difference in strains from gages 10 and 11 was partly due to widthwise bending but also due to a deviation of the gages from perfect circumferential alignment. The hole in this specimen was 11.11 mm (0.438 in.) in diameter, and installing both gages properly aligned in a hole that size was difficult. It is interesting to note the strains at location 14 were lower than the strains at locations 13 and 15. This indicates the stress was not uniform across the width of the specimen. Ideally, in testing holes in this configuration, a uniform state of stress should be developed at some cross section before the hole. Whether the strain was uniform at some point between the doubler and the hole could be determined from these three measurements. If a uniform stress state is not developed, the true response of an open-hole cannot be determined. If the doubler were too close to the hole, there would be a danger of biasing the stresses around the hole.

Figure 45 shows the load-strain response for open-hole aluminum specimen 11. Bending effects were remarkably low, but again the strain was not uniform across the specimen width. In this case it is also not clear whether there were a region between the hole and doubler where the tensile stress was uniform across the width.

The stress concentration factor for the aluminum specimens could be computed from the strain data. Since aluminum is homogeneous and isotropic, strain concentration factors and stress concentration factors are identical. This is not so for composites, however. Table 1 gives the pertinent data for computing the stress concentration factor, based on the gross stress, for specimen 1. The value was calculated to be 3.25. The gross area of the specimen was 195 mm^2 (0.302 in.^2), while the net area was 146 mm^2 (0.227 in.^2). Similarly, table 2 presents the pertinent data for computing the stress concentration factors for specimen 11. Based on the gross area of 548 mm^2 (0.850 in.^2), the stress concentration factor was 3.15. Using the net area at 480 mm^2 (0.774 in.^2), the stress concentration factor was 2.75. All the strain concentration figures are based on a maximum strain level less than 0.2 percent. Figures 46 and 47 show the load-head displacement relations for the two specimens.

Since extrapolation of strain data to the edge of the hole was inaccurate, only those composite specimens gaged inside the hole could be used to determine strain concentration factors. Thus only data from open-hole specimens 1 and 11 were useful for this purpose. These two specimens, unlike their aluminum counterparts, did not have a row of gages between the hole and the doubler to measure the gross strain. The value of E , determined from testing double-lap, single-hole specimen 11, in combination with the applied axial load and the cross-sectional area, were used to compute gross strain. This computed value of gross strain was then used to determine the strain concentration factors. Table 3 illustrates the data for specimen 1 while table 4 presents similar information for specimen 11. The gross strain concentration factor for specimen 1 was computed to be 3.95. The net area for specimen 1 was 152 mm^2 (0.235 in.^2) and the gross area was 202 mm^2 (0.3131 in.^2), resulting in a net strain concentration factor of 2.96. For specimen 11, the strain concentration factor based on gross area was 3.32. The net area of the specimen was 451 mm^2 (0.699 in.^2), and the gross area was 575 mm^2 (0.799 in.^2). Thus the net strain concentration factor for specimen 11 was 2.90.

Figure 48 indicates how these values of strain concentration factors agree with commonly accepted values for homogeneous isotropic materials taken from reference 4. The figure indicates the concentration factor as a function of the ratio of the hole diameter to specimen width. Indicated on the figure are the values for the aluminum and the composite material specimens. The aluminum should match the accepted values, except the data used to generate the solid curve came from a variety of sources and experimental methods. Thus there is expected to be some scatter band associated with the data, and knowing this bandwidth would be useful. Based on the figure, the measurements from the aluminum appear conservative. It should be mentioned that misalignment of the strain gage inside the hole would cause the strain gage to register low. It is felt any conservatism in the strain readings of the aluminum was also reflected in measurements in the composite specimens. For the aluminum specimen, the smaller the gage, the more accurate was the strain measurement. However, for the composite material, the strain gage must be of a certain size to cover a sufficient area so the effects of matrix and fibers are averaged or smeared. Also, the gage widths were chosen to match the specimen thickness, and this dictated the gage length for off-the-shelf gages. It is safe to say, however, based on the data, that the strain concentration

factors for the quasi-isotropic specimens were higher than for the identical aluminum specimen, and it is most likely safe to generalize that statement for all values of W/D .

Double-Lap, Double-Hole Specimens

One of the basic issues which could be studied with the strain measurements from the double-lap, double-hole specimens was the amount of load transferred past the first bolt to be reacted by the second bolt. Also the question of uniformity of the strain across the specimen, particularly before the first bolt, could be investigated. The former issue, coupled with information on the increase in load-carrying capacity due to the addition of a second bolt, over and above the single-bolt configuration, could be useful in joint design.

One measure of uniformity of strain across the specimen is the ratio of the strain from the center gage to the average of the strain from the two outer gages. Such a ratio is plotted in figures 49 and 50 as a function of W/D and percent ultimate load. Figure 49 shows this ratio for the row of gages between the doubler and the first bolt while figure 50 indicates the ratio for the row of gages between the two bolts. A uniform strain across the joint would result in this ratio being unity. One joint tested had a W/D of 2.35 due to a mis-drilled hole; two joints had $W/D = 4$; two had $W/D = 6$; and two had $W/D = 8$. The figures are shown with data plotted to either side of $W/D = 4, 6$, and 8 to avoid clutter in order to illustrate the trend with percent ultimate load as well as the scatter in the data. The specimen plotted just to the left of $W/D = 8$, and having the values of the ratio less than unity, failed in the doubler. Thus the load distribution between the doubler and the first bolt for this specimen might not be typical.

Between the doubler and the first bolt, the strain ratio was generally different than unity. However, for all specimens with $W/D = 4$ and 6 , the ratio was not too different than one. For these specimens, the first setup was apparently close to an ideal situation of uniform stress before the first bolt. For the large-hole specimen ($W/D = 2.35$) and the specimen with the doubler failure, a uniform state of stress had not been developed. For the ratios between the doubler and the first bolt, there was no overwhelming trend as to how the uniformity varied with load, although the ratio generally increased with load. This indicates a redistribution of stresses with load

level, a nonlinear effect. Between the bolts, the strain ratio was quite different than unity and the ratio definitely increased with load level.

One measure of load transfer past the first bolt was the ratio of strain behind the first bolt to strain ahead of it. More specifically, for the situation at hand, the strain level between the doubler and the first bolt was compared with the strain level between the two bolts. The average of the strains from the two outer gages before the first bolt was compared with the average of the strains from the two outer gages behind the bolt. This was accomplished by forming the ratio of the strains after the first bolt to the strains before the first bolt. Likewise, the strains from the middle gages were ratioed. Figure 57 shows the ratio for the outer gages, using W/D and load level as parameters, and figure 52 shows similar information for the centerline gages. There did not appear to be a definite trend with W/D, but in general the ratio decreased slightly for increasing load. The average of all ratios was 0.42. The numbers presented here are based on measurements of one to three hole diameters from the hole. It would be wrong, for example, to assume the peak stress at the second hole was only 42 percent of the peak stress at the lead hole. This information would be very useful, but these strain ratios can only give a rough indication of the strain distribution. A complete picture of the strain in a bolted joint would require a different technique, such as a photoelastic model, birefringent coatings or interferometry.

CONCLUDING REMARKS

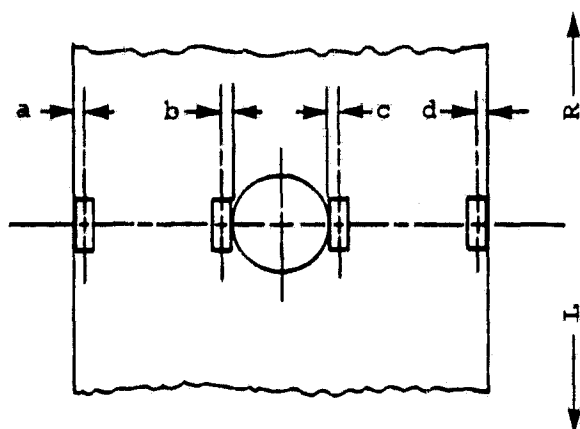
In summary, installation of strain gages on the bolted joint specimens has provided some useful information. First, it appears that if strain gages are to be used to determine strain concentration factors, the only way to accurately determine the strain at a hole edge is to install a gage circumferentially inside the hole. The strain gradients are too steep to measure accurately the hole-edge strains by using a gage on the upper surface or by extrapolating strain data from a series of gages along a radius away from the hole. Second, based on the results from the strain-gaged aluminum specimens, strain concentration calculations based on data from a circumferentially installed gage may be slightly conservative but certainly give legitimate design numbers. Third, for identical geometries, quasi-isotropic layups produce higher strain concentration values than isotropic materials,

indicating the nonisotropy affects the results to a degree. Underlying all this is the possibility that, in an effort to conserve material, specimens may be made too short to allow a uniform state of stress to develop between the load introduction and the test hole.

For the double-lap, double-hole specimens, it appears that roughly 42 percent of the load passes the first bolt to be reacted by the second bolt. Any comments regarding the value of peak stress at the lead hole compared to the value of stress at the second hole would be erroneously using global strain measurements to predict local behavior. The nonuniformity of the strain across the specimens was no doubt a function of the distance between the doubler and the lead bolt and the distance between the two bolts. The strain could be made uniform by simply making the specimen longer. A more important issue is how close the second bolt can be put to the lead bolt before the load-carrying performance of both bolts is degraded.

APPENDIX A

LOCATION OF GAGES ON COMPOSITE OPEN-HOLE SPECIMENS



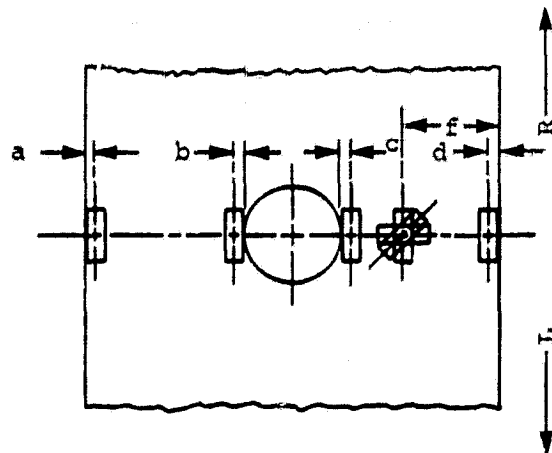
e same as d but for
gage on back

distances measured to
centerline scribe-
marks on gages

Specimen		<u>a</u>	<u>b</u>	<u>c</u>	<u>d</u>	<u>e</u>
OH-1	mm	1.191	1.389	1.389	1.191	1.191
	in.	0.0469	0.0547	0.0547	0.0469	0.0469
OH-4	mm	3.175	1.389	1.389	3.175	3.175
	in.	0.1250	0.0547	0.0547	0.1250	0.1250
OH-7	mm	1.389	3.373	1.389	3.373	3.967
	in.	0.0547	0.1328	0.0547	0.1328	0.1562

(cont'd)

APPENDIX A (CONCL'D)



e same as d but for
gage on back

distances measured to
centerline scribe-
marks on gages

Specimen		<u>a</u>	<u>b</u>	<u>c</u>	<u>d</u>	<u>e</u>	<u>f</u>
OH-5	mm	1.191	3.373	1.191	3.373	3.373	5.755
	in.	0.0469	0.1328	0.0469	0.1328	0.1328	0.2266
OH-9	mm	1.389	3.175	1.389	3.373	3.373	8.334
	in.	0.0547	0.1250	0.0547	0.1328	0.1328	0.3281
OH-11	mm	1.588	3.373	1.588	3.373	3.373	5.755
	in.	0.0625	0.1328	0.0625	0.1328	0.1328	0.2266

APPENDIX B

STRAIN GAGE SPECIFICATIONS FOR COMPOSITE OPEN-HOLE SPECIMENS

Specimen Number	Gage Location	Gage Type ²	Gage Factor
4, 5, 7 and 9 ¹	1, 7, 8	CEA-06-125UW-350	2.14 ± 0.5%
	2, 3	EA-06-062AQ-350	2.075 ± 0.5%
	4, 5, 6 ³	WK-06-060WR-350	2.10 ± 1.0%
1	1, 7, 8	EA-06-062AQ-350	2.075 ± 0.5%
	2, 3	EA-06-062AQ-350	2.075 ± 0.5%
	9, 12	EA-06-090DH-350	2.13 ± 0.5%
	10, 11	EA-06-090DH-350	2.13 ± 0.5%
11	1, 7, 8	CEA-06-125UW-350	2.14 ± 0.5%
	2, 3	EA-06-062AQ-350	2.075 ± 0.5%
	4, 5, 6	WK-06-060WR-350	2.10 ± 1.0%
	9, 12	EA-06-125AC-350	2.115 ± 0.5%
	10, 11	EA-06-125AC-350	2.115 ± 0.5%

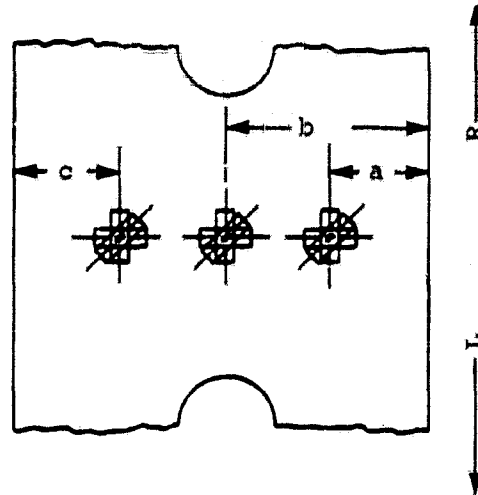
¹ See figures 5, 6, 7, and 8.

² Micro-Measurement designation.

³ Rosettes on specimens 5 and 9 only.

APPENDIX C

LOCATION OF STRAIN GAGES ON DOUBLE-LAP, SINGLE-HOLE SPECIMEN 11



distances measured to
centerline scribe-
marks on gage

Units	Dimension		
	a	b	c
mm	24.21	48.81	24.21
in.	0.9531	1.9218	0.9531

APPENDIX D

STRAIN GAGE SPECIFICATION FOR DOUBLE-LAP,
SINGLE-HOLE SPECIMEN 11

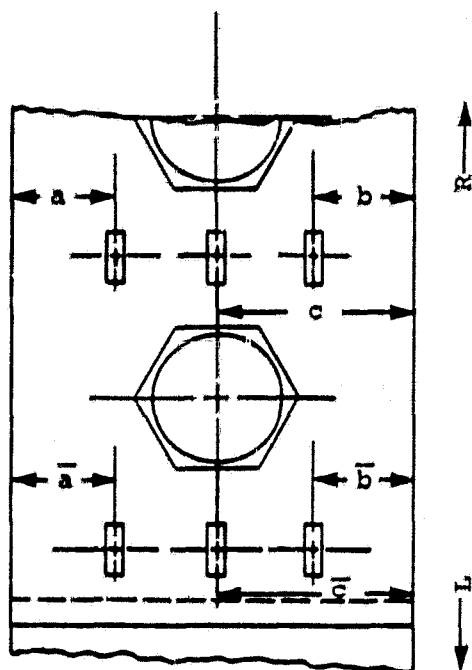
<u>Gage Location¹</u>	<u>Gage Type²</u>	<u>Gage Factor</u>
1-2-3, 4-5-6, 7-8-9	WA-06-250WR-350	2.12 ± 1.0%

¹ See figure 9.

² Micro-Measurements designation.

APPENDIX E

LOCATION OF STRAIN GAGES ON DOUBLE LAP, DOUBLE HOLE SPECIMENS



distances measured to
centerline scribe-
marks on gages

Specimen Number		<u>a</u>	<u>a</u> ⁻	<u>b</u>	<u>b</u> ⁻	<u>c</u>	<u>c</u> ⁻
DLDH-1	mm	11.11	10.91	10.91	10.72	22.03	22.42
	in.	0.4375	0.4297	0.4297	0.4219	0.8672	0.8828
DLDH-3	mm	17.07	16.67	16.67	16.87	32.94	32.94
	in.	0.6719	0.6562	0.6562	0.6641	1.2969	1.2734
DLDH-7	mm	22.03	22.03	22.42	22.03	44.65	44.65
	in.	0.8672	0.8672	0.8828	0.8672	1.7578	1.7578
DLDH-17	mm	10.91	12.10	10.52	10.12	22.22	23.02
	in.	0.4297	0.4766	0.4141	0.3984	0.8750	0.9062
DLDH-18	mm	12.30	12.10	9.921	9.723	23.22	22.82
	in.	0.4844	0.4766	0.3906	0.3828	0.9141	0.8984
DLDH-20	mm	16.73	15.68 ¹	16.87	17.07	32.94	32.94
	in.	0.6328	0.6172	0.6641	0.6719	1.2969	1.2969
DLDH-22	mm	21.43	21.63	22.22	21.63	44.25	44.45
	in.	0.8438	0.8516	0.8750	0.8516	1.7422	1.7500

¹ Center of 0-45-90 rosette.

APPENDIX F

STRAIN GAGE SPECIFICATIONS FOR DOUBLE-LAP, DOUBLE HOLE SPECIMENS

<u>Specimen Number</u>	<u>Gage Location</u>	<u>Gage Type²</u>	<u>Gage Factor</u>
1, 3, 7, 17, 18 and 22 ¹	1, 2, 3, 4, 5, 6	CEA-06-250UW-350	2.125 ± 0.5%
20 ¹	1, 2, 3, 4, 5, 6	CEA-06-250UW-350	2.125 ± 0.5%
		WA-06-060WR-350	2.10 ± 1.5%

¹ See figure 10.

² Micro-Measurement gage designation.

REFERENCES

1. Hyer, M.W.; and Lightfoot, M.C.: Composite Bolted-Joint Specimens: Experimental Results. NASA CR-158964, 1978.
2. Hyer, M.W.; and Lightfoot, M.C.: Ultimate Strength of High-Load-Capacity Composite Bolted Joints. 5th ASTM Conference on Composite Materials: Testing and Design, March 1978.
3. Daniel, I.M.; Rowlands, R.E.; and Whiteside, J.B.: Effects of Material and Stacking Sequence on Behavior of Composite Plates with Holes. Experimental Mech., Vol. 14, No. 1, Jan. 1974, pp. 1-9.
4. Peterson, R.E.: Stress Concentration Factors. John Wiley and Sons (New York), 1974, p. 150.

Table 1. Strain concentration data for aluminum open-hole specimen 1
(strain values, e , in microstrain).

N	Load		e_{13}	e_{14}	e_{15}	e_{10}	e_{11}	e_{gross}	e_{hole}	K_{gross}
		lb								
2170	486		171	139	171	531	481	160	506	3.16
3505	788		284	237	288	858	775	270	816	3.02
8304	1867		553	464	581	1991	1812	533	1901	3.57

Avg = 3.25

$$e_{\text{gross}} = \frac{e_{13} + e_{14} + e_{15}}{3}$$

$$e_{\text{hole}} = \frac{e_{10} + e_{11}}{2}$$

$$K_{\text{gross}} = \frac{e_{\text{hole}}}{e_{\text{gross}}}$$

Table 2. Strain concentration data for aluminum open-hole specimen 11
(strain values, e , microstrain).

N	Load		e_{13}	e_{14}	e_{15}	e_{10}	e_{11}	e_{gross}	e_{hole}	K_{gross}
		lb								
8540	1920		224	214	236	719	722	225	720	3.20
12491	2808		336	326	342	1042	1045	335	1044	3.12
24946	5608		690	643	678	2090	2097	670	2094	3.12

Avg = 3.15

$$e_{\text{gross}} = \frac{e_{13} + e_{14} + e_{15}}{3}$$

$$e_{\text{hole}} = \frac{e_{10} + e_{11}}{2}$$

$$K_{\text{gross}} = \frac{e_{\text{hole}}}{e_{\text{gross}}}$$

Table 3. Strain concentration data for composite open-hole specimen 1
(strain values, e , in microstrain).

Load	N	lb	e_{10}	e_{11}	e_{gross}	e_{hole}	K_{gross}
9510		2138	3192	3365	837	3278	3.92
19246		4327	6473	6723	1694	6598	3.89
28774		6496	9991	10197	2542	10094	3.97
38480		8651	13653	13721	3386	13687	4.04

Avg = 3.95

$$E = 56.26 \text{ MPa } (8.16 \times 10^6 \text{ psi})$$

$$e_{\text{gross}} = \frac{\text{Load}}{EA_{\text{gross}}}$$

$$A_{\text{gross}} = 2.02 \times 10^{-4} \text{ m}^2 (0.3131 \text{ in.}^2)$$

$$e_{\text{hole}} = \frac{e_{10} + e_{11}}{2}$$

$$K_{\text{gross}} = \frac{e_{\text{hole}}}{e_{\text{gross}}}$$

Table 4. Strain concentration data for composite open hole, specimen 11
(strain values, e , in microstrain).

N	Load		e_{10}	e_{11}	e_{gross}	e_{hole}	K_{gross}
		lb					
24020		5400	2786	2742	828	2764	3.34
47200		10610	5384	5362	1628	5373	3.30
73700		16570	8413	8485	2542	8449	3.32
97500		21920	11089	11288	3363	11188	3.33
E = 56.26 MPa (8.16×10^6 psi)							Avg = 3.32

$$e_{gross} = \frac{\text{Load}}{EA_{gross}}$$

$$A_{gross} = 5.154 \times 10^{-4} \text{ m}^2 \text{ (0.7988 in.}^2\text{)}$$

$$e_{hole} = \frac{e_{10} + e_{11}}{2}$$

$$K_{gross} = \frac{e_{hole}}{e_{gross}}$$

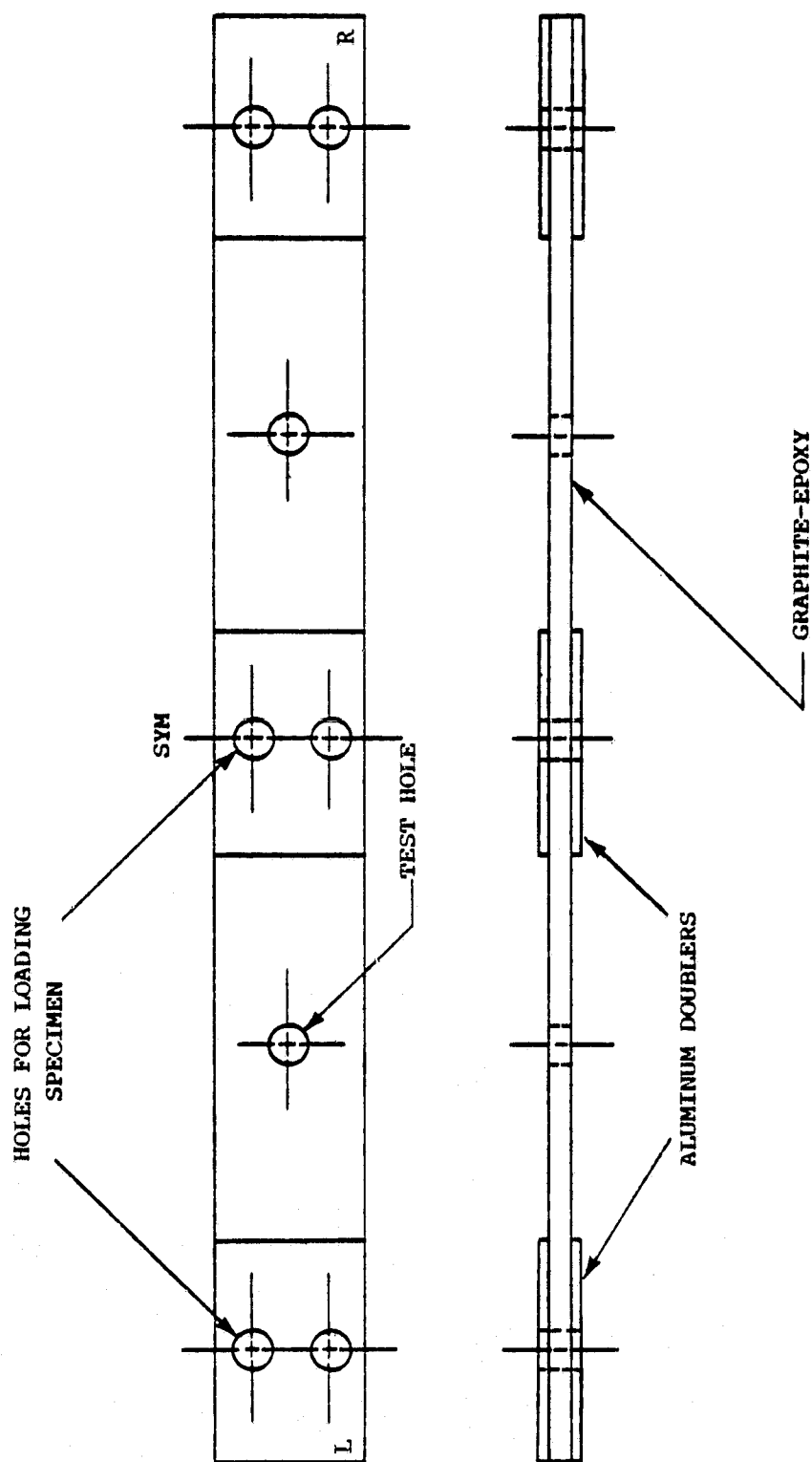


Figure 1. Specimens for open-hole tests.

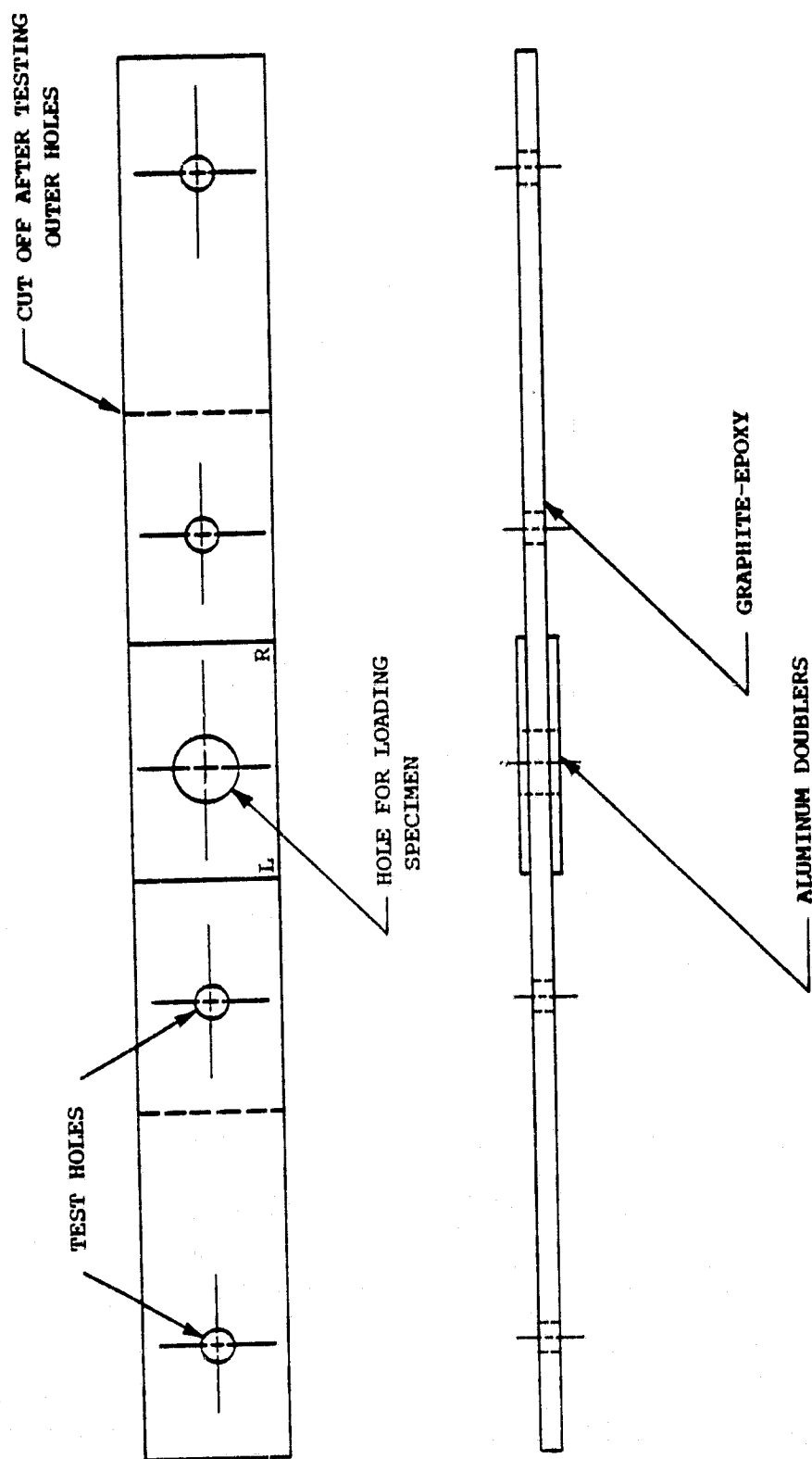


Figure 2. Specimens for double-lap, single-hole tests.

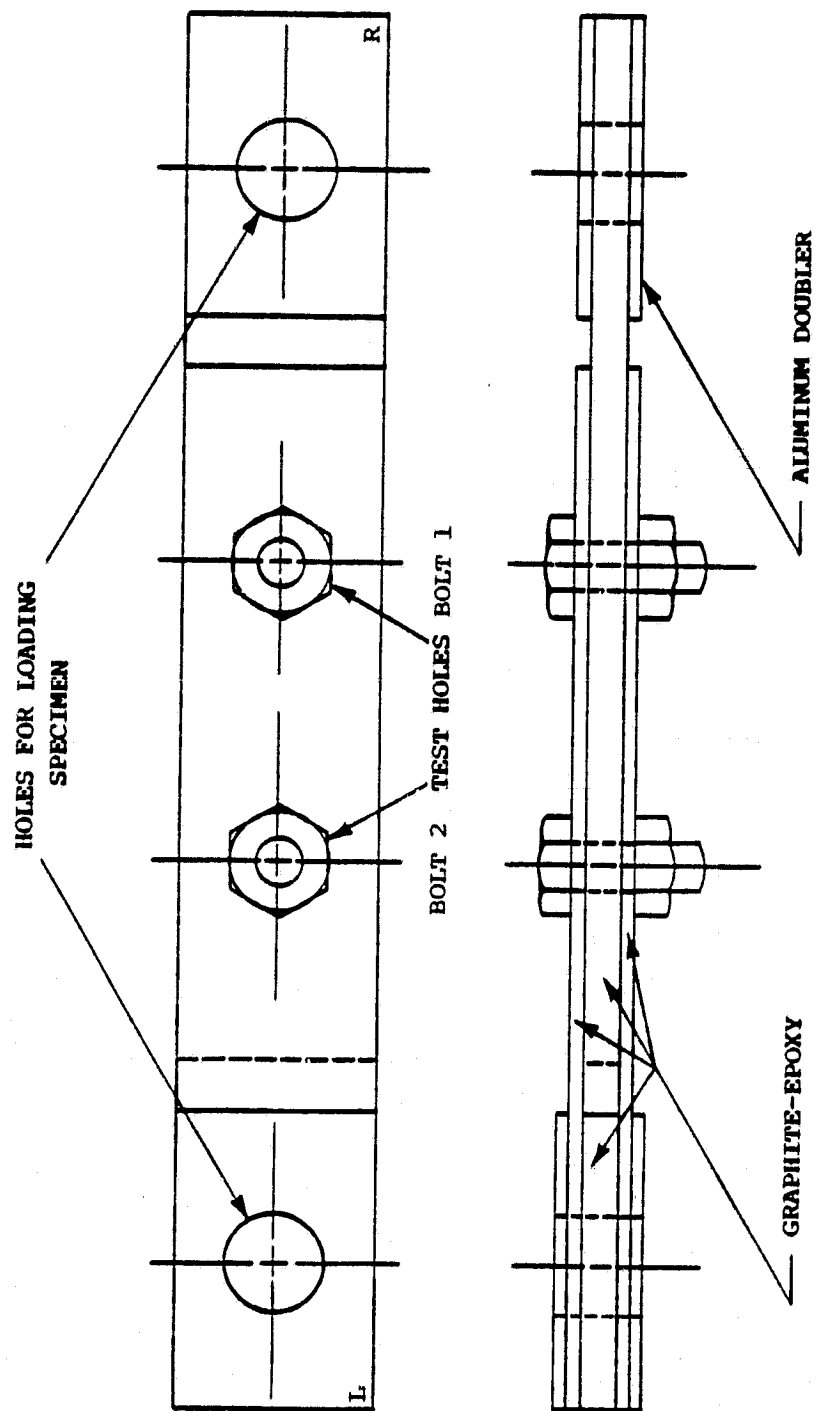


Figure 3. Specimens for double-lap, double-hole tests.

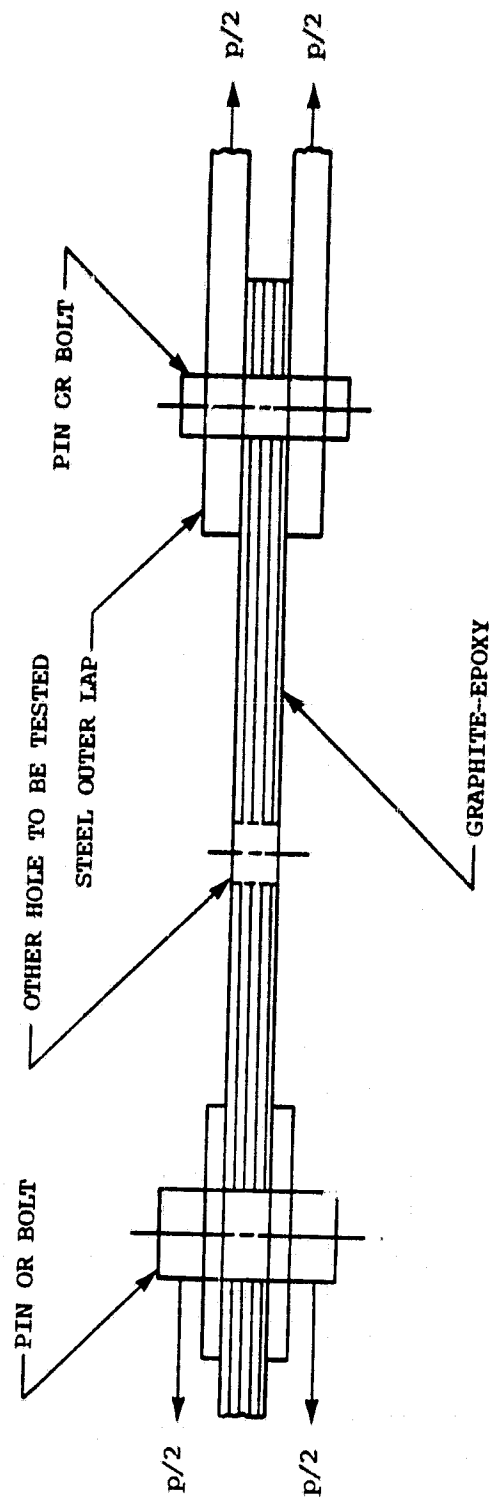


Figure 4. Double-lap, single-hole test setup.

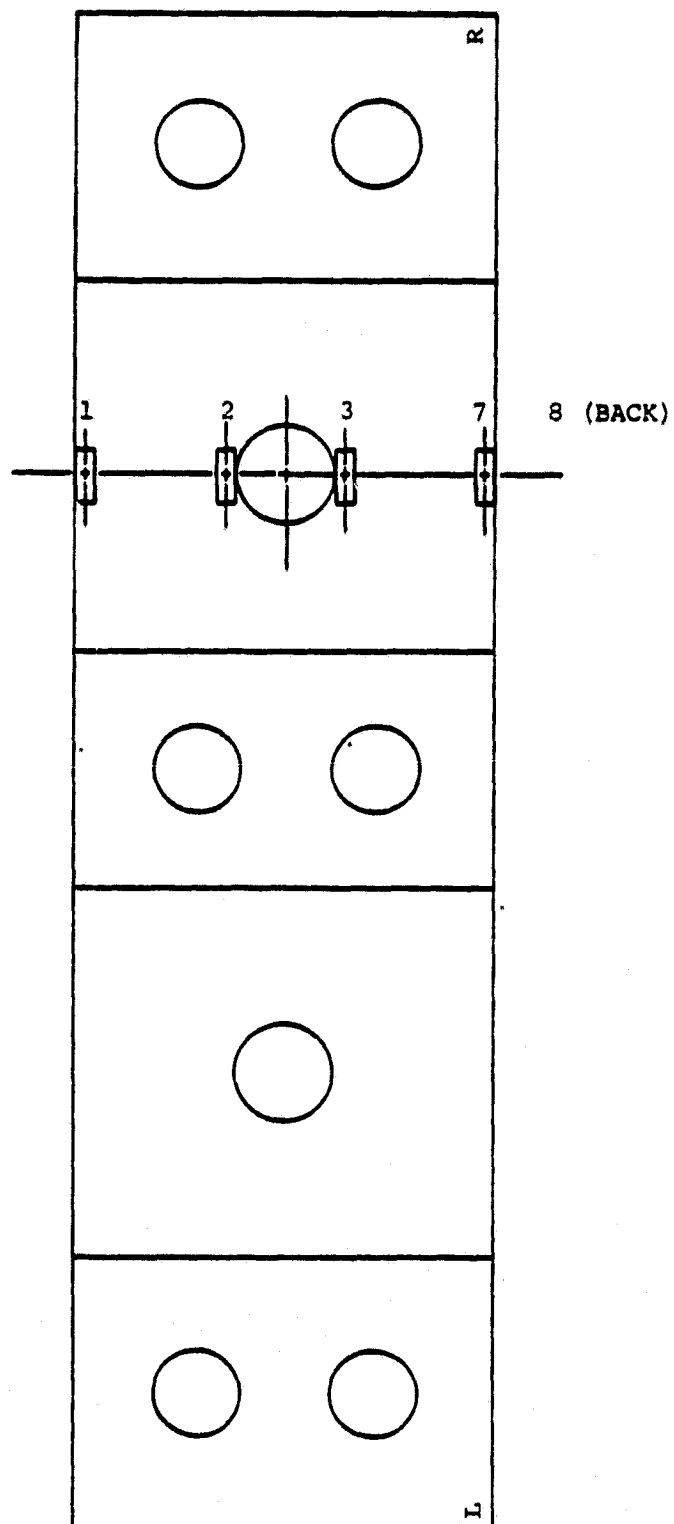


Figure 5. Strain gage locations for open-hole specimens 4 and 7.

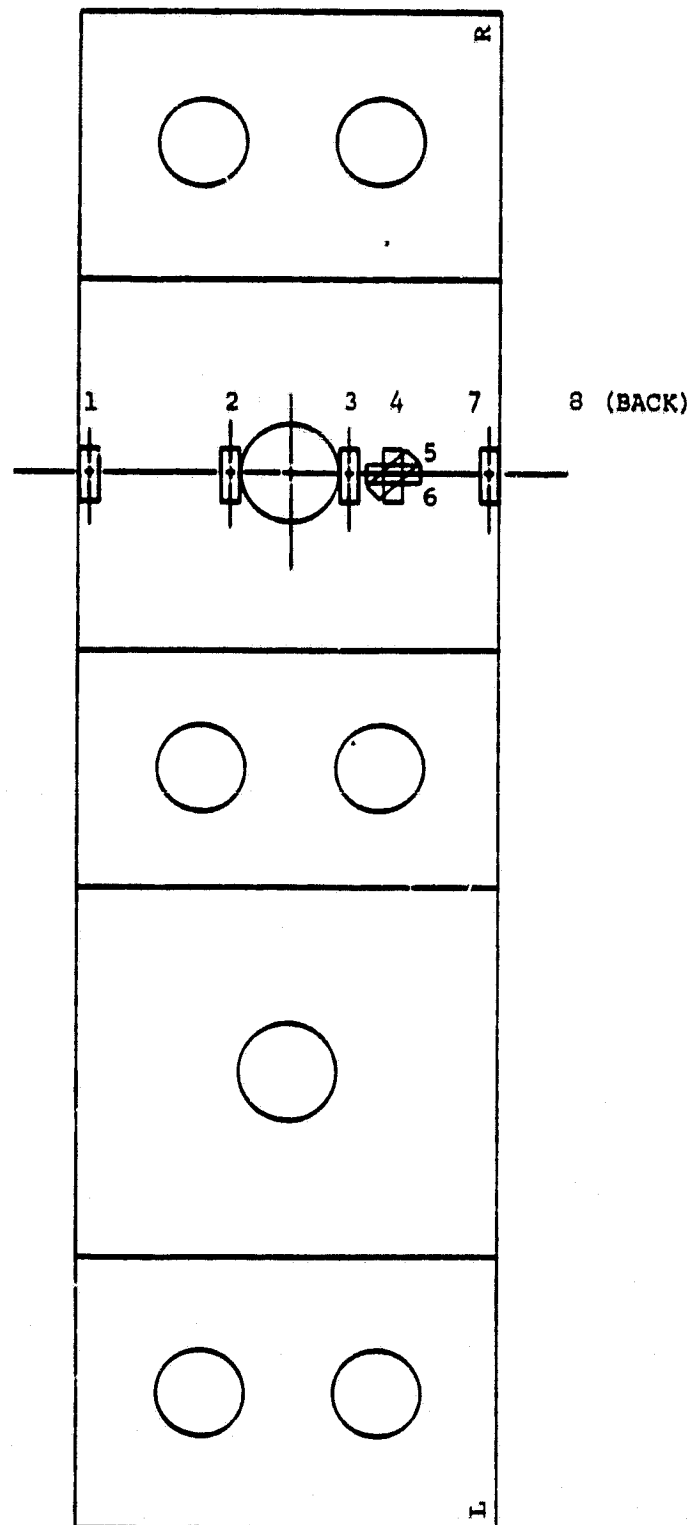


Figure 6. Strain gage locations for open-hole specimens 5 and 9.

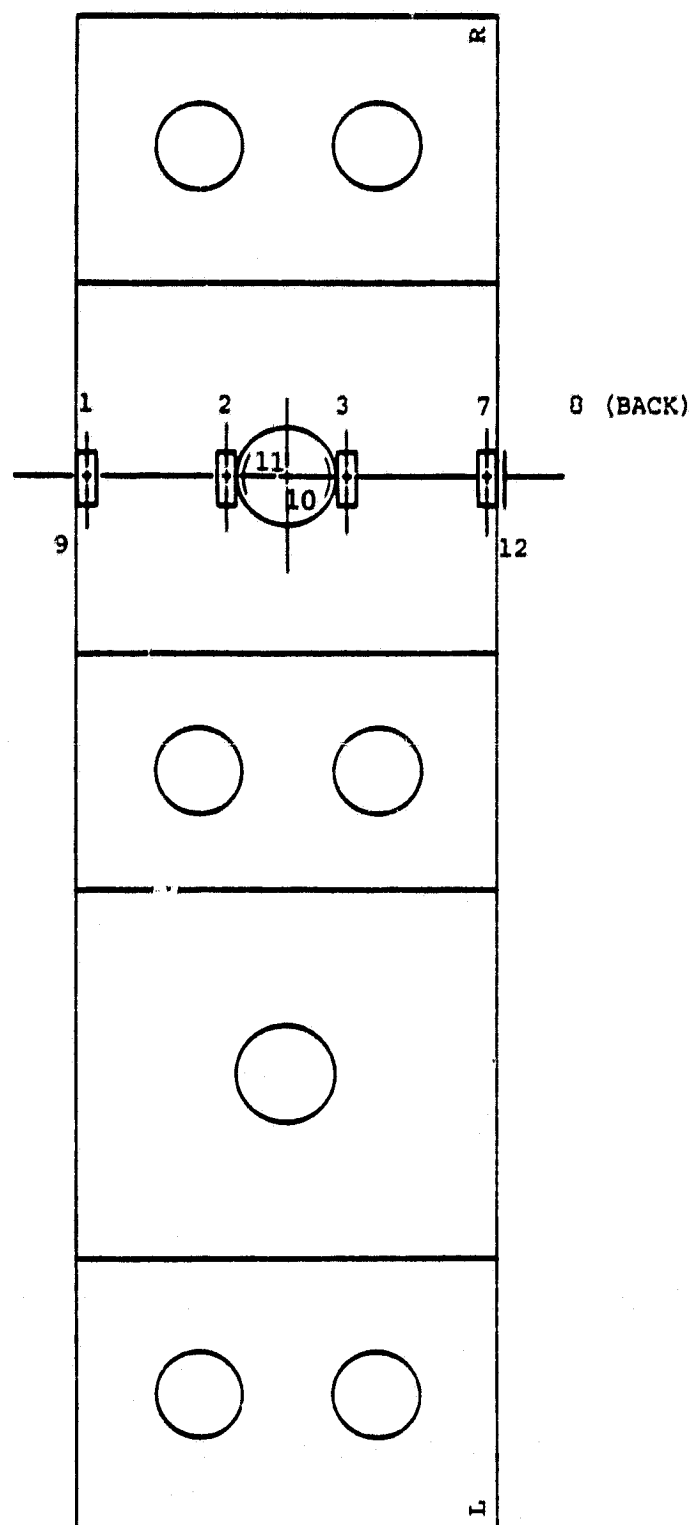


Figure 7. Strain gage locations for open-hole specimen 1.

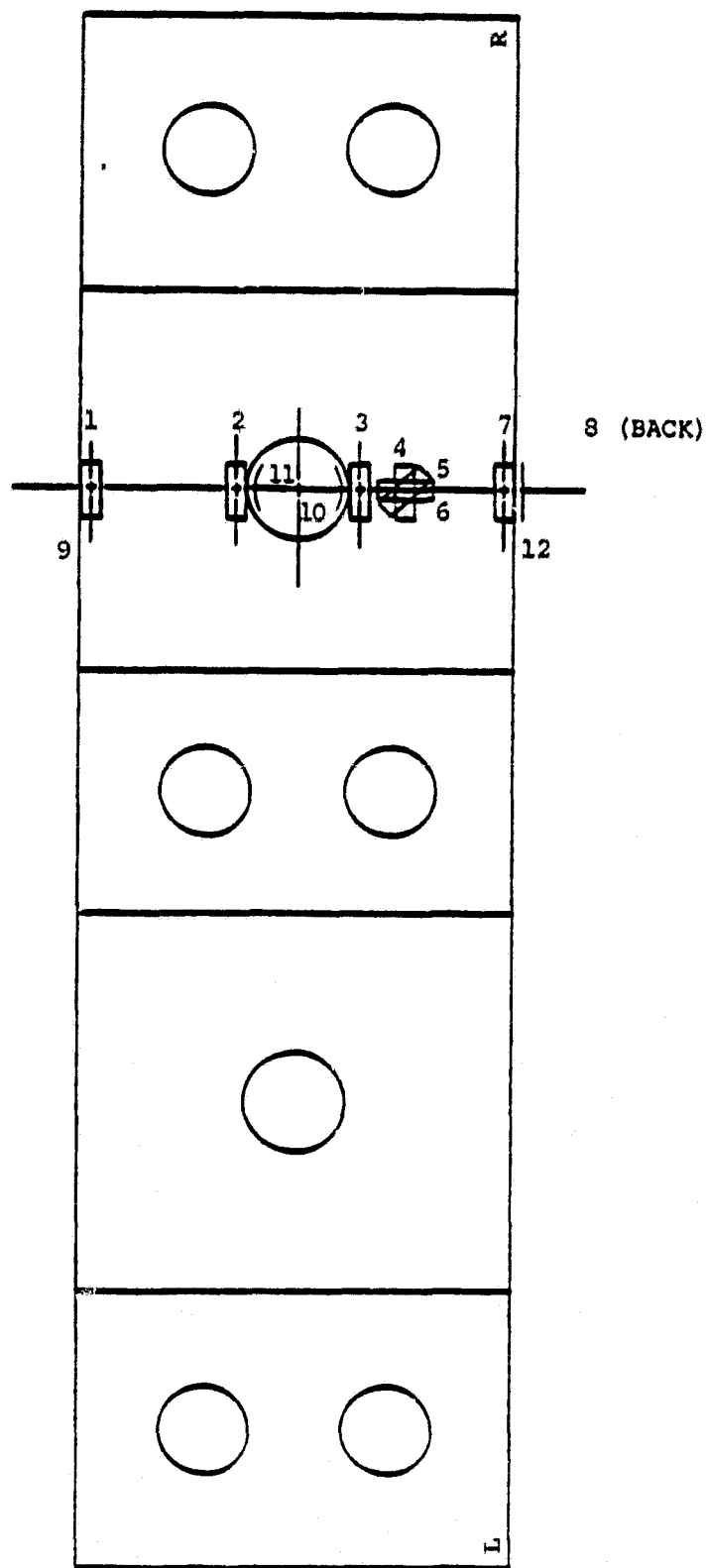
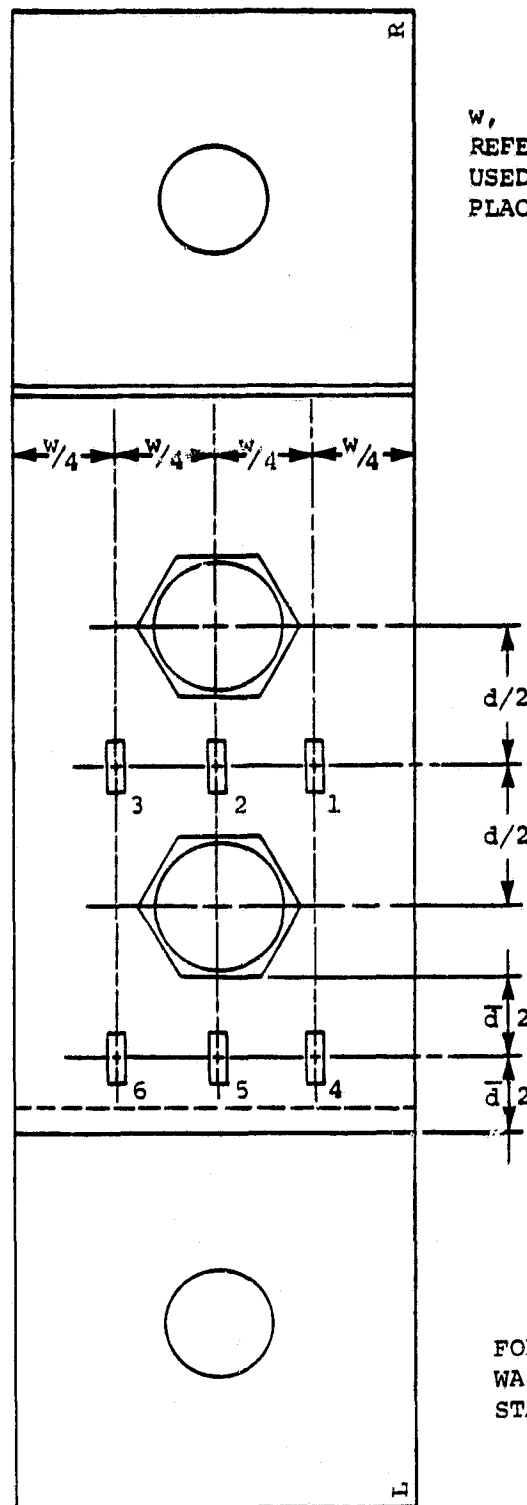


Figure 8. Strain gage location for open-hole specimen 11.



w , d , AND \bar{d} ARE IDENTIFIED IN REFERENCE 1, BUT THE NOTATION IS USED HERE TO INDICATE THE SYMMETRIC PLACEMENT OF THE GAGES

FOR SPECIMEN 20, GAGE 6 WAS REPLACED WITH A STACKED ROSETTE

Figure 10. Strain gage locations for double-lap, double-hole specimens.

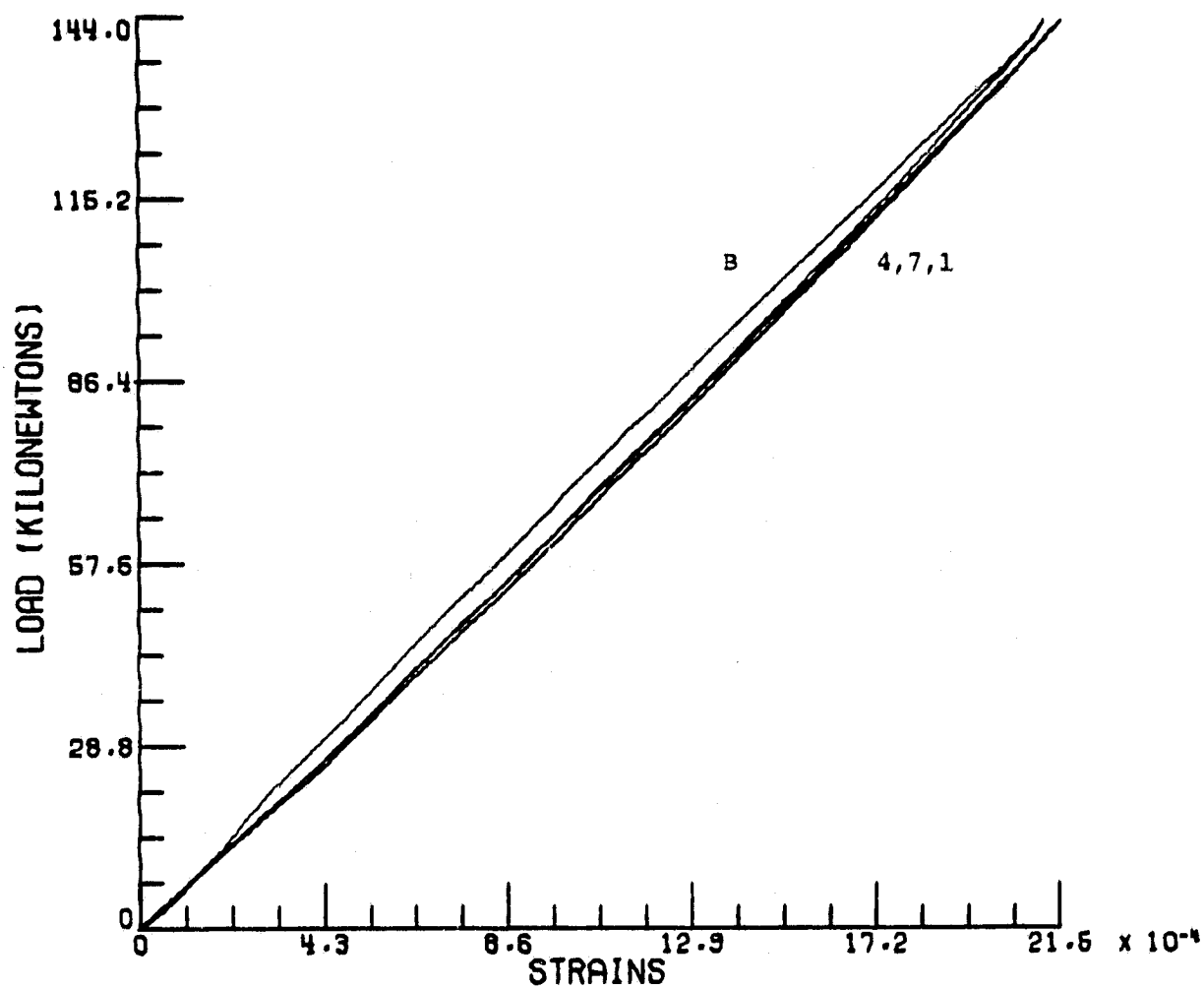


Figure 11. Load-strain responses for double-lap, single-hole specimen 11, axial gages.

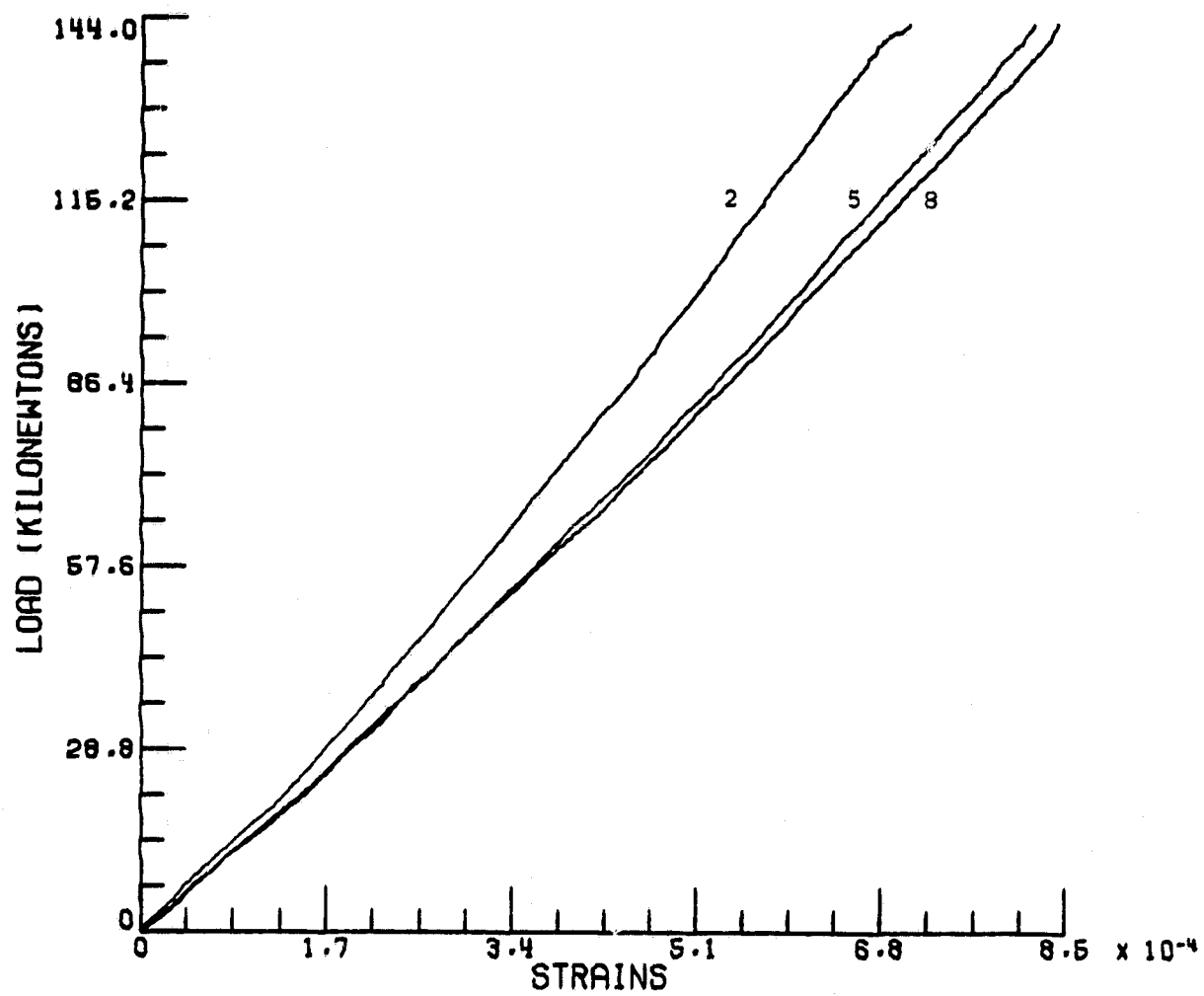


Figure 12. Load-strain responses for double-lap, single-hole specimen 11, lateral gages.

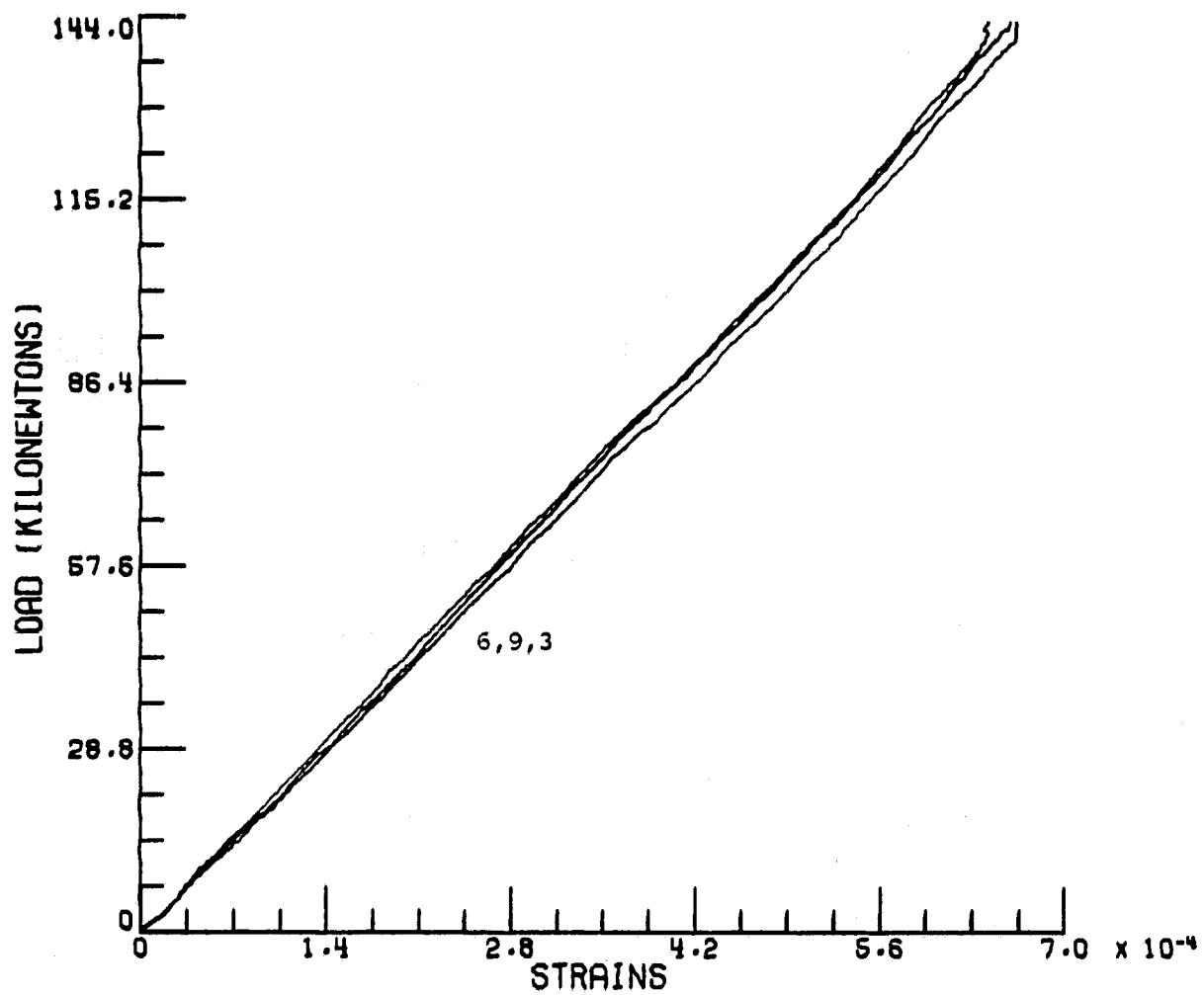


Figure 13. Load-strain responses for double-lap, single-hole specimen 11, 45° gages.

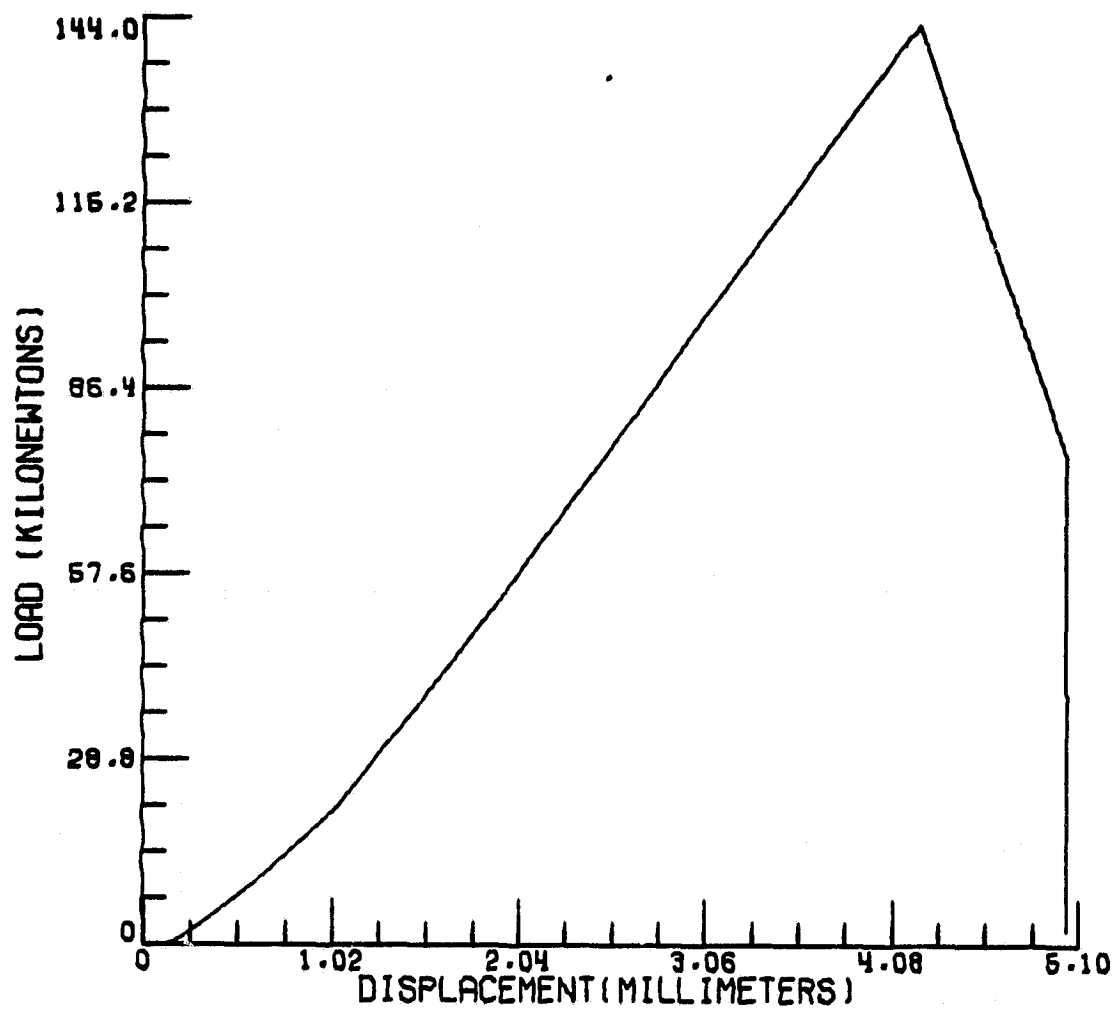


Figure 14. Load-head displacement for double-lap, single-hole specimen 11.

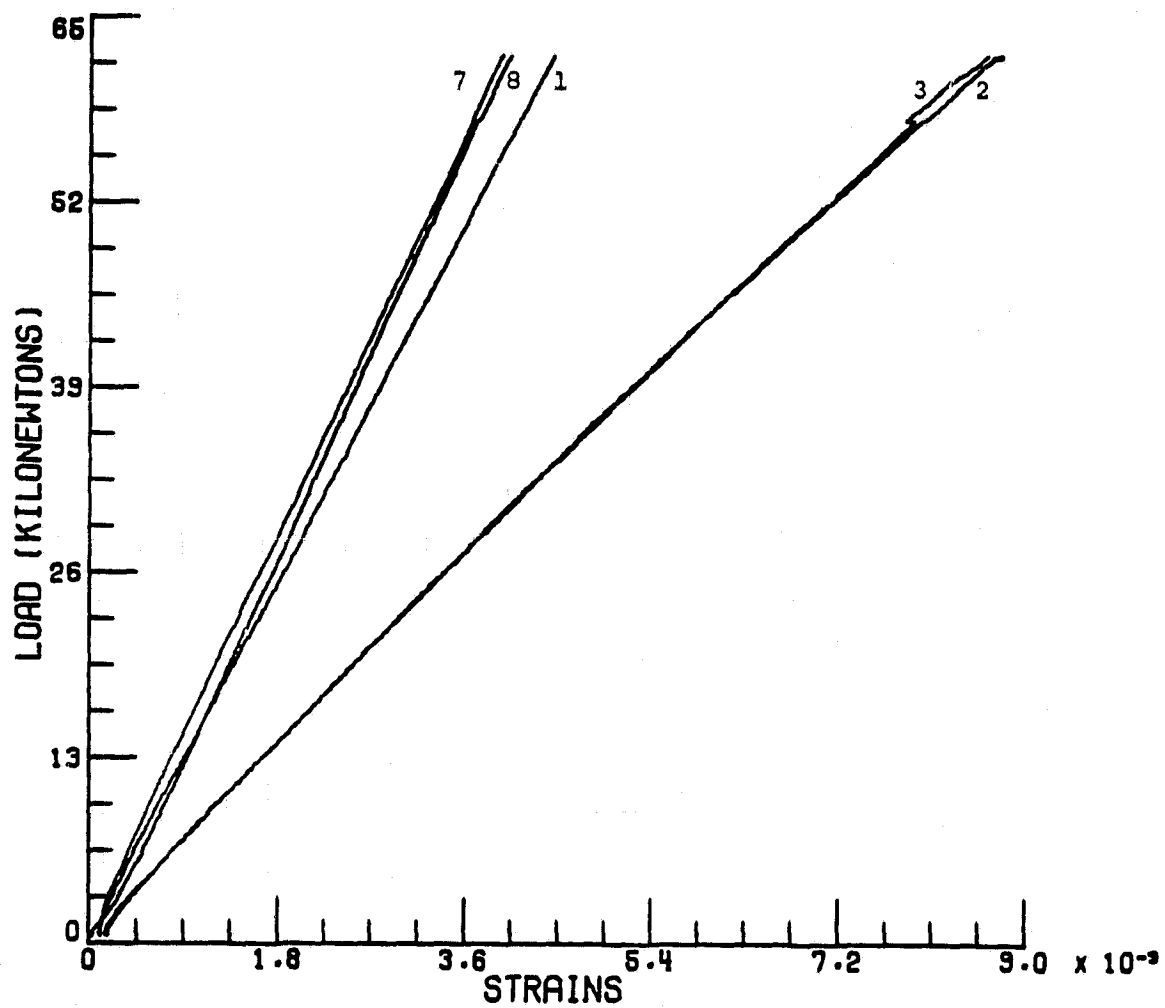


Figure 15. Load-strain responses for open-hole specimen 4.

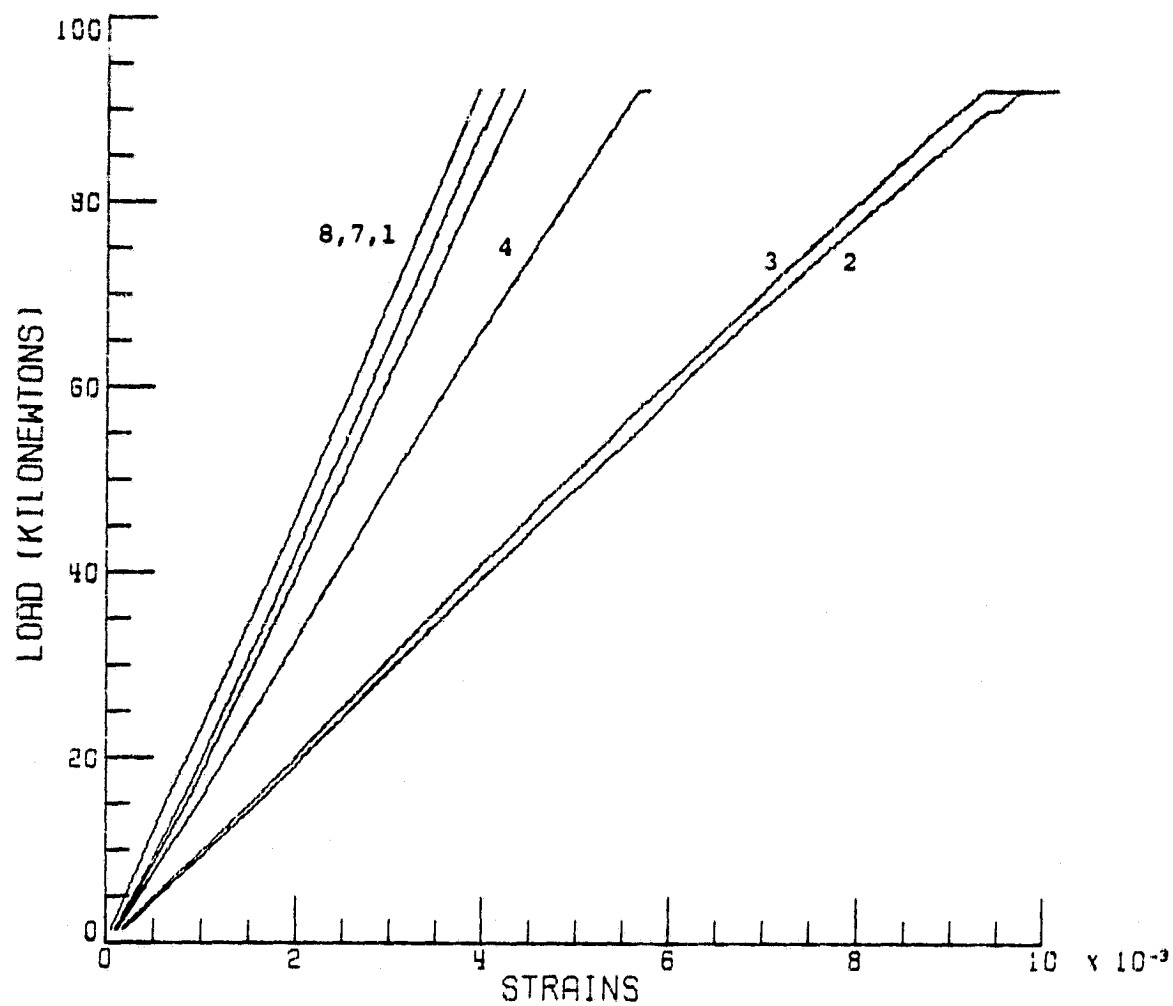


Figure 16. Load-strain responses for open-hole specimen 5.

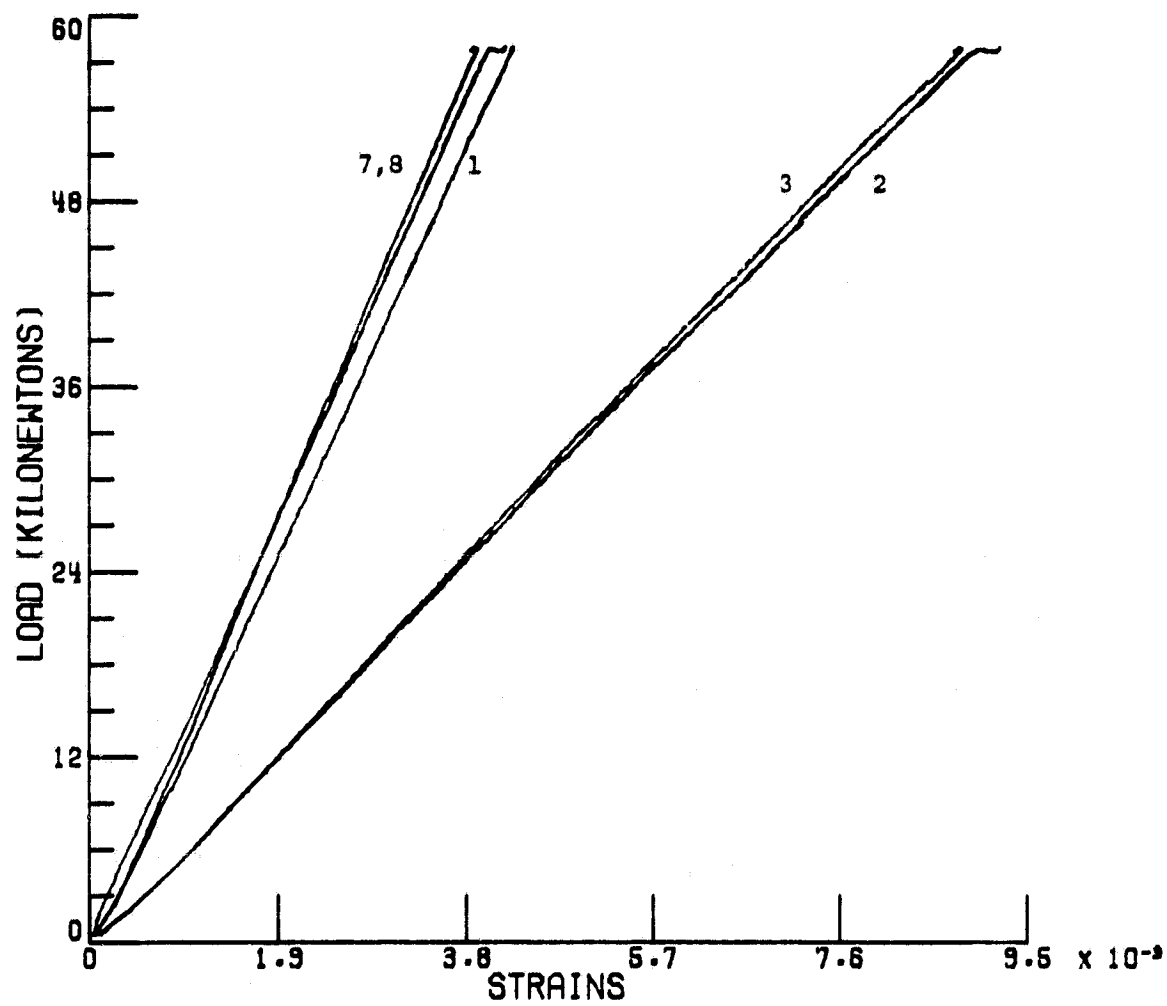


Figure 17. Load-strain responses for open-hole specimen 7.

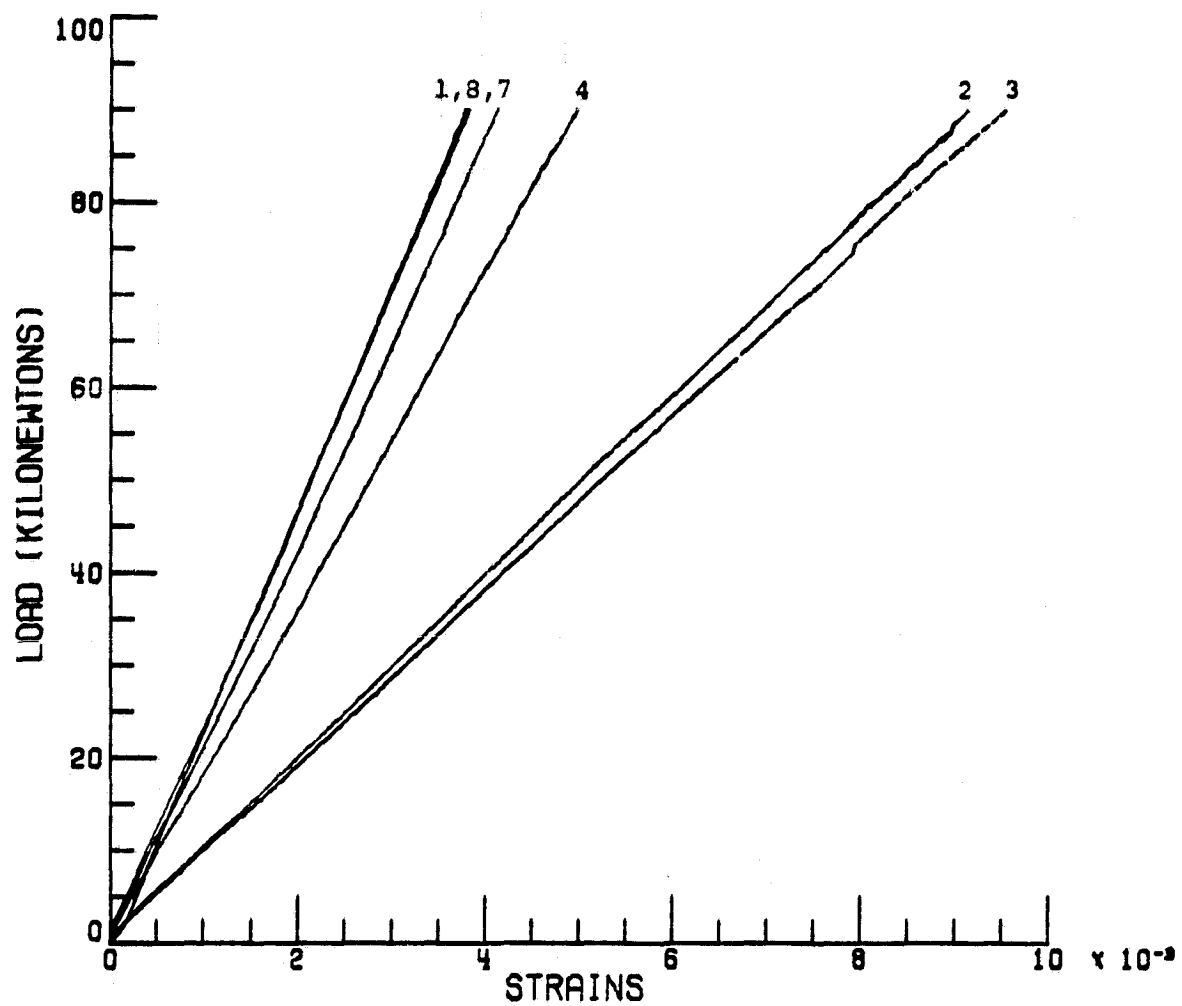


Figure 18. Load-strain responses for open-hole specimen 9.

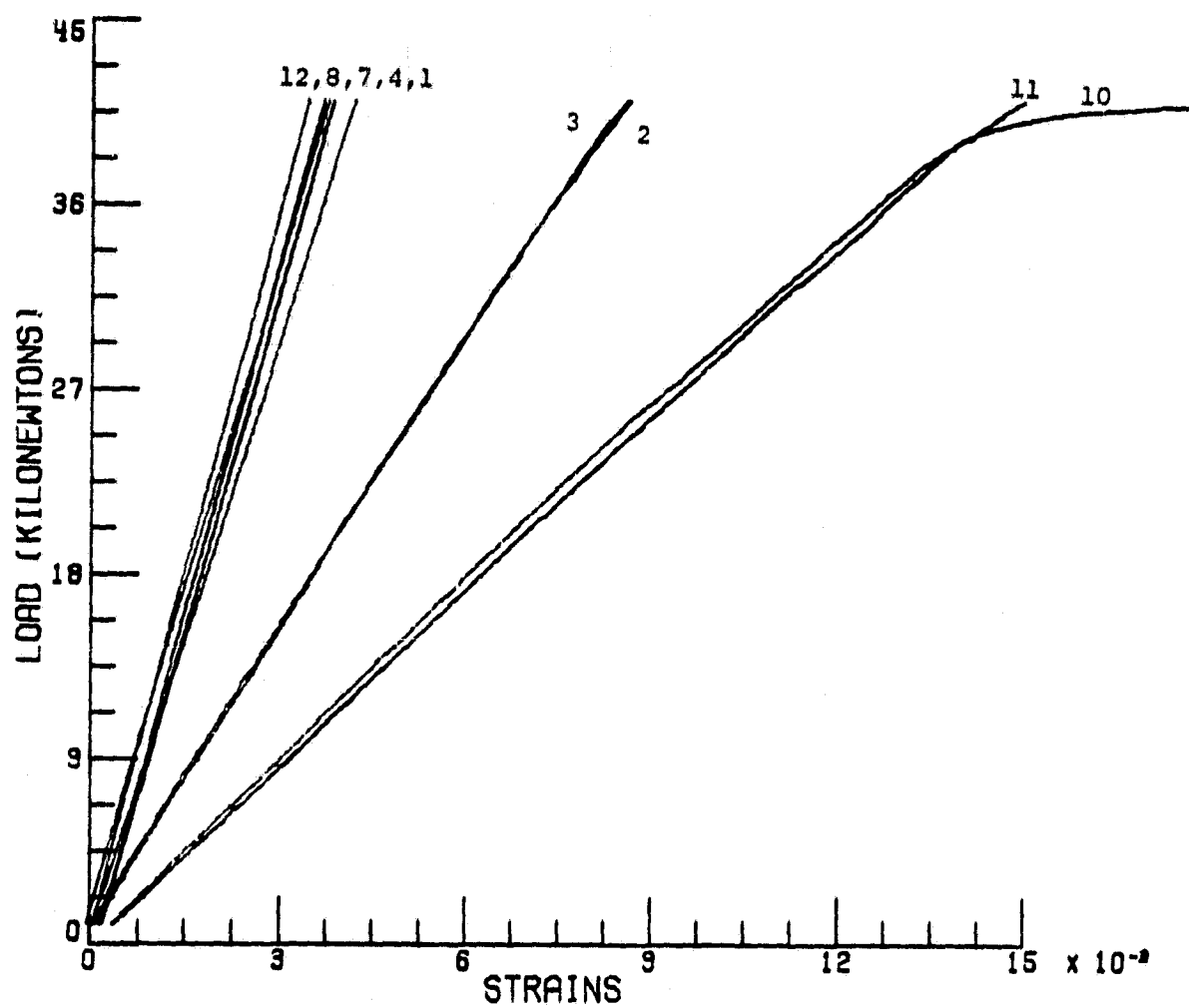


Figure 19. Load-strain responses for open-hole specimen 1.

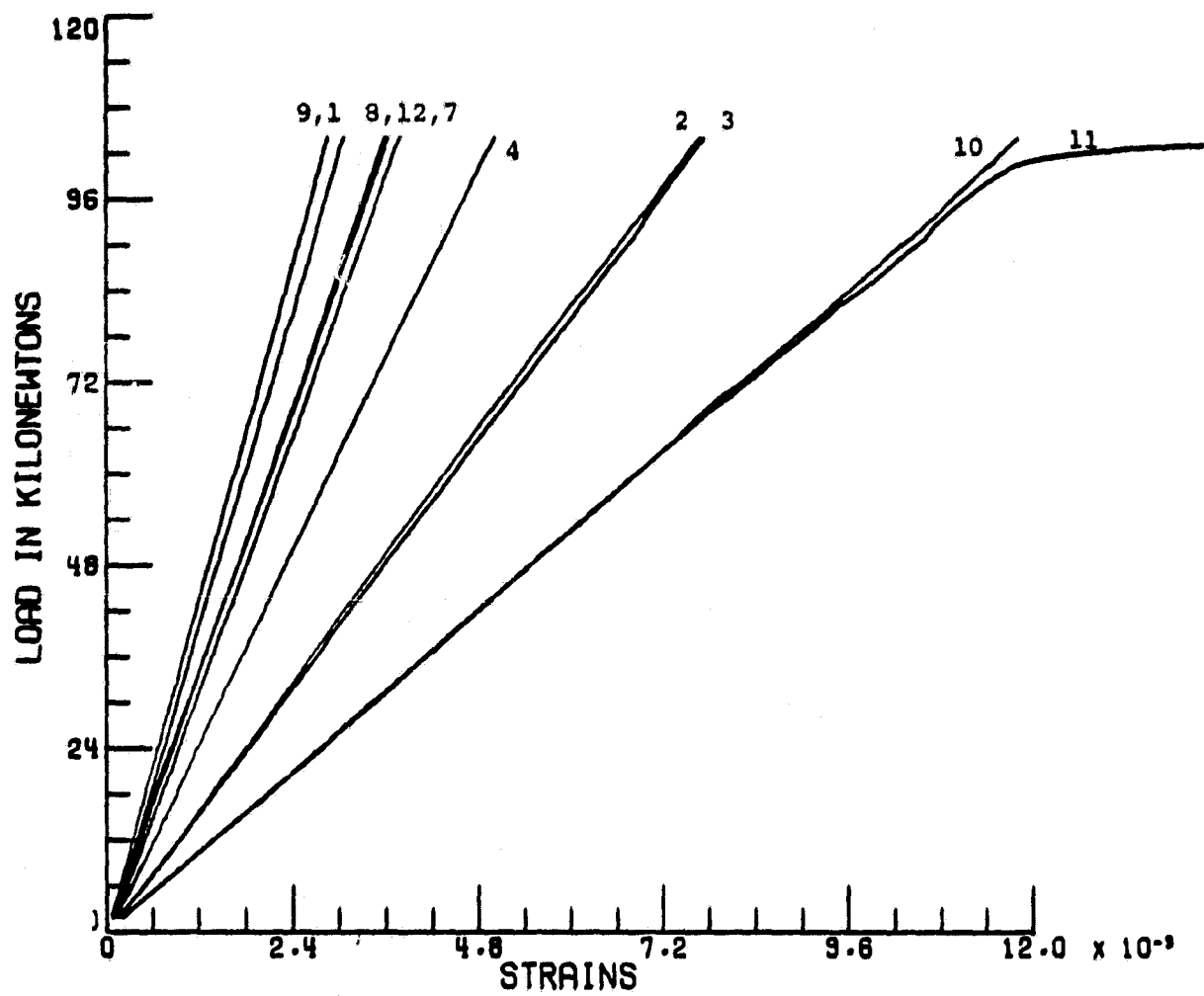


Figure 20. Load-strain responses for open-hole specimen 11.

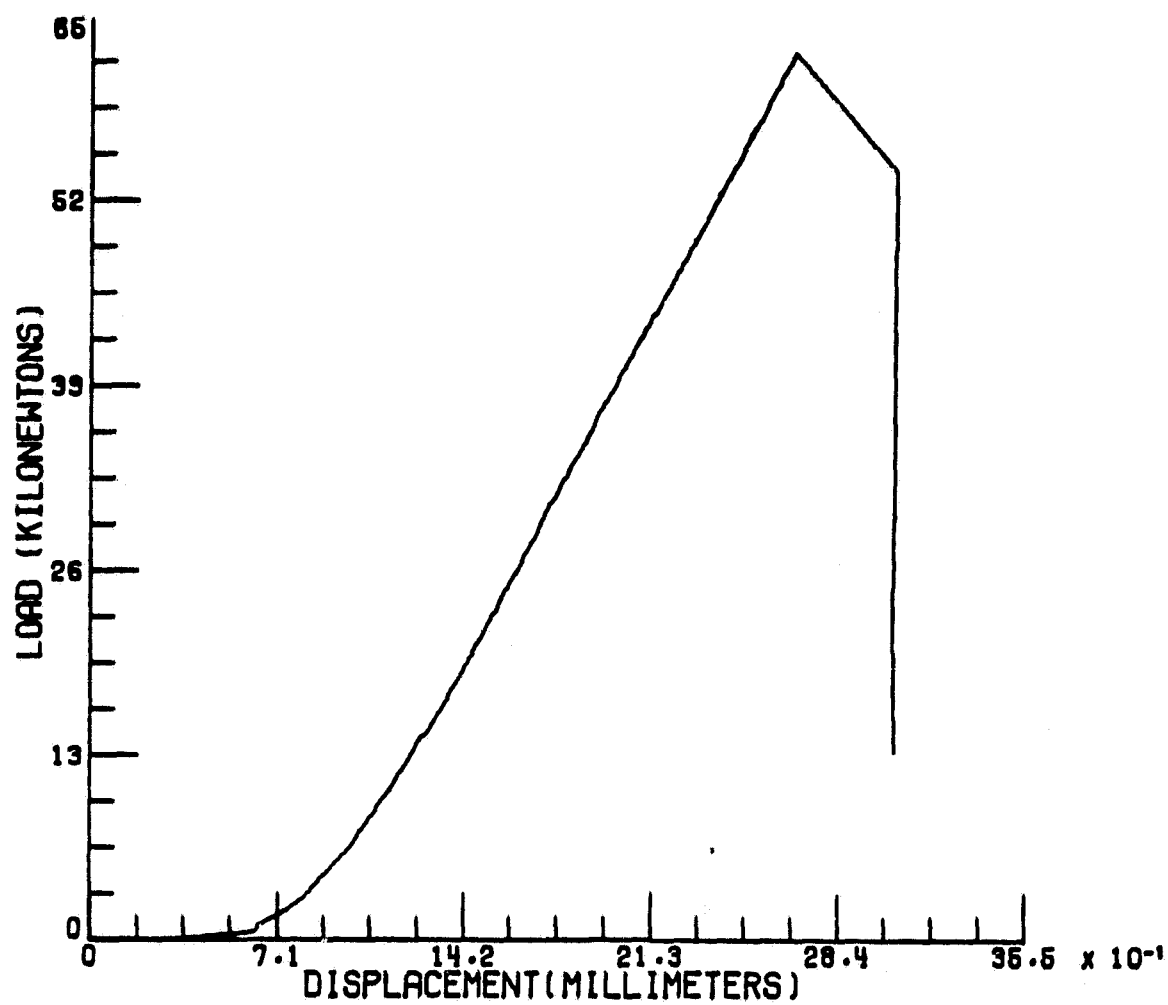


Figure 21. Load-head displacement for open-hole specimen 4.

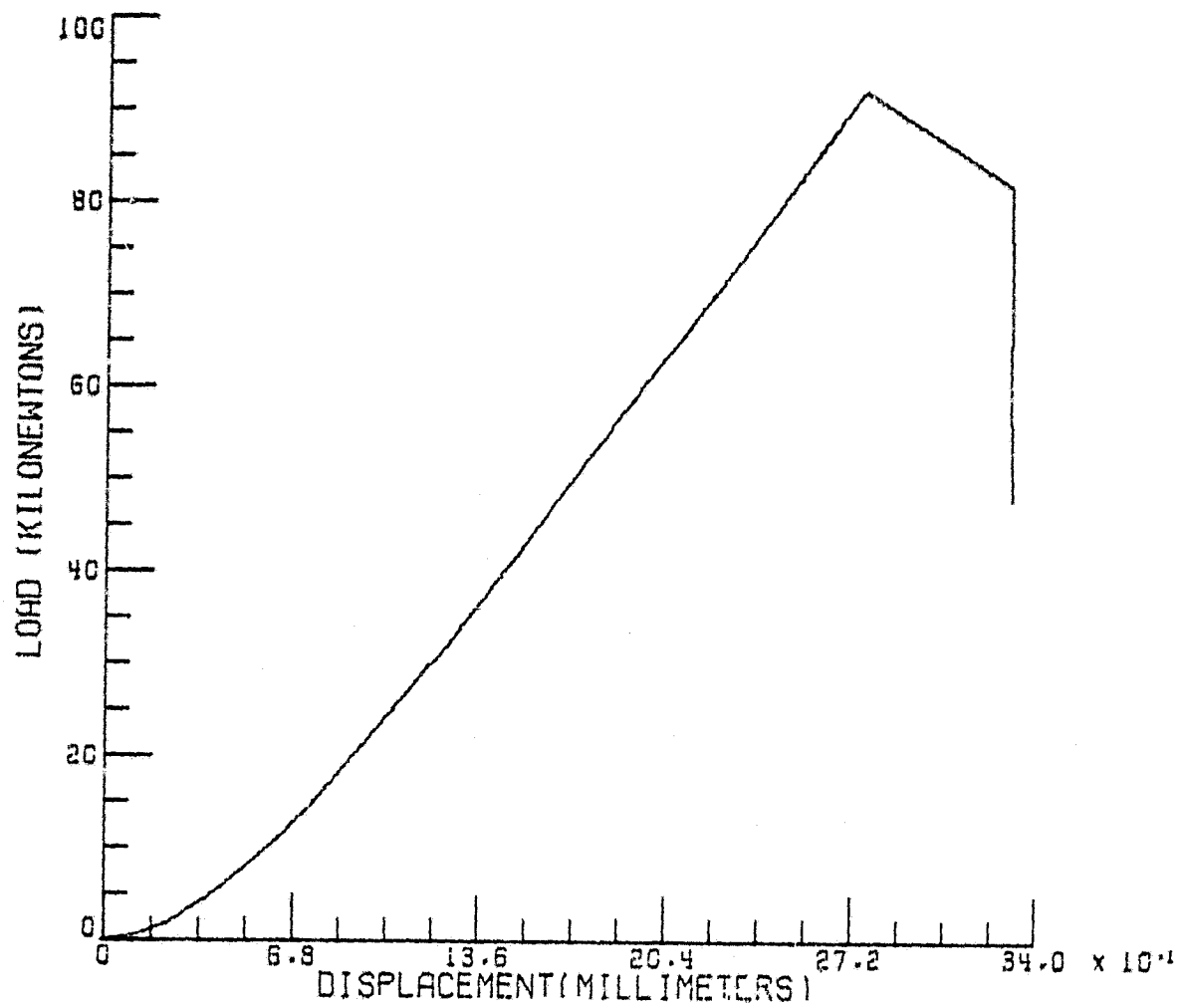


Figure 22. Load-head displacement for open-hole specimen 5.

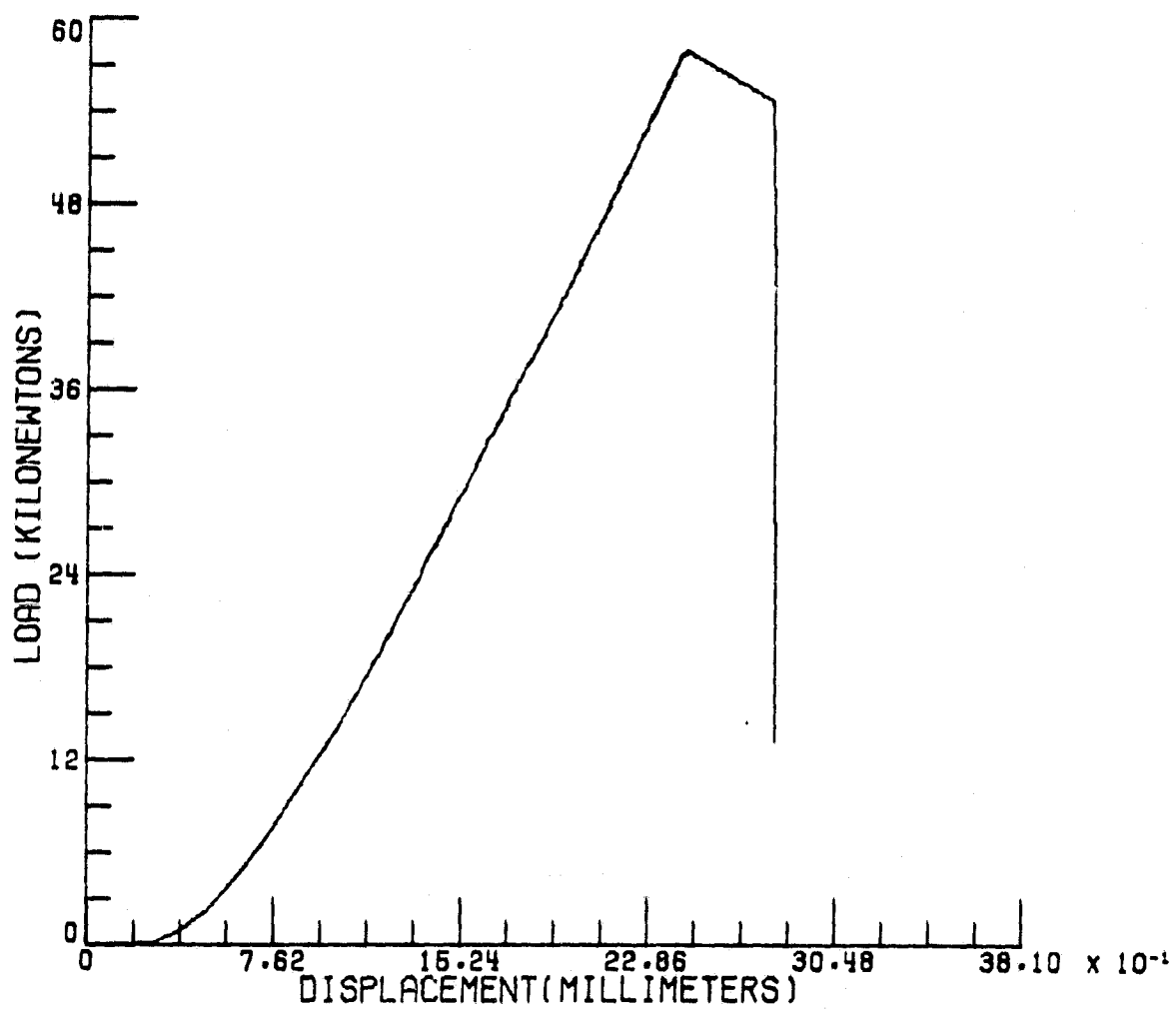


Figure 23. Load-head displacement for open-hole specimen 7.

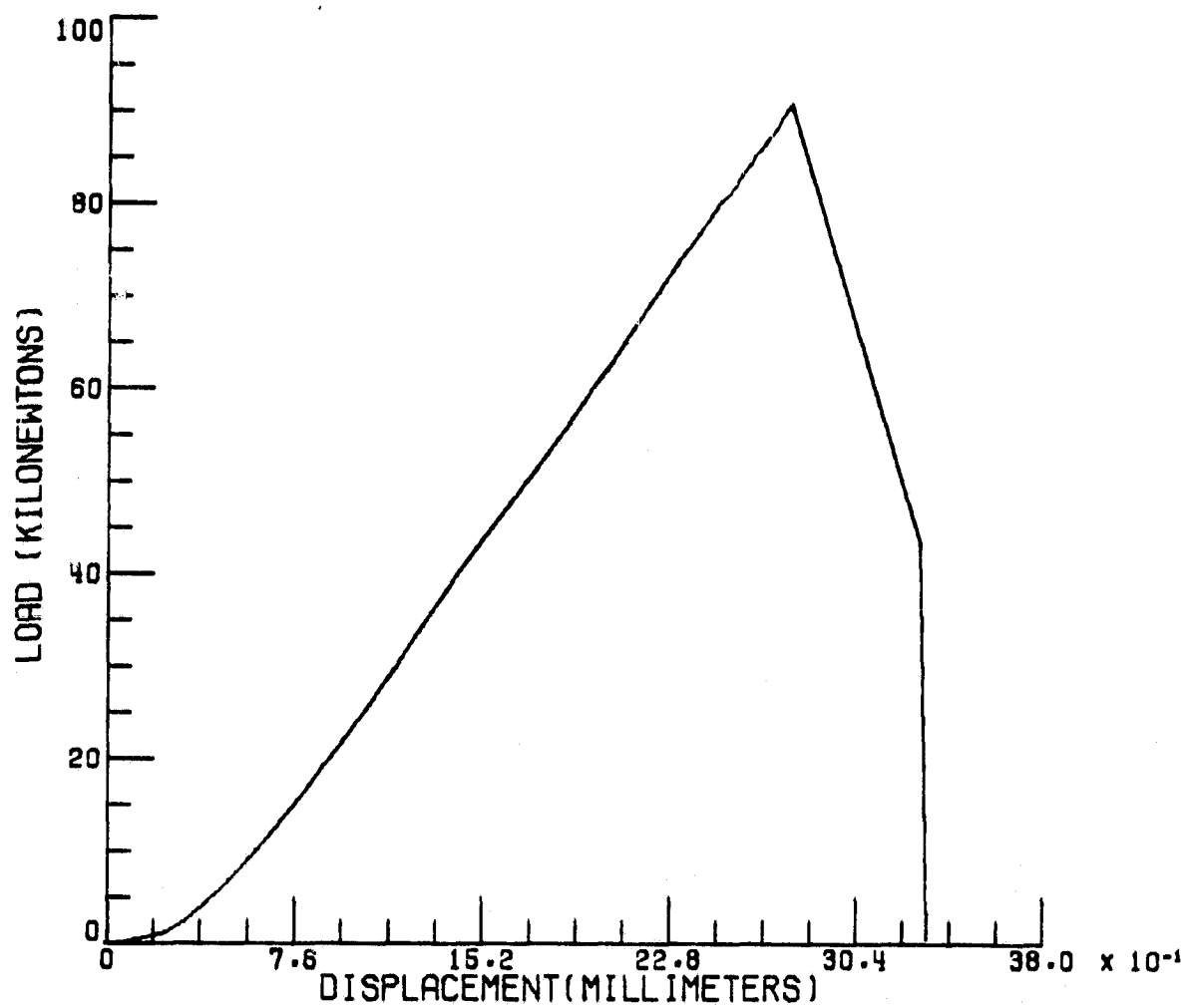


Figure 24. Load-head displacement for open-hole specimen 9.

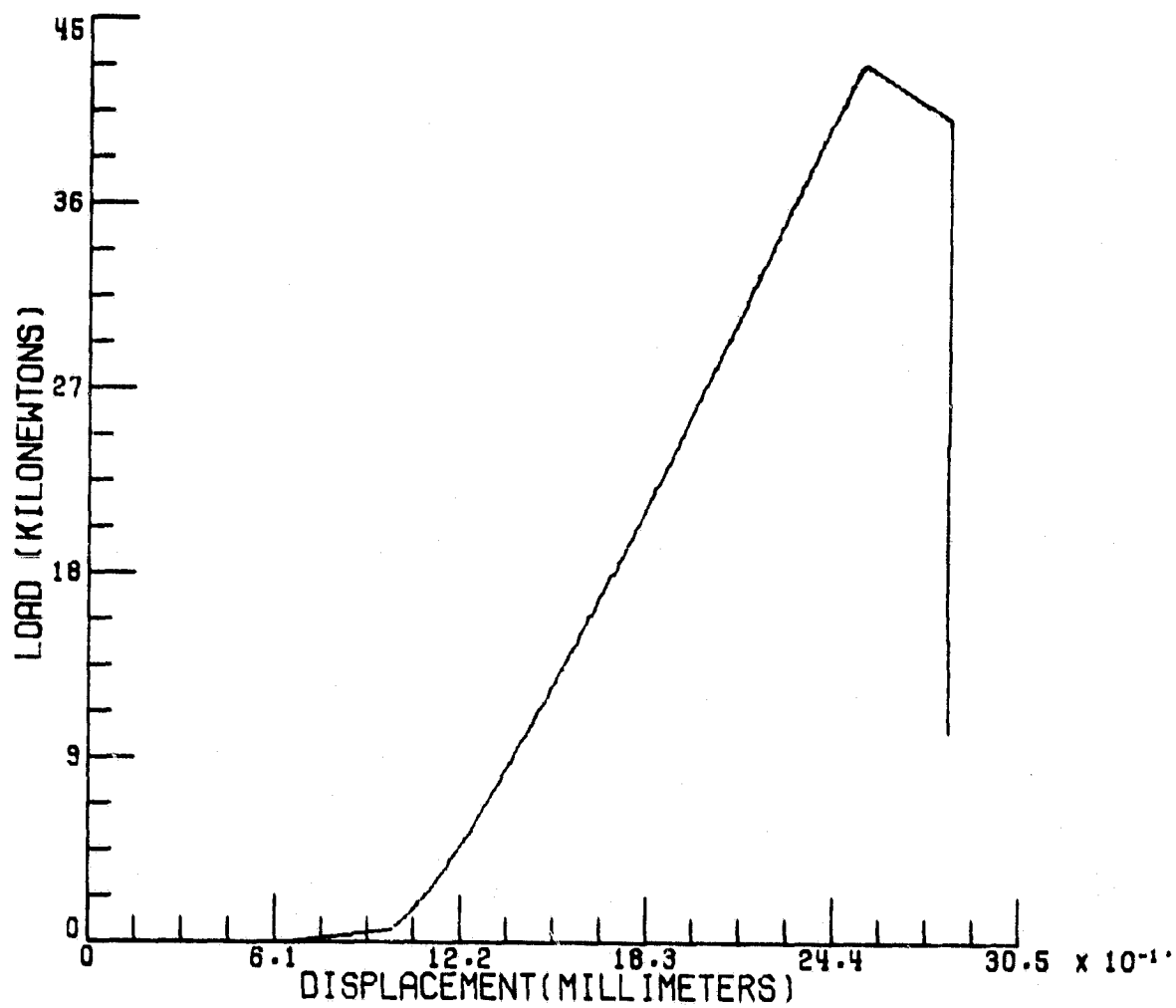


Figure 25. Load-head displacement for open-hole specimen 1.

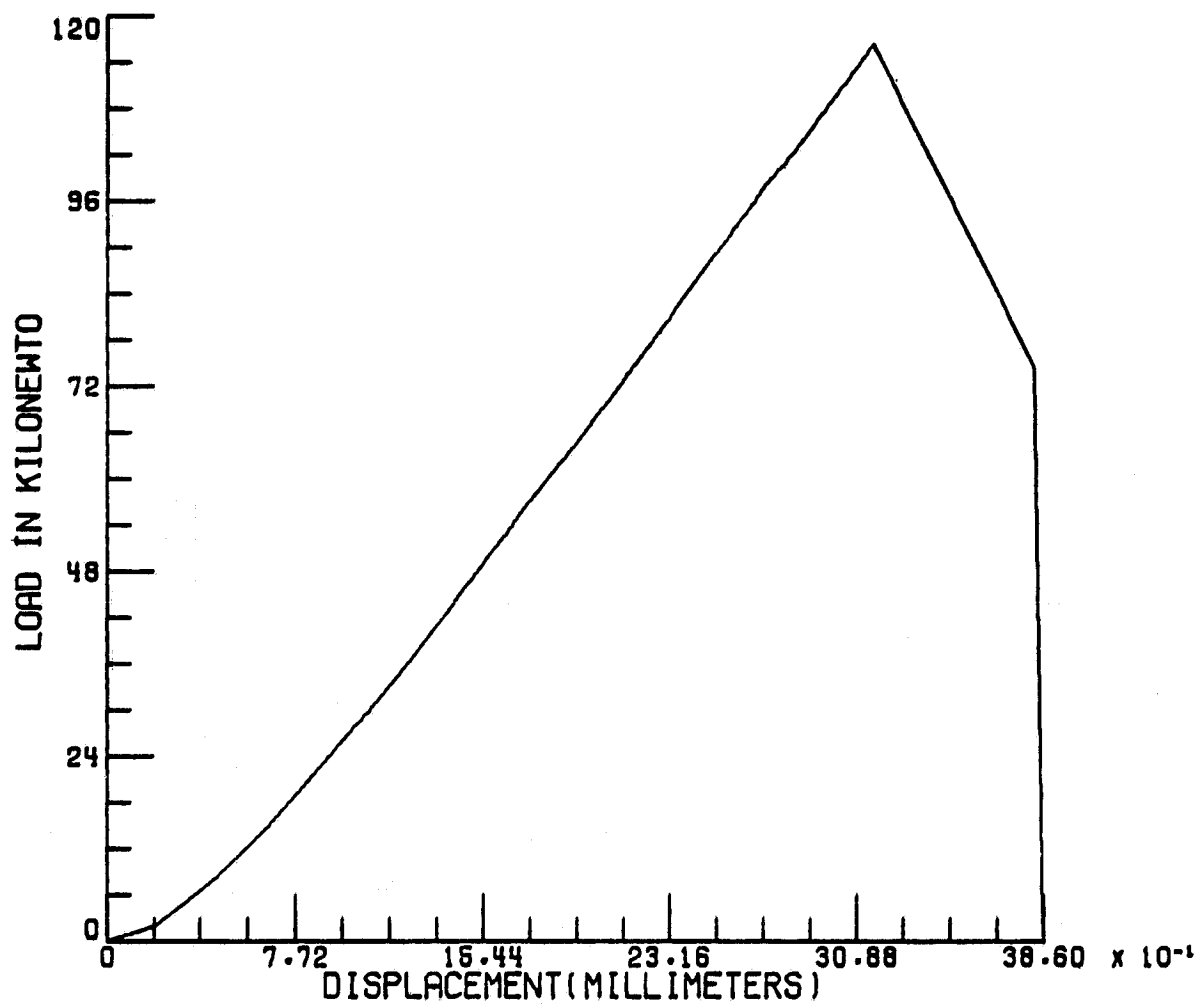


Figure 26. Load-head displacement for open-hole specimen 11.

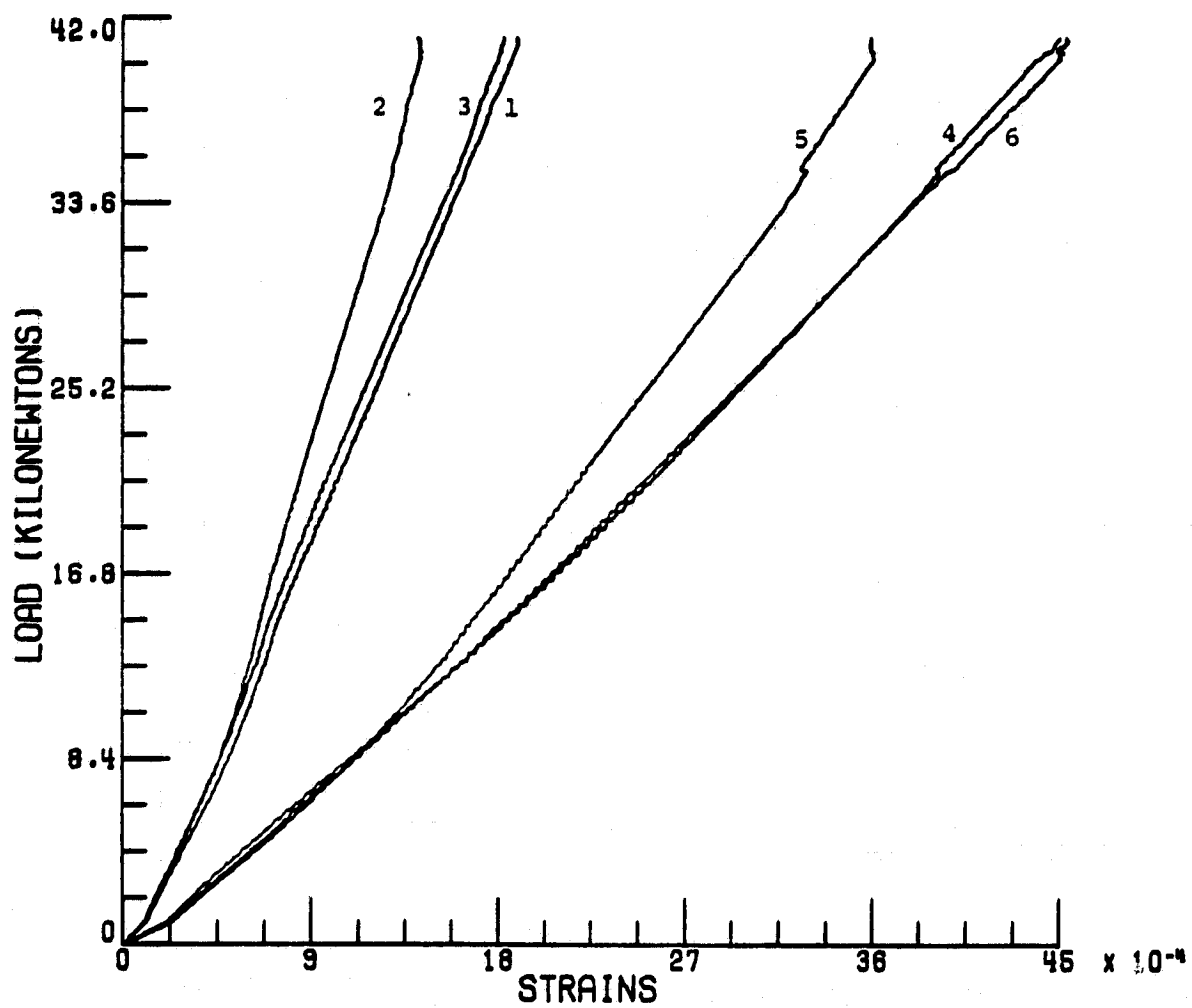


Figure 27. Load-strain responses for double-lap, double-hole specimen 1.

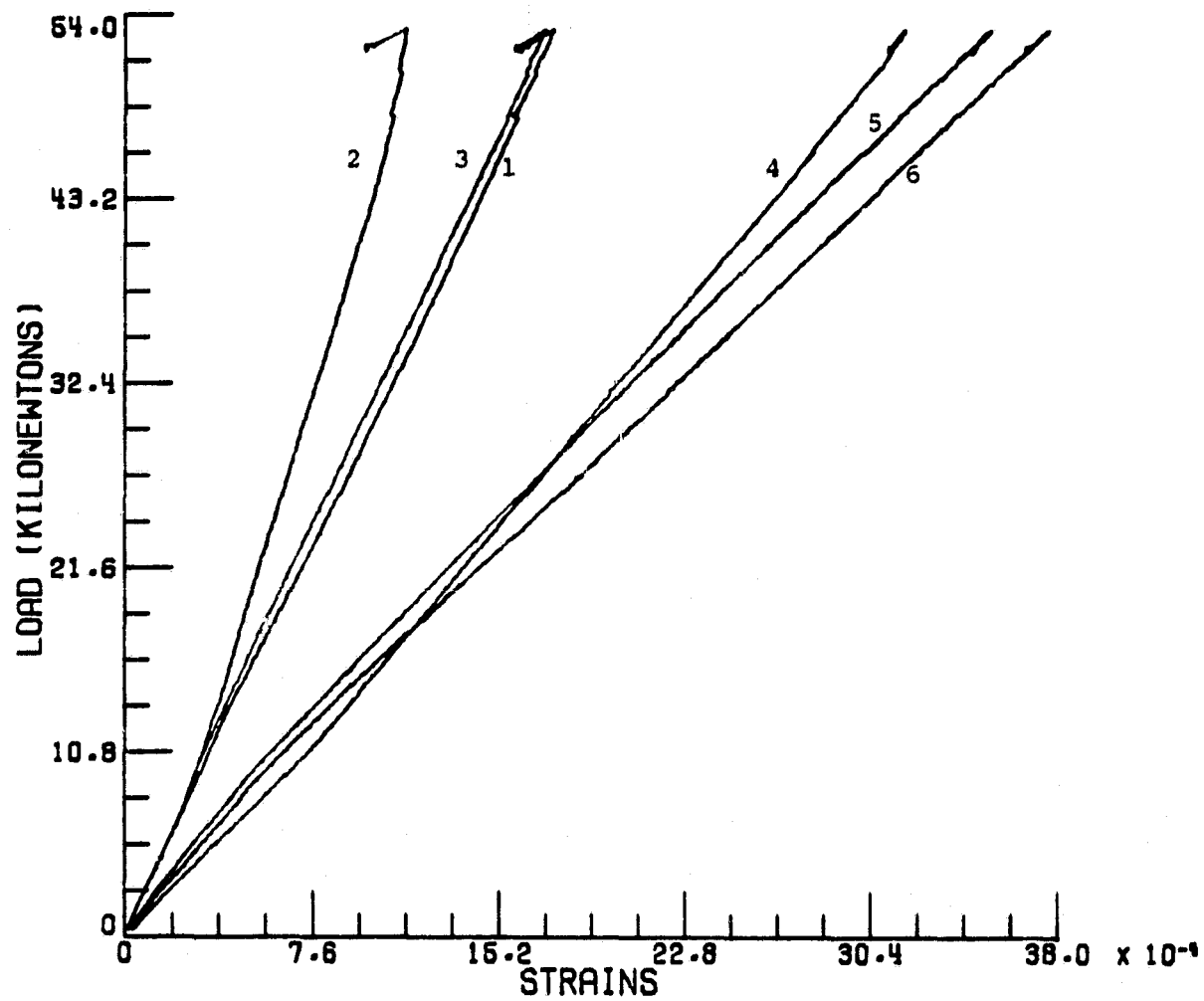


Figure 28. Load-strain responses for double-lap, double-hole specimen 3.

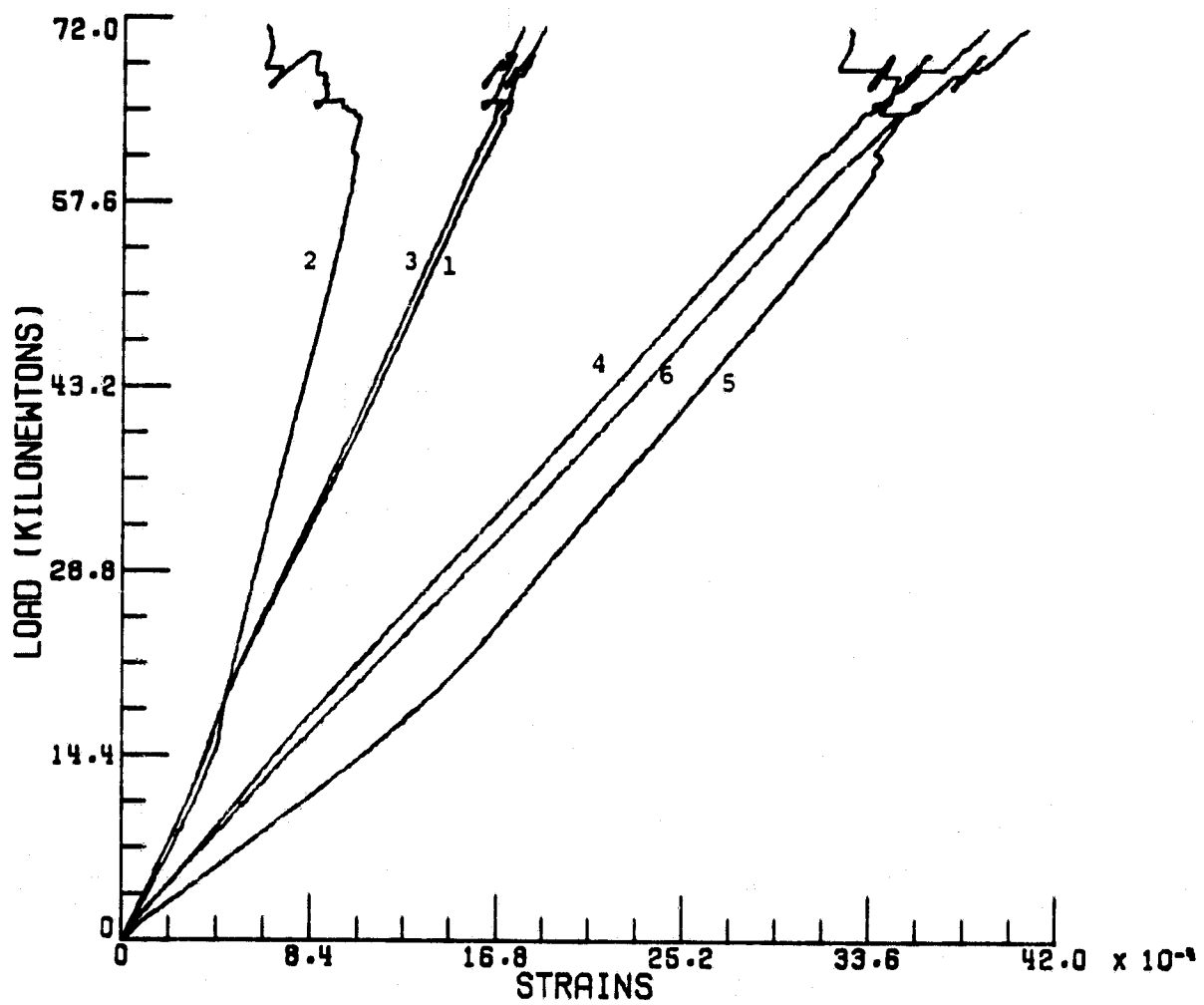


Figure 29. Load-strain responses for double-lap, double-hole specimen 7.

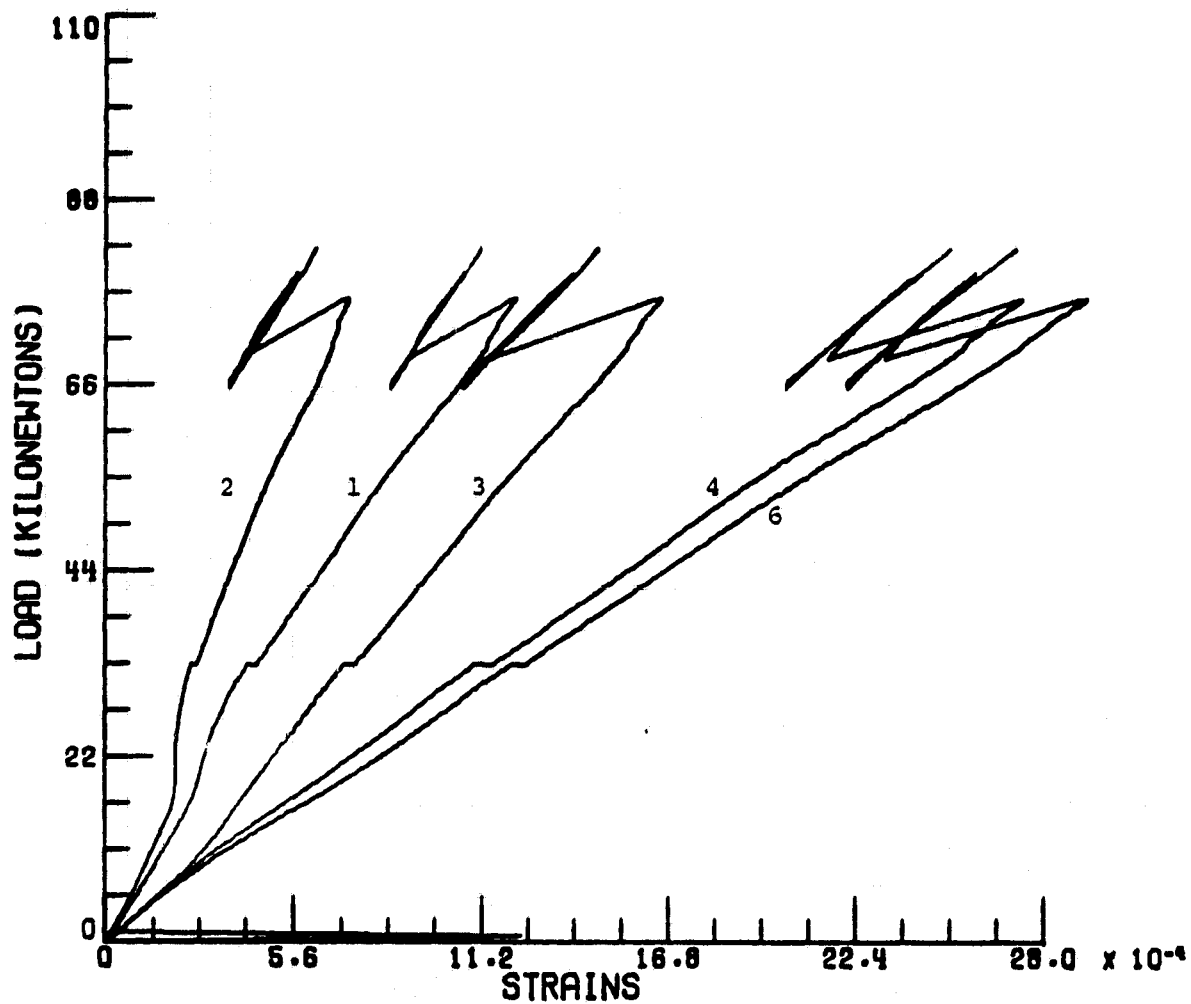


Figure 30. Load-strain responses for double-lap, double-hole specimen 17.

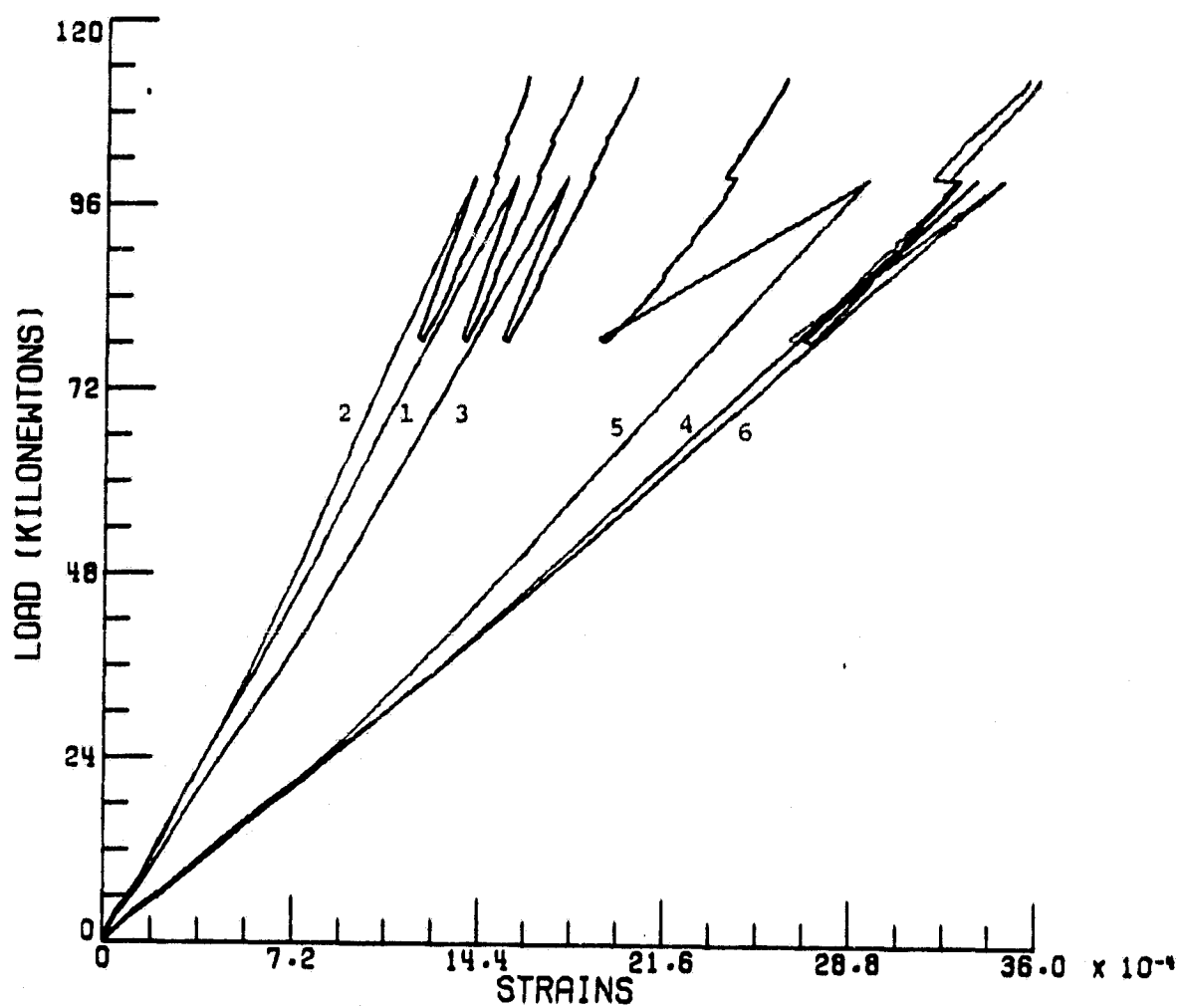


Figure 31. Load-strain responses for double-lap, double-hole specimen 18.

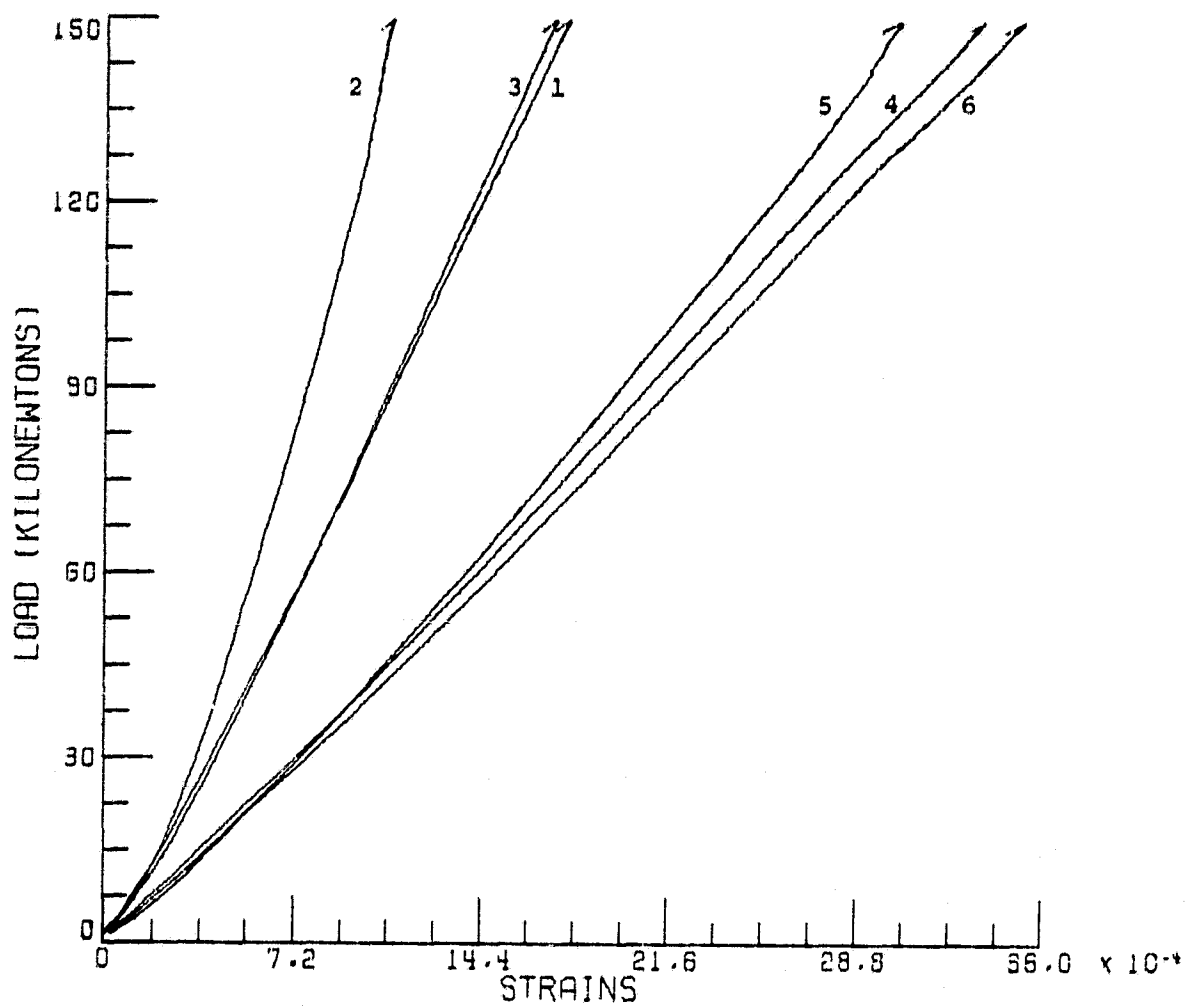


Figure 32. Load-strain responses for double-lap, double-hole specimen 20.

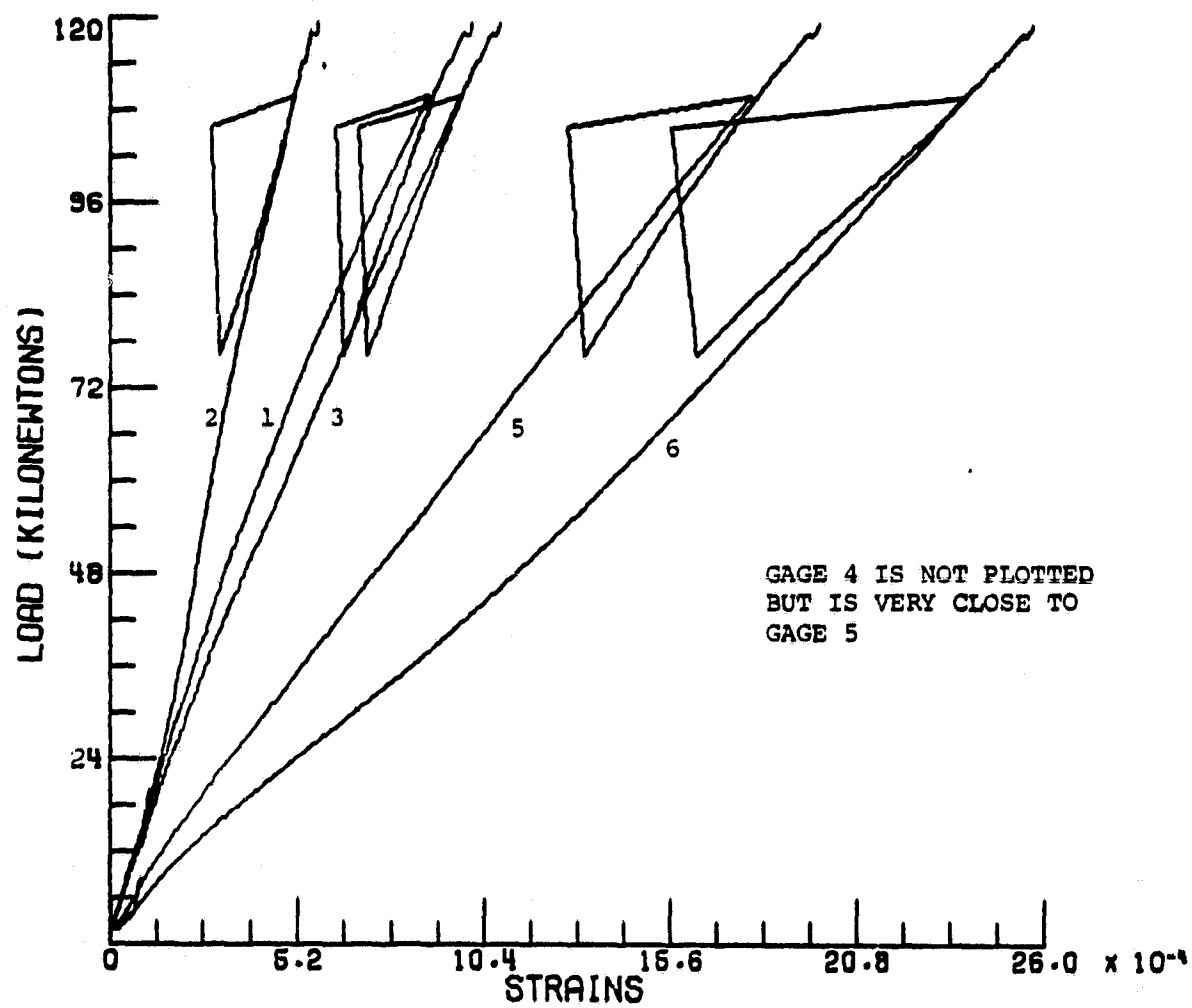


Figure 33. Load-strain responses for double-lap, double-hole specimen 22.

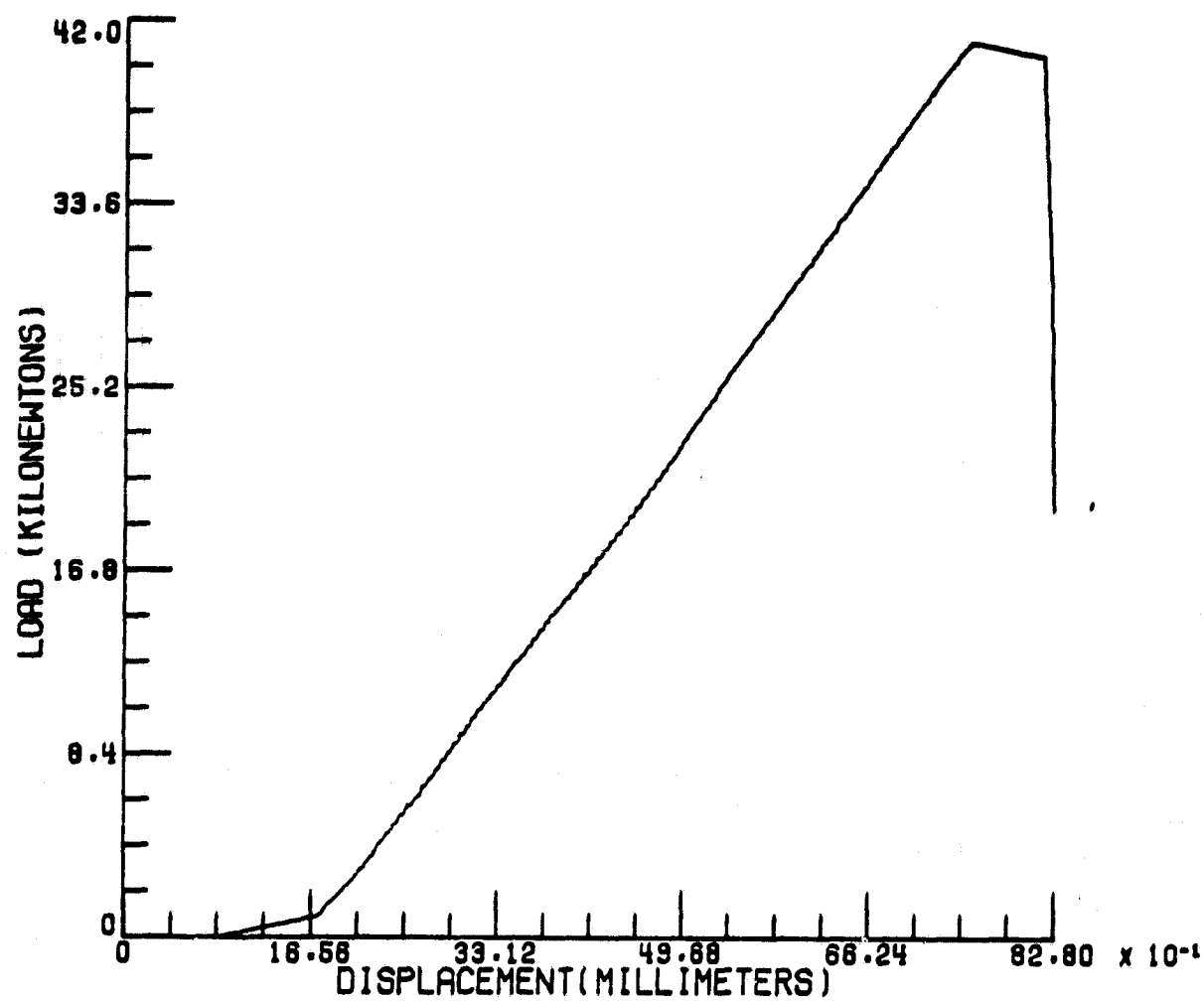


Figure 34. Load-head displacement for double-lap, double-hole specimen 1.

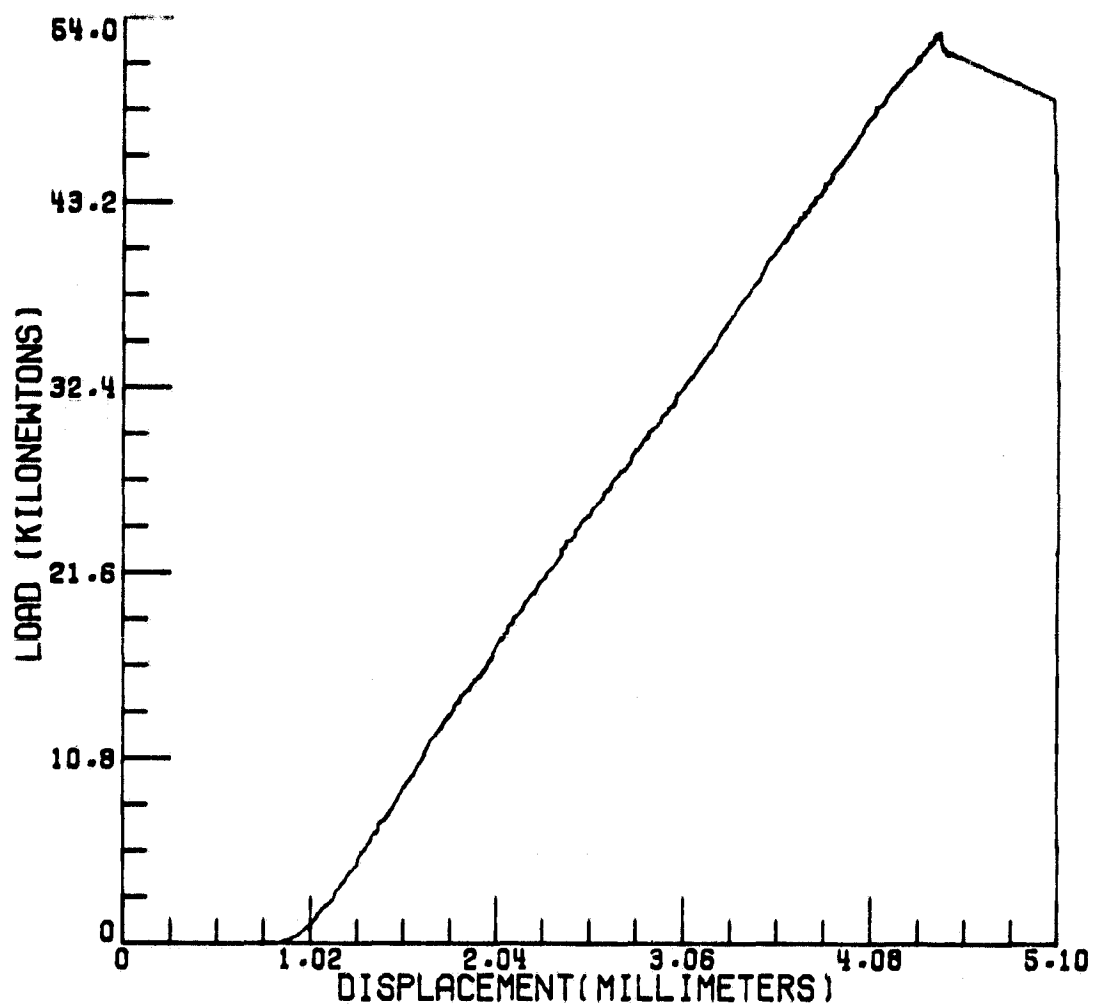


Figure 35. Load-head displacement for double-lap, double-hole specimen 3.

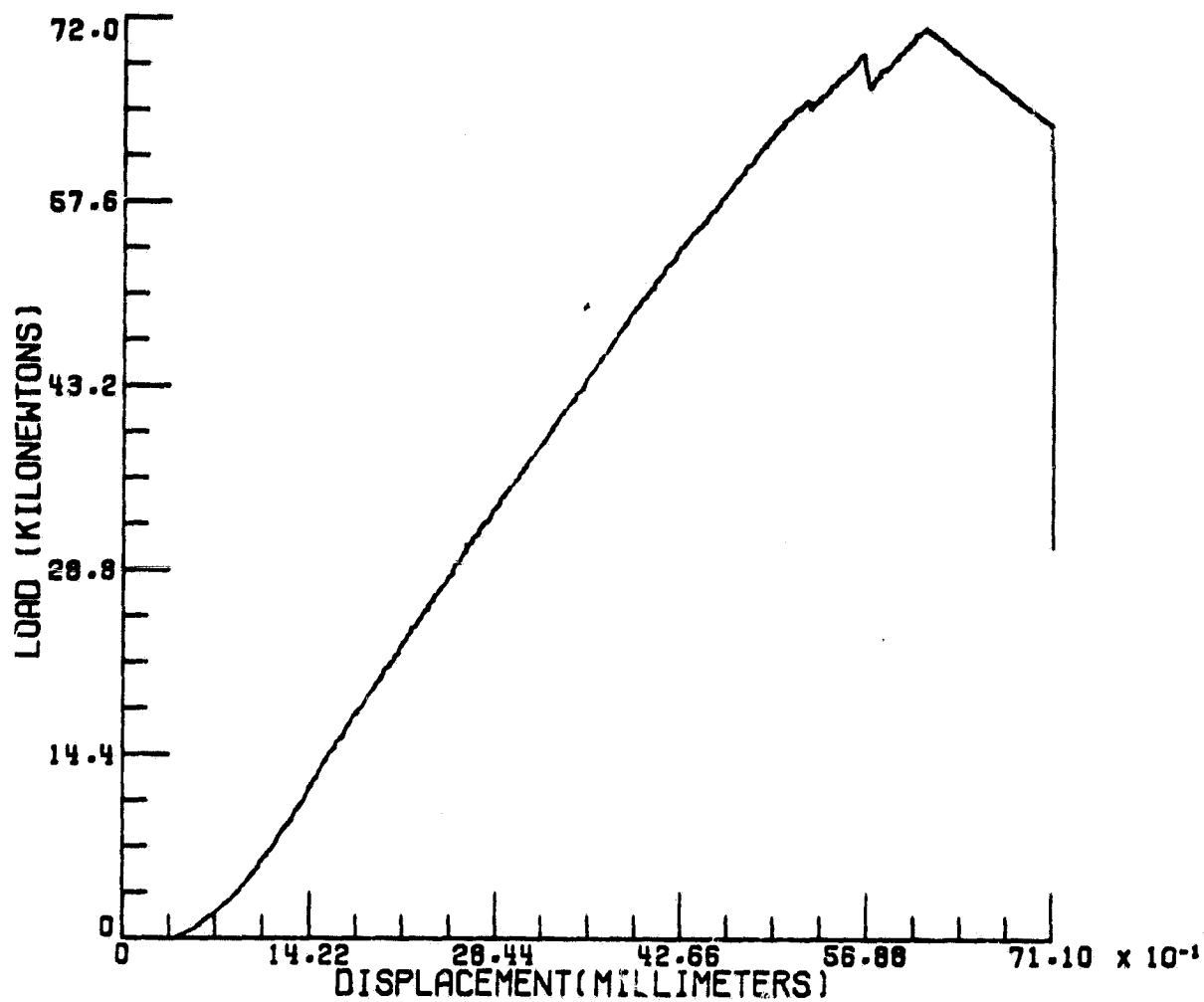


Figure 36. Load-head displacement for double-lap, double-hole specimen 7.

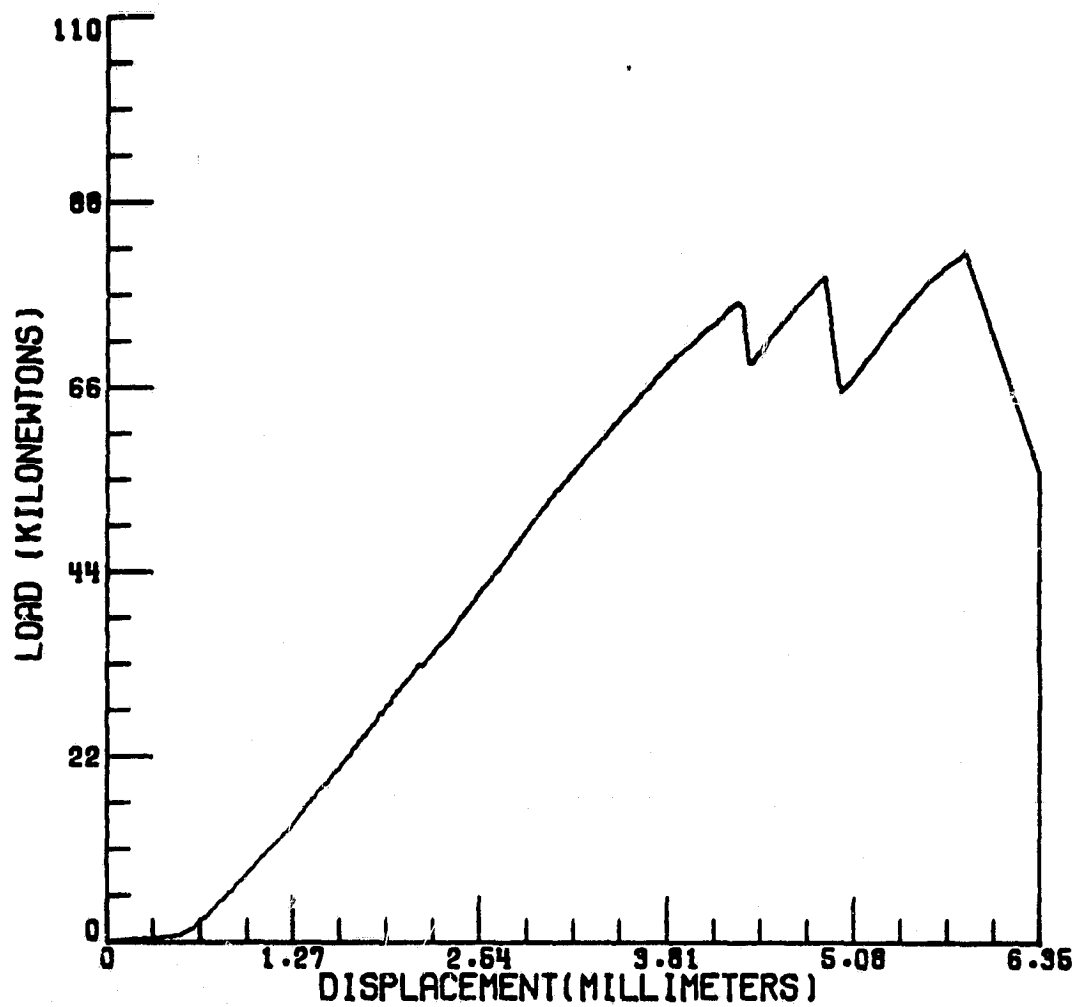


Figure 37. Load-head displacement for double-lap, double-hole specimen 17.

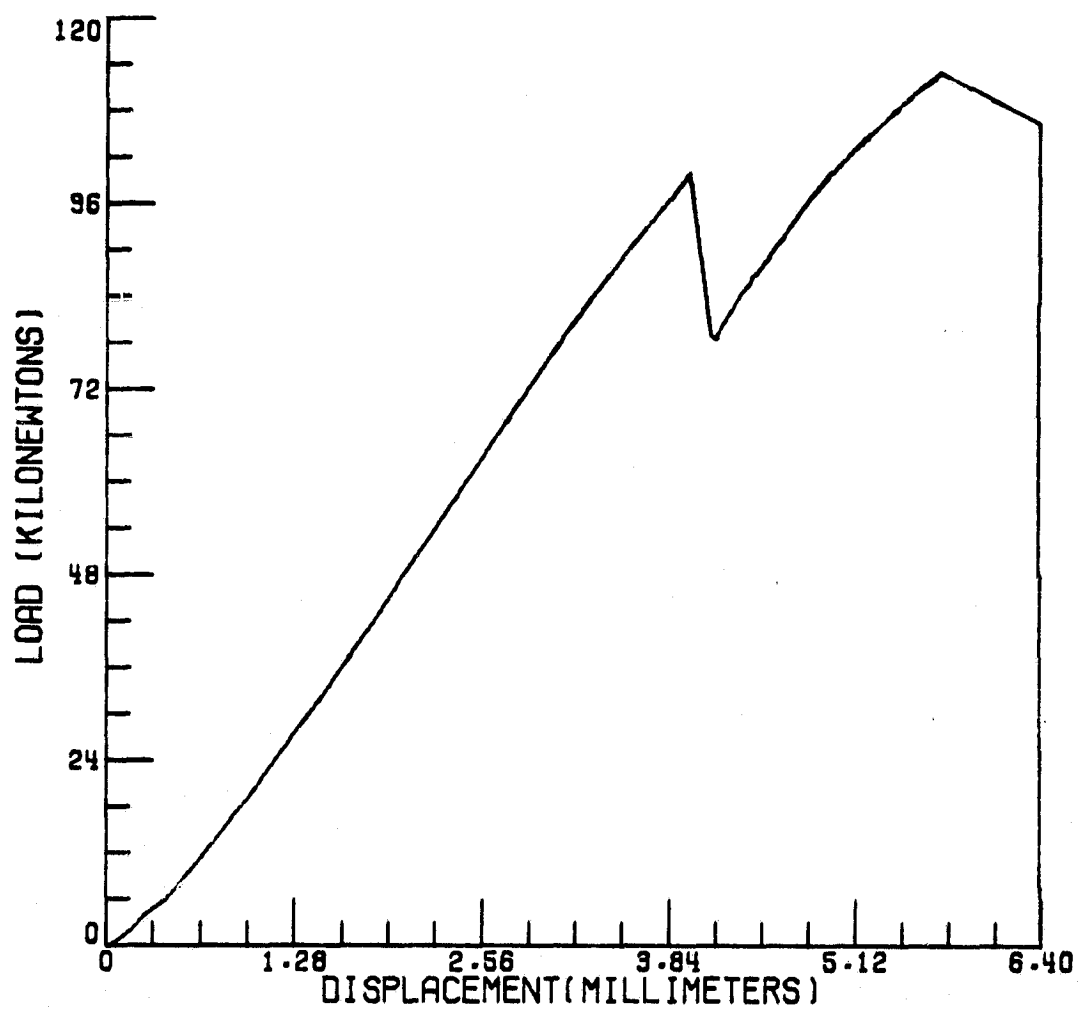


Figure 38. Load-head displacement for double-lap, double-hole specimen 18.

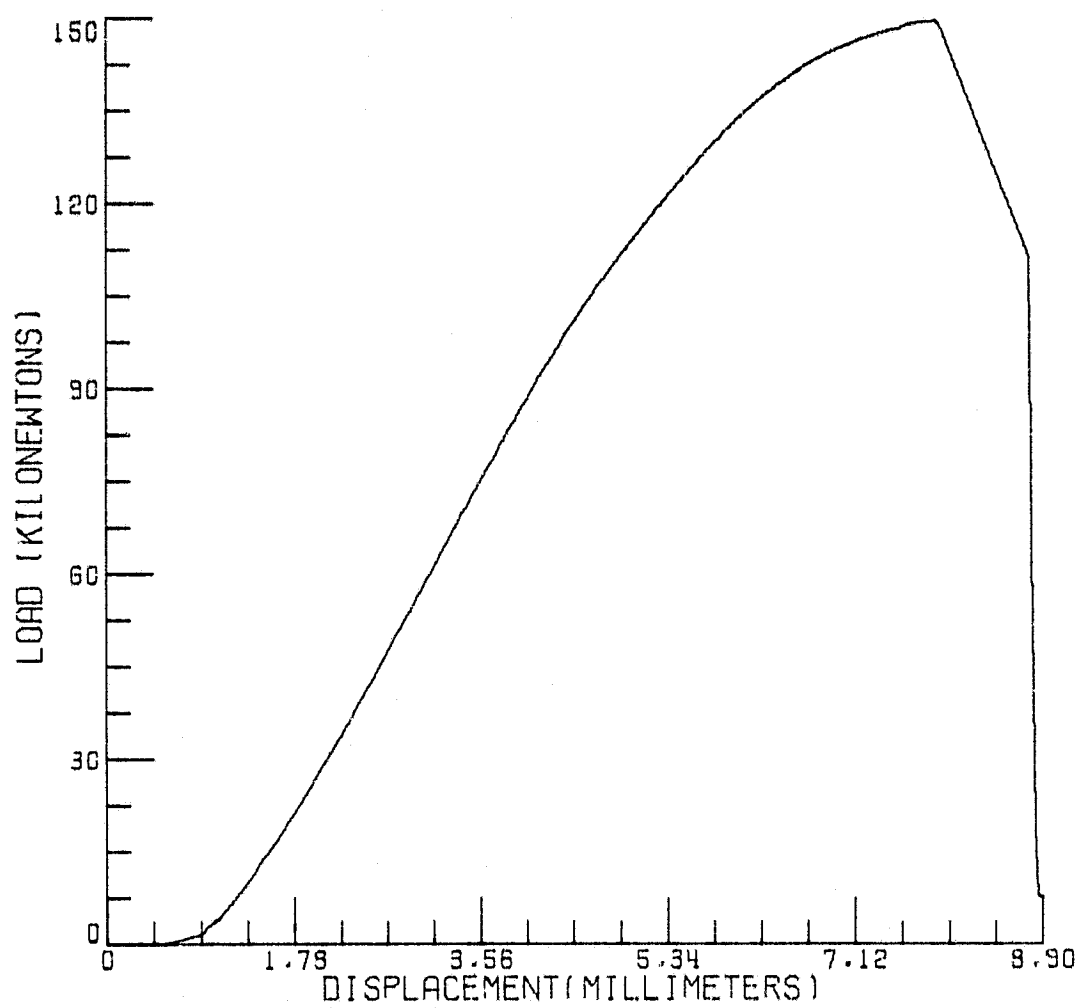


Figure 39. Load-head displacement for double-lap, double-hole specimen 20.

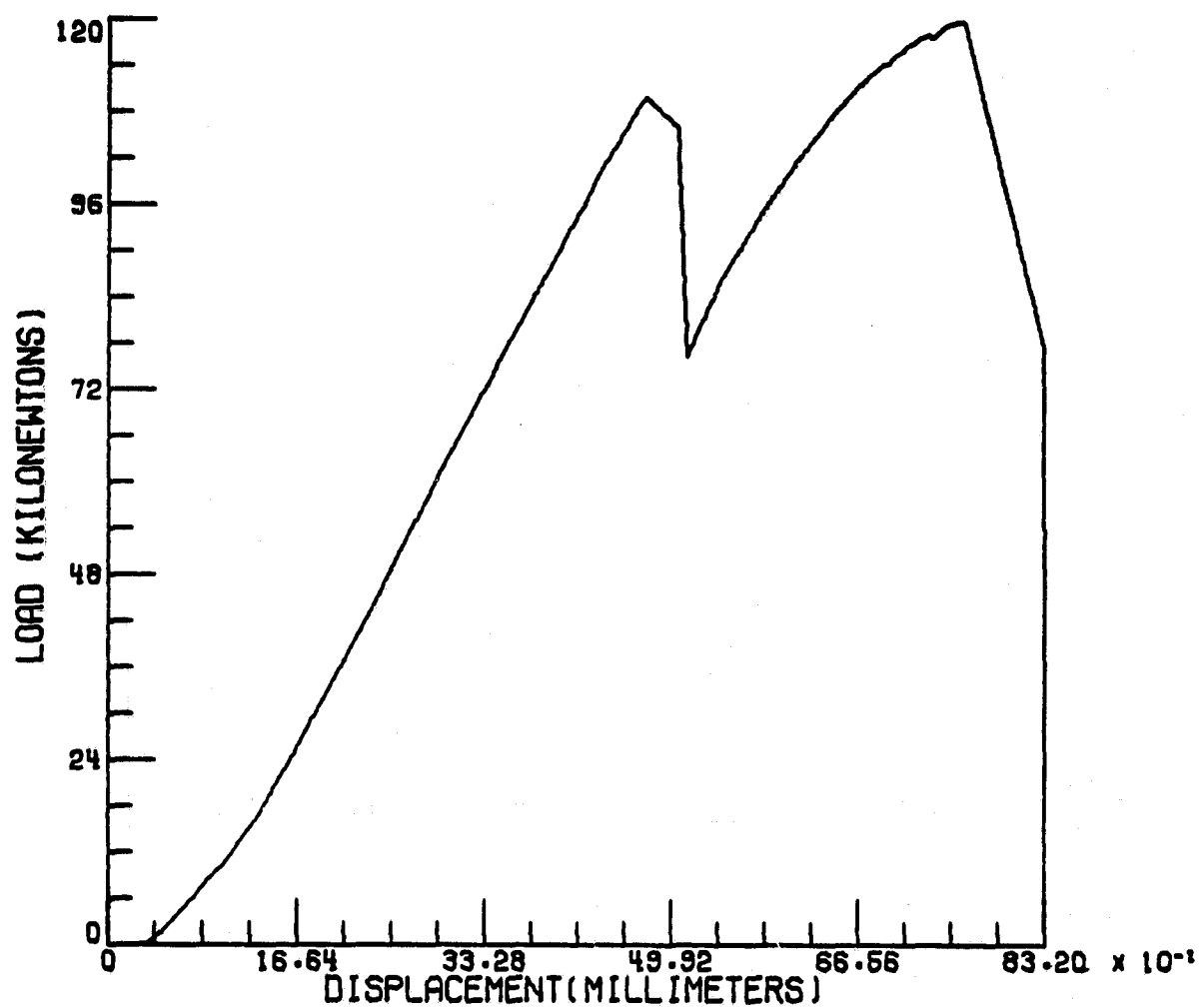


Figure 40. Load-head displacement for double-lap, double-hole specimen 22.

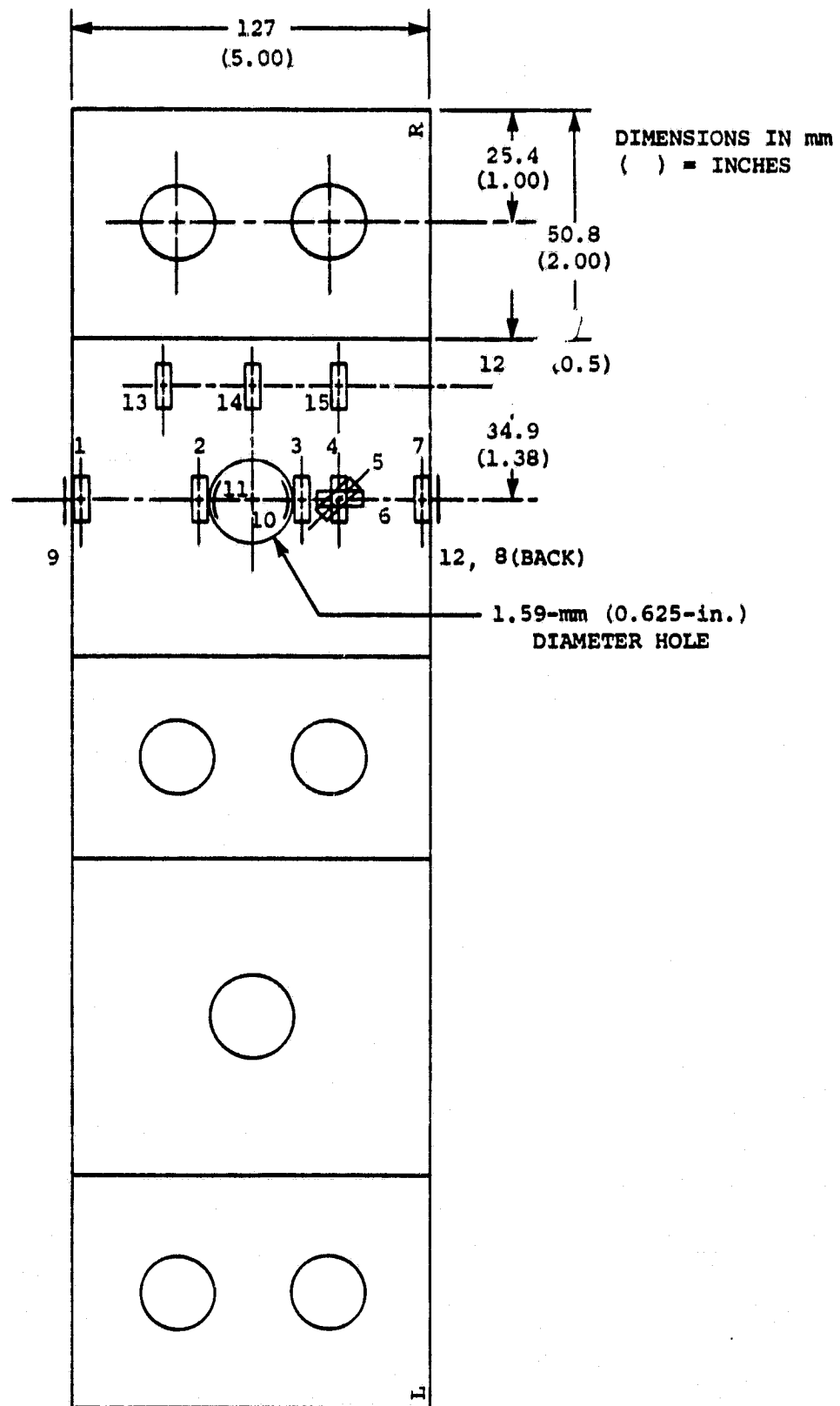
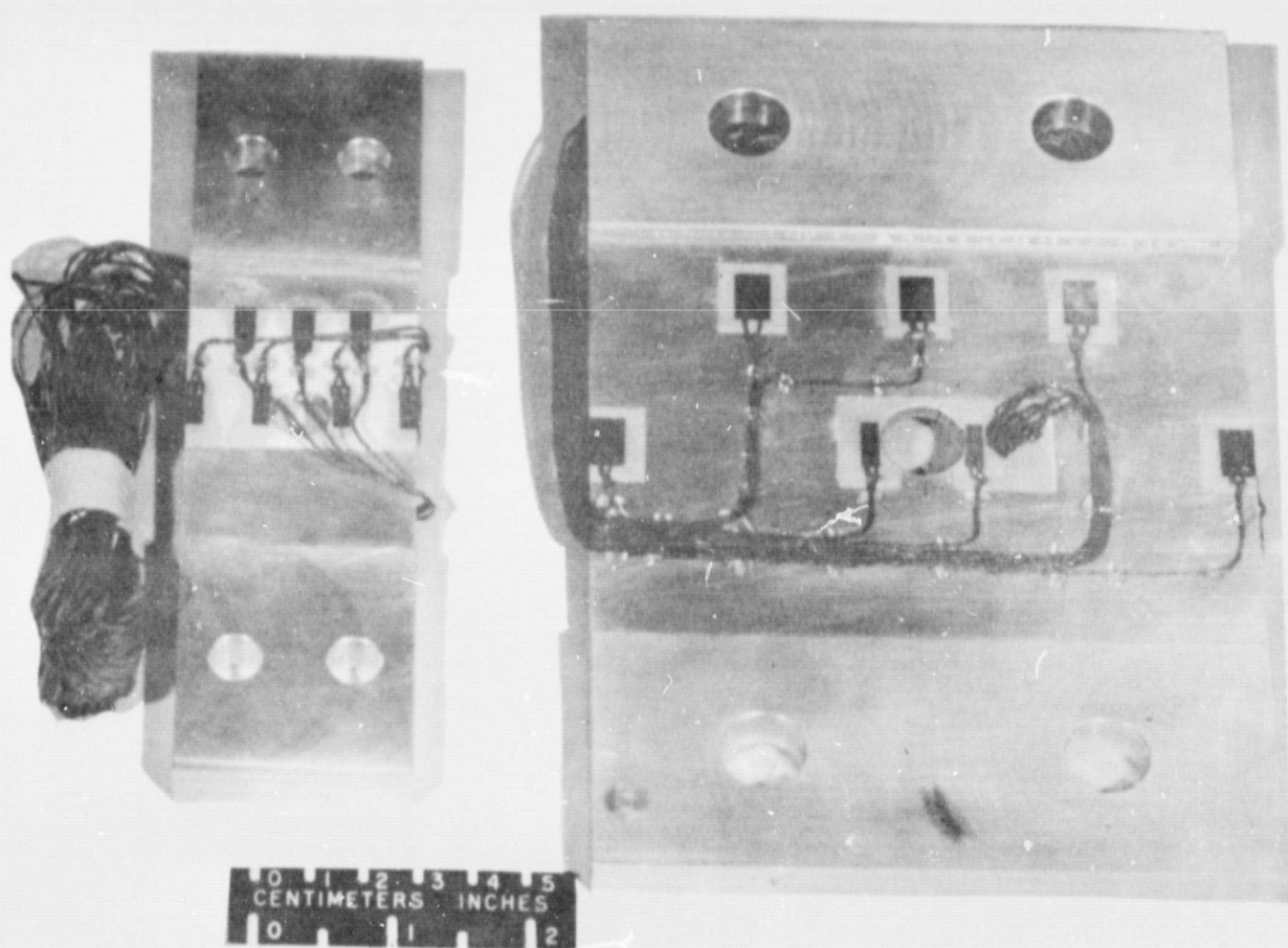


Figure 42. Strain gage locations for aluminum open-hole specimen 11.

Figure 43. Aluminum open-hole specimens 1 (left)
and 11 (right).



ORIGINAL PAGE IS
OF POOR QUALITY

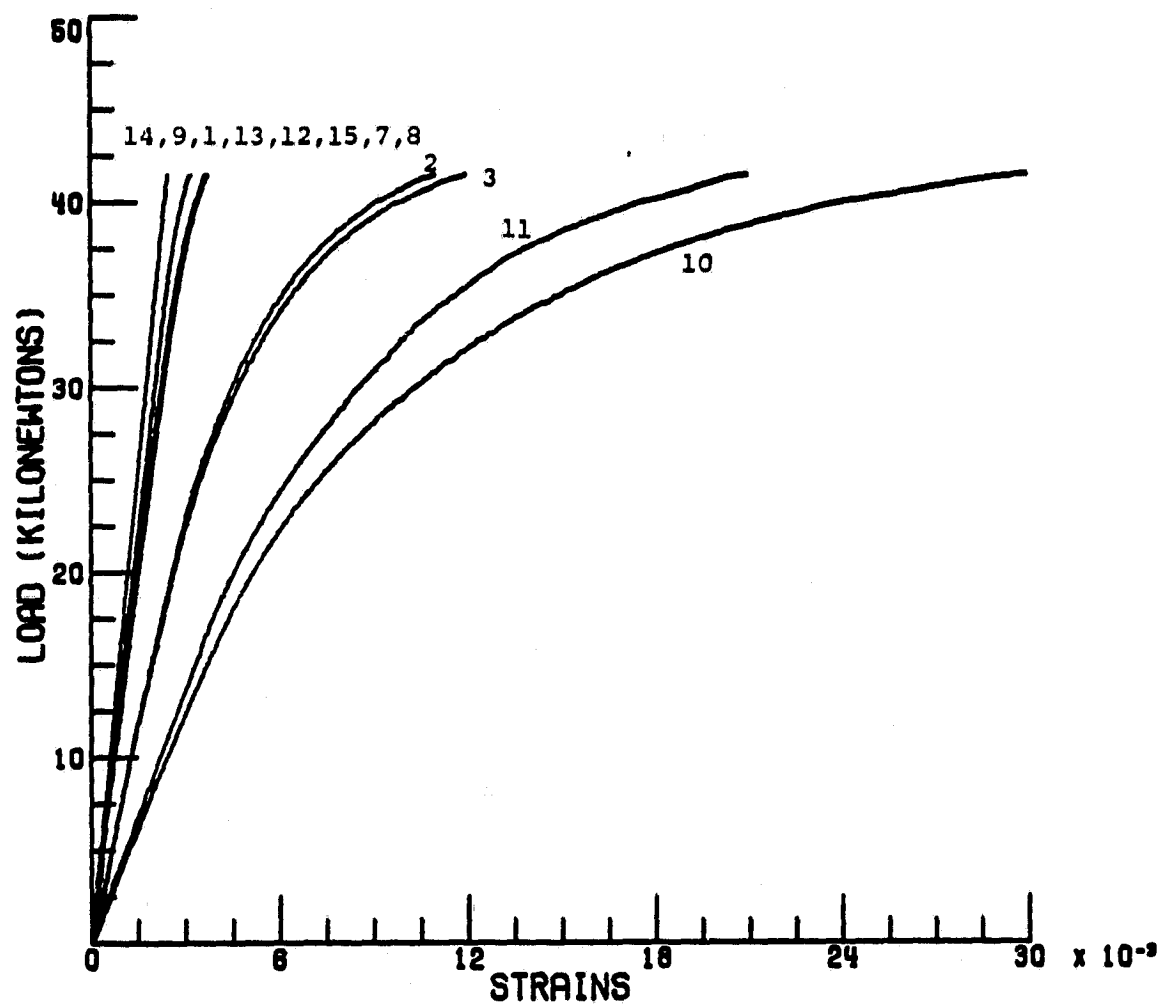


Figure 44. Load-strain responses for aluminum open-hole specimen 1.

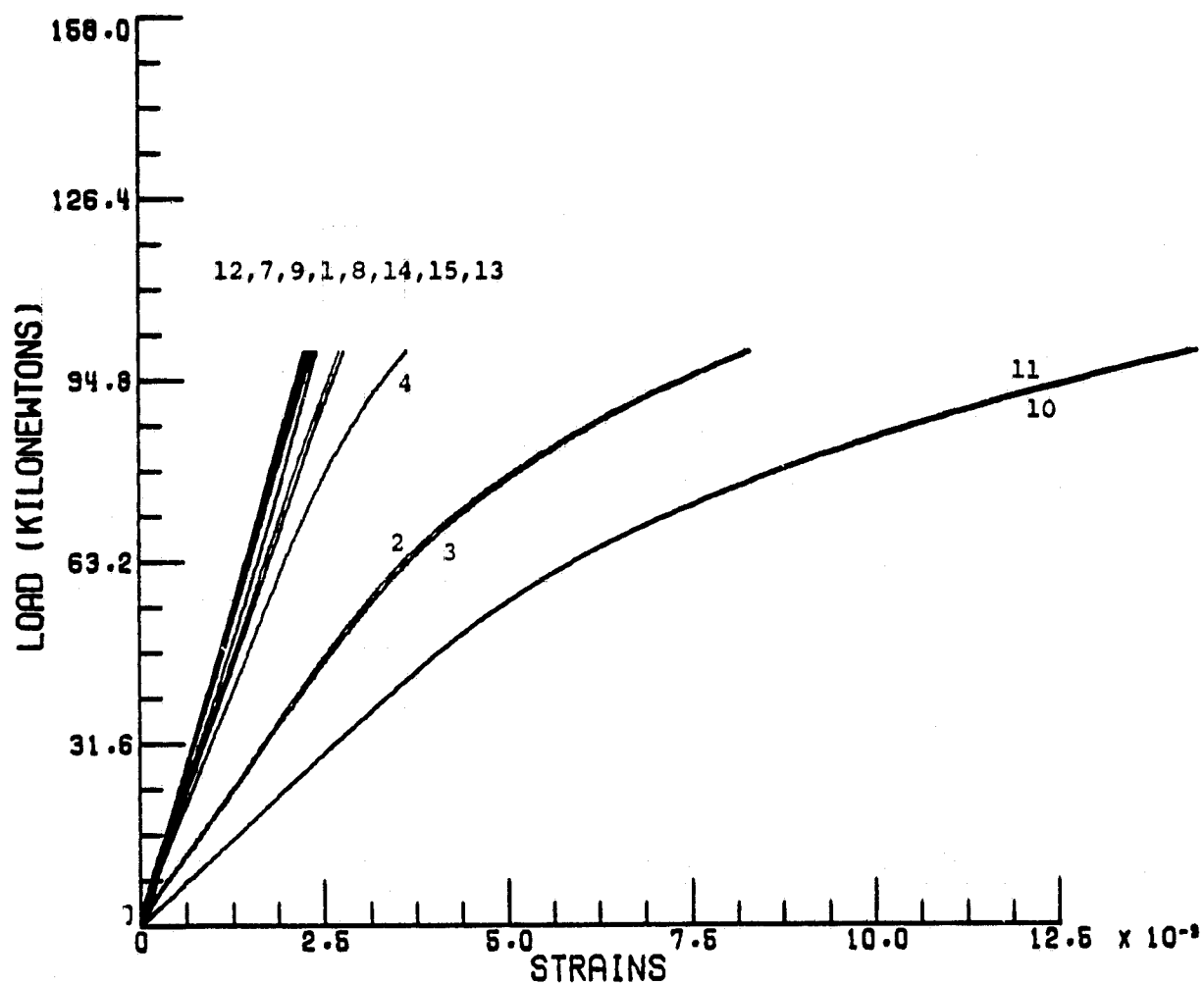


Figure 45. Load-strain responses for aluminum open-hole specimen 11.

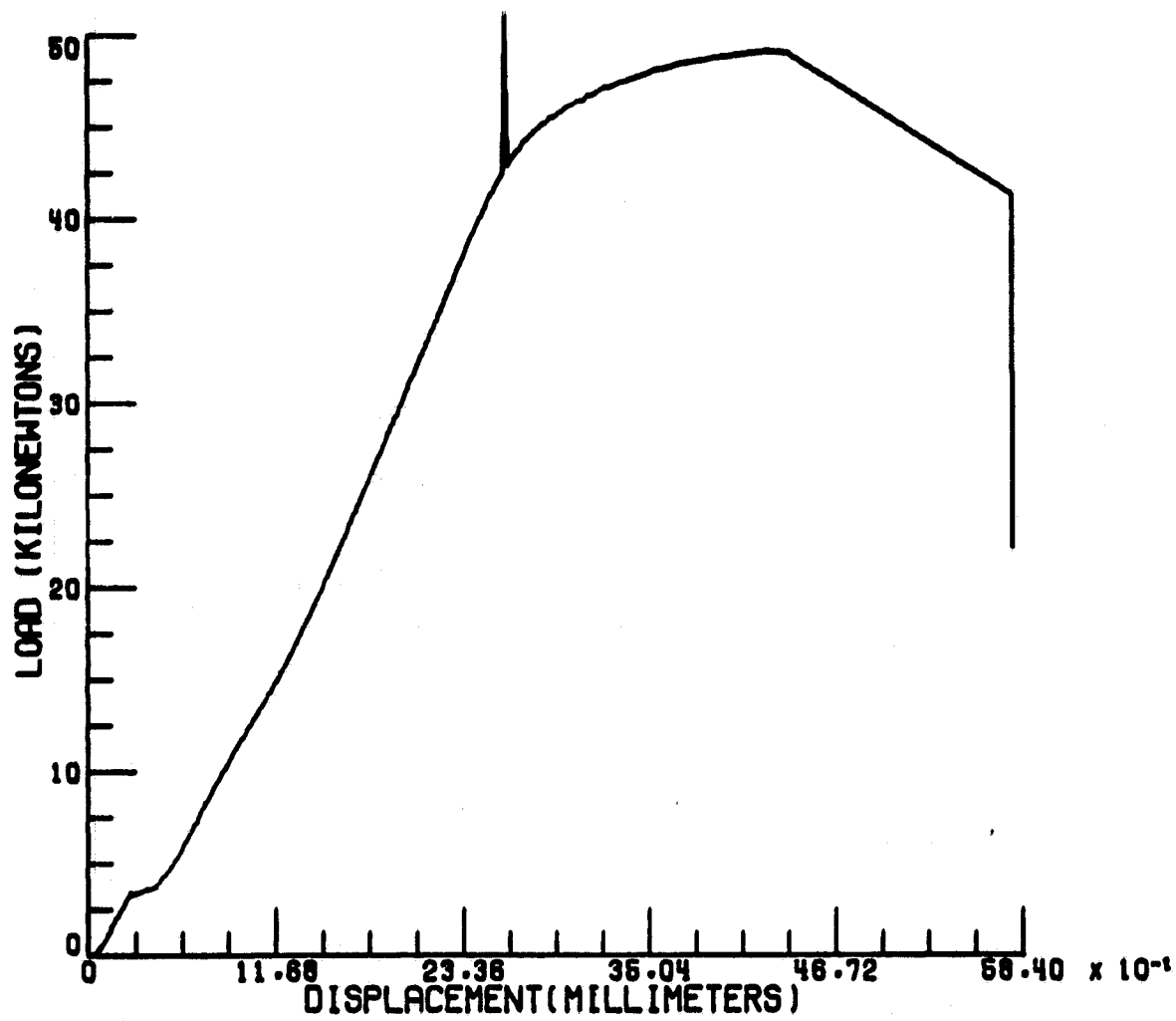


Figure 46. Load-head displacement for aluminum open-hole specimen 1.

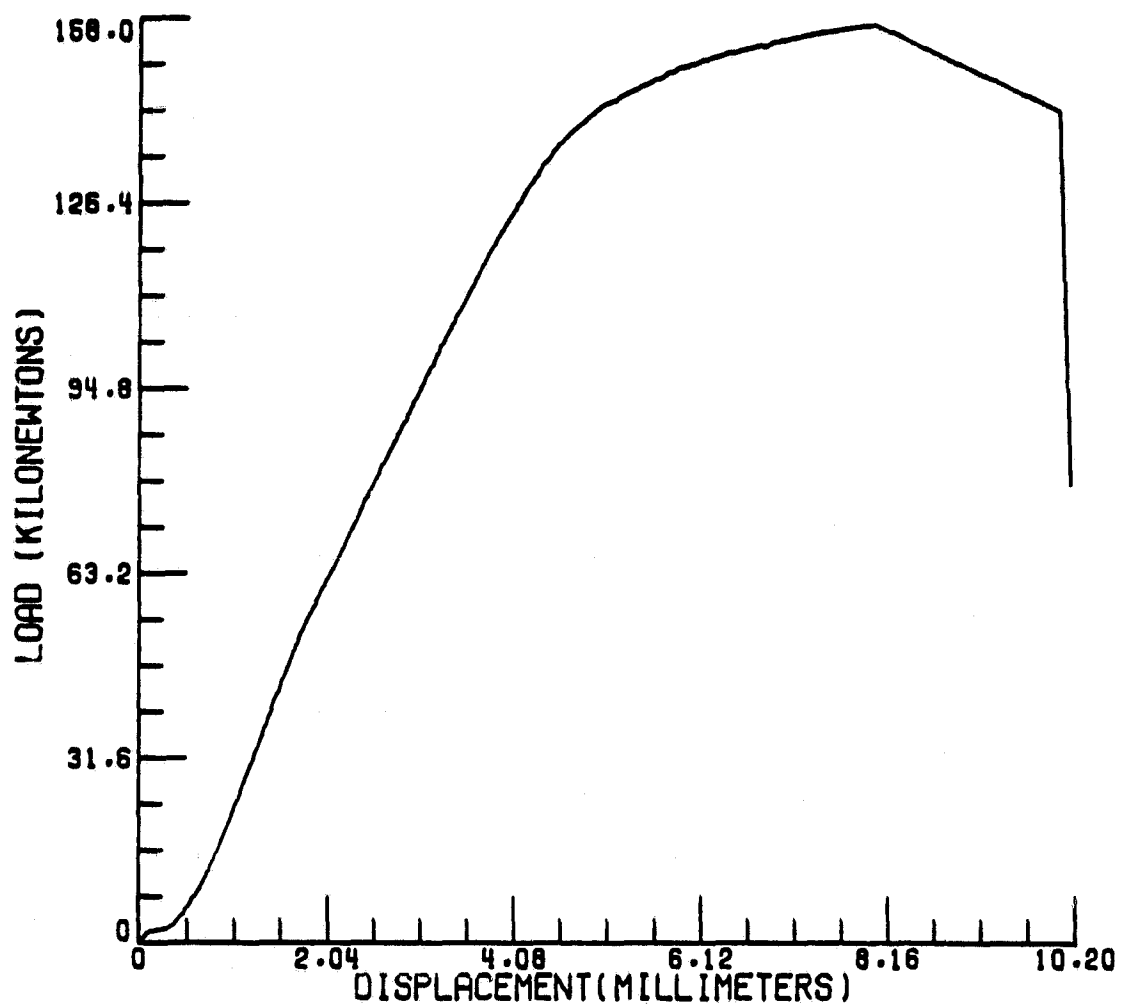


Figure 47. Load-head displacement for aluminum open-hole specimen 11.

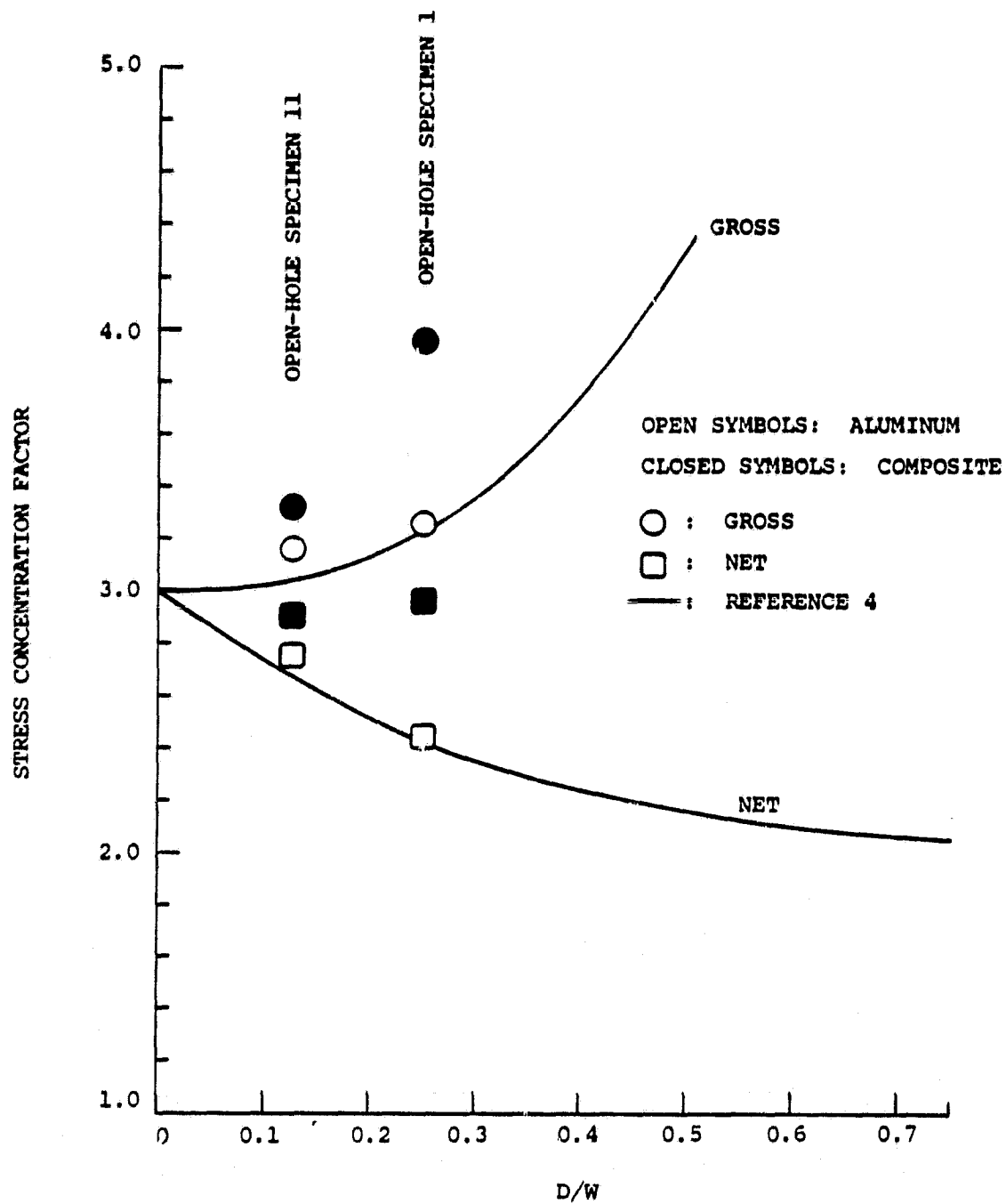


Figure 48. Stress concentration factors for aluminum and composite specimens 1 and 11.

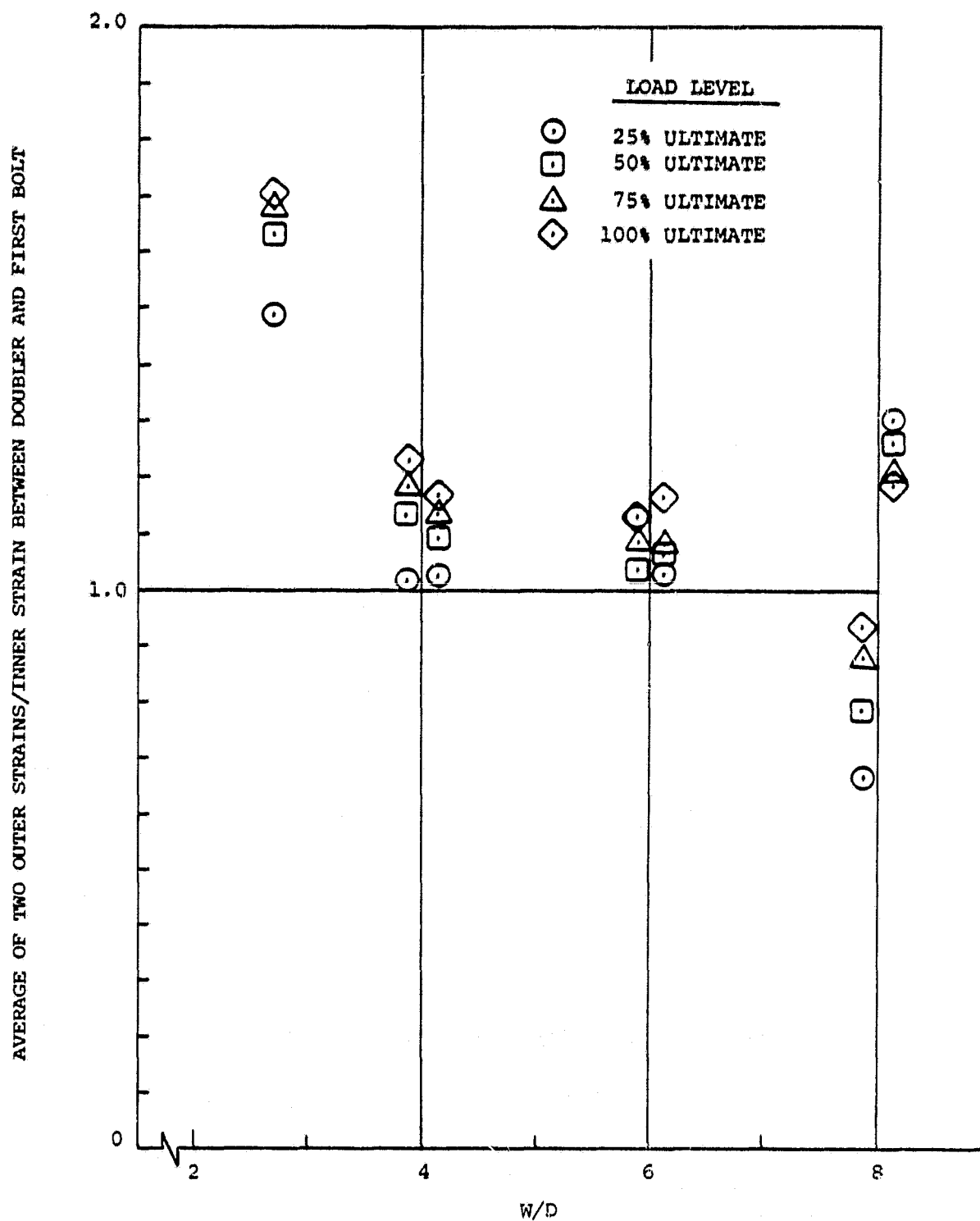


Figure 49. Uniformity of strain across double-lap, double-hole specimens between doubler and first bolt.

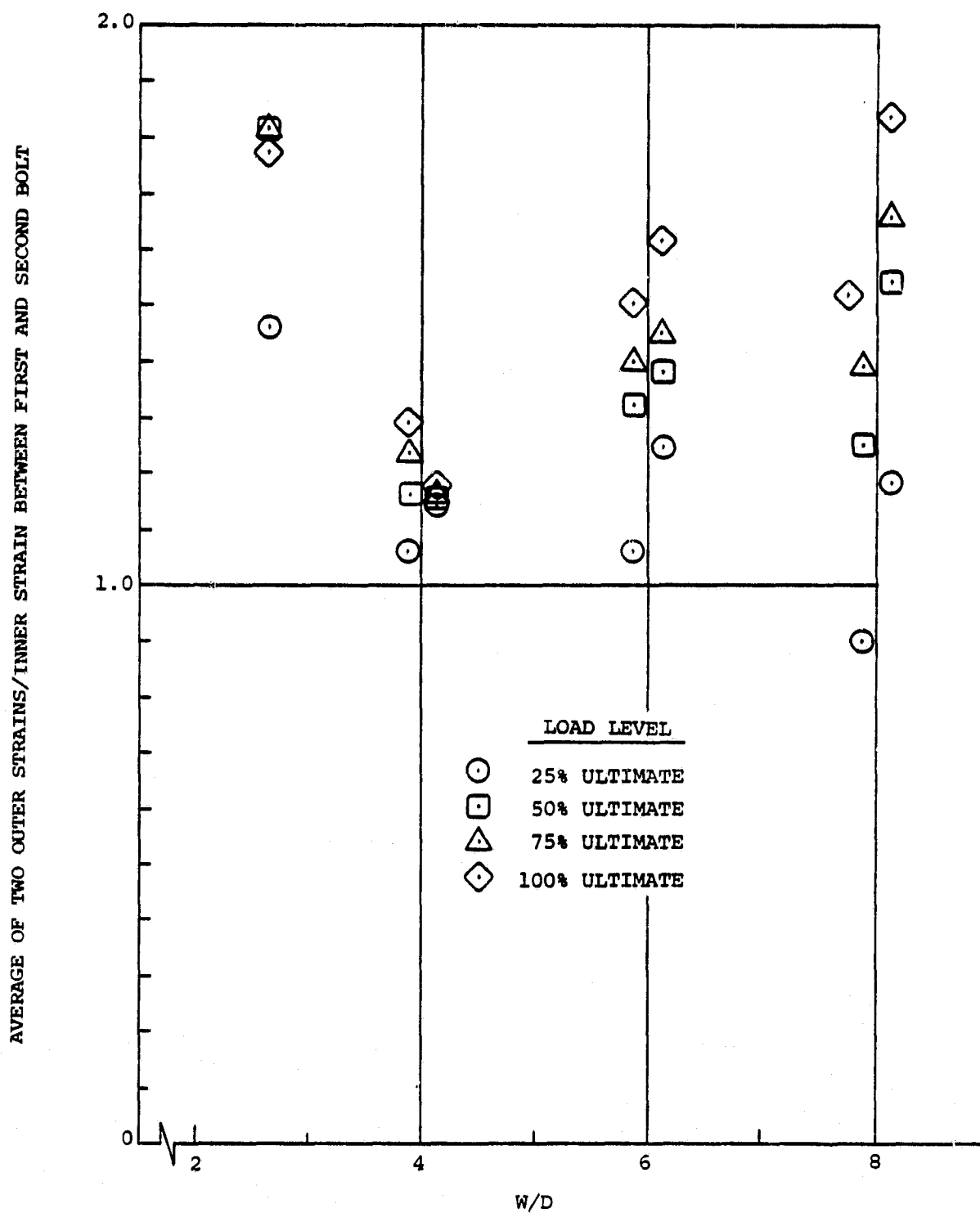


Figure 50. Uniformity of strain across double-lap, double-hole specimens between bolts.

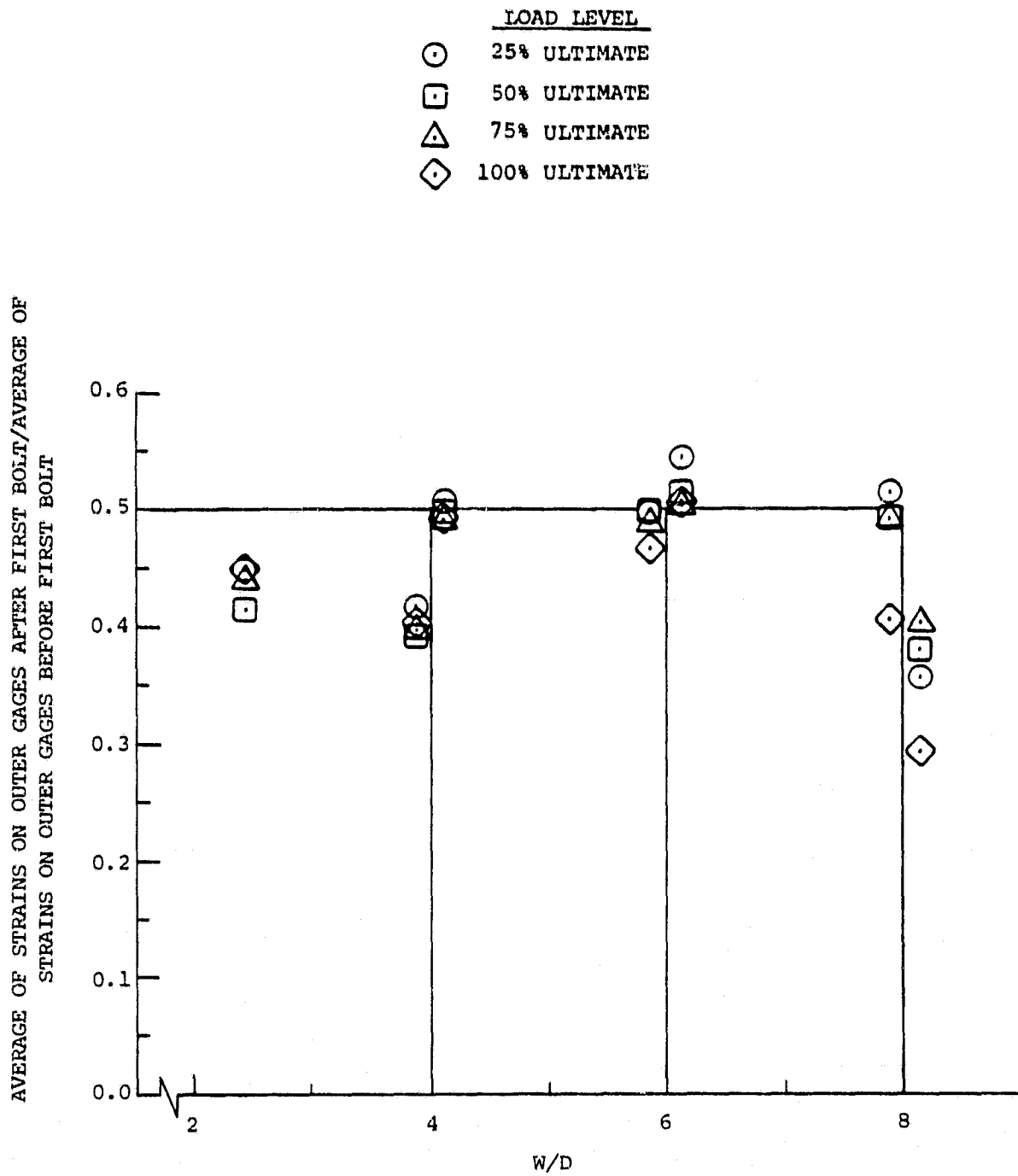


Figure 51. Ratio of strains before and after first bolt in double-lap, double-hole specimens, outer gages.

STRAIN ON CENTERLINE GAGE AFTER FIRST BOLT/STRAIN ON
CENTERLINE GAGE BEFORE FIRST BOLT.

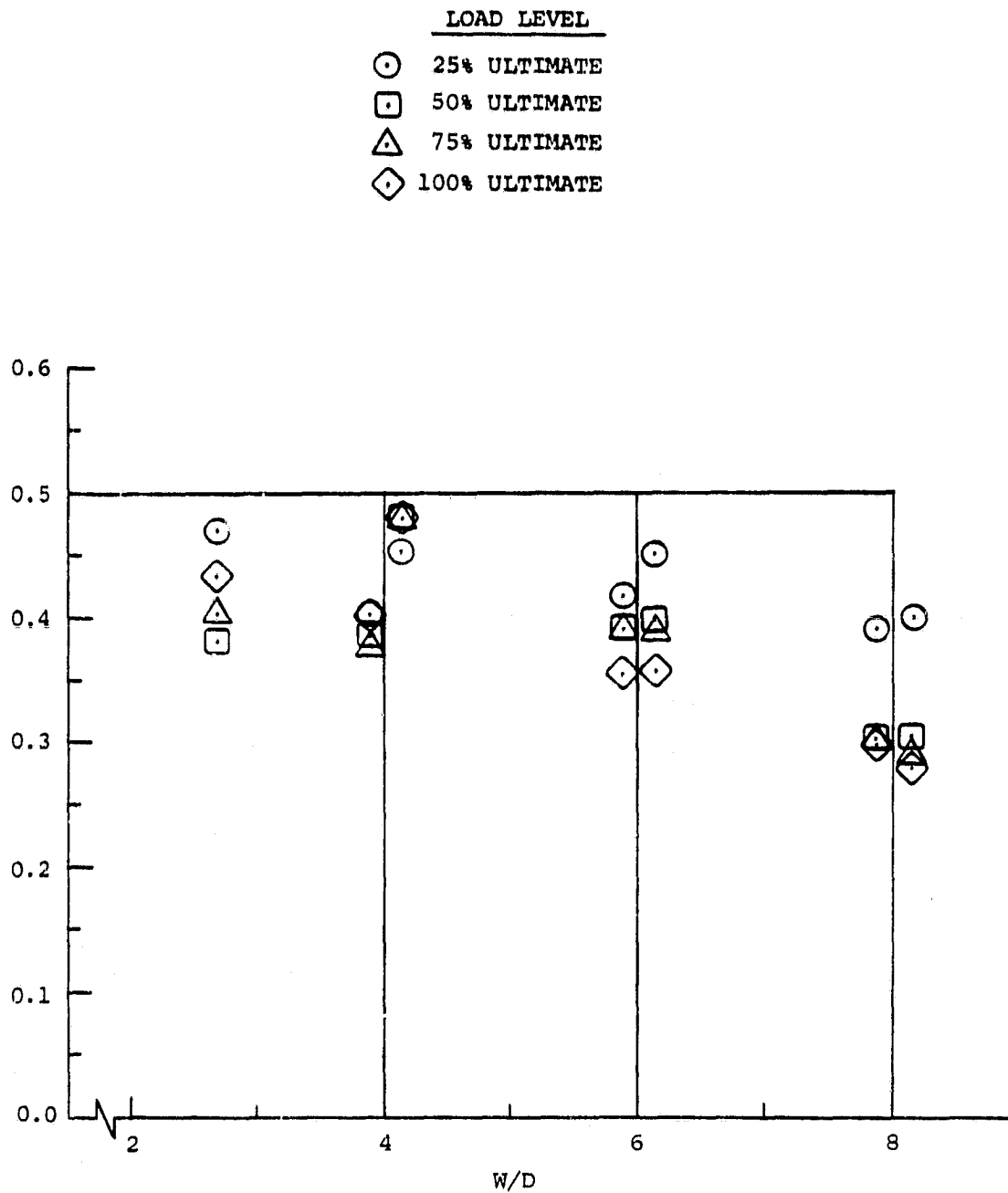


Figure 52. Ratio of strains before and after first bolt in double-lap, double-hole specimen, centerline gages.